UNIVERSIDAD DE CHILE
FACULTAD DE CIENCIAS FÍSICAS Y MATEMÁTICAS
DEPARTAMENTO DE INGENIERÍA ELÉCTRICA

PCR3BP PROBLEM: TRANSFER ORBIT EVALUATION FROM LEO ORBIT TO LUNAR ORBIT OF A SIX UNITS CUBESAT SATELLITE

**TESIS PARA OPTAR AL GRADO DE
MAGÍSTER EN CIENCIAS DE LA INGENIERÍA, MENCIÓN ELÉCTRICA**

RODRIGO FERNANDO SILVA FERNÁNDEZ

PROFESOR GUÍA:
MARCOS DÍAZ QUEZADA

MIEMBROS DE LA COMISIÓN:
LEOPOLDO SOTO NORAMBUENA
RENÉ MÉNDEZ BUSSARD
CÉSAR FUENTES GONZÁLEZ

SANTIAGO DE CHILE
2021

RESUMEN DE LA MEMORIA PARA OPTAR AL GRADO DE: magíster en ciencias de la ingeniería, mención eléctrica
POR: Rodrigo Fernando Silva Fernández
FECHA: 31/05/2021
PROFESOR GUIA: Marcos Díaz Quezada

PCR3BP PROBLEM: TRANSFER ORBIT EVALUATION FROM LEO ORBIT TO LUNAR ORBIT OF A SIX UNITS CUBESAT SATELLITE

La Luna ha sido objeto de admiración y asombro para los seres humanos desde tiempos antiguos. Casi está en la naturaleza humana observar e incluso tener el deseo de alcanzar la Luna. En tiempos modernos, aterrizar en la Luna significaba la conquista del espacio en el contexto de la *Carrera Espacial*. El programa Apollo lo consiguió con sus misiones, pero desde entonces la presencia de humanos ha sido practicamente nula.Por otro lado, el crecimiento de los satélites de estándar Cubesat en los últimos años ha sido exponencial, haciendo que los Cubesats jueguen un rol central en la industria espacial. Aún más, las misiones de Cubesats a la Luna han empezado a ser desarrolladas. Hoy surge un nuevo interés en ir a la Luna y poner a la primera mujer en suelo lunar, esto es propuesto por el programa Artemis, el cual tiene por meta iniciar una nueva era de humanos en la Luna. Con todo esto, pareciera ser que los satélites Cubesat pueden ser un componente clave en el desarrollo de las actividades en la Luna, convirtiéndose en un área de investigación interesante. Un primer paso en esta dirección podría ser la evaluación de una órbita de transferencia desde la Tierra a la Luna, desde una órbita LEO a una órbita lunar. Para ello, este trabajo presenta y resuelve las ecuaciones de un Cubesat de seis unidades en el marco del Problema de los Tres Cuerpos Restringido Plano y Circular (PCR3BP). Se encuentra que para las condiciones propuestas en este trabajo, se necesitará alrededor de medio kilogramo de combustible para transferir un Cubesat con masa inicial de ocho kilogramos desde una órbita LEO a una órbita lunar. También, dependiendo de la frecuencia de operación del propulsor, el satélite tomará entre cuatro a 16 meses en viajar desde una órbita LEO a una órbita lunar. Este trabajo muestra que es posible transferir un satélite Cubesat desde una órbita LEO a una órbita lunar con las restricciones caractéristicas de un Cubesat. Un siguiente paso en esta investigación sería replicar este estudio pero en tres dimensiones, trabajando en el contexto del Problema de Tres Cuerpos Restringido y Circular (CR3BP).

PCR3BP PROBLEM: TRANSFER ORBIT EVALUATION FROM LEO ORBIT TO LUNAR ORBIT OF A SIX UNITS CUBESAT SATELLITE

Abstract

The Moon has been an object of admiration and has astonished human beings since ancient times. It is part of human nature to watch and desire to reach the Moon. In modern times, landing on the Moon has meant the conquest of space in the context of the *Space Race*. The Apollo program accomplished this with its missions, but since then the presence of humans on the Moon has been practically null. On the other hand, the growth of the Cubesat satellite standard in the last years has been exponential, making the cubesats playing a central role in the space industry. Even more, cubesats missions to the Moon has began to be developed. Today, there is a new interest to go to the Moon and put the first woman in lunar soil, this is proposed by the Artemis program, which has for goal to initiate a new era of humans on the Moon. With all of this, it seems that the cubesats satellites may be a key component in the development of the activities on the Moon, becoming an interesting area of research. One first step in this direction could be the evaluation of a transfer orbit from Earth to the Moon, from a LEO orbit to a lunar orbit. To do this, this work presents and solves the equations of motion of a Cubesat satellite of six units in the framework of the *Planar Circular and Restricted 3 Body Problem* (PCR3BP). It is found that for the conditions proposed in this work, it will take around half of a kilogram of fuel to transfer a Cubesat of initial mass of eight kilograms from LEO orbit to a lunar orbit. Also, depending on the operation frequency of the thruster, the satellite will take between four to sixteen months to transfer from LEO to lunar orbit. This work shows that it is possible to transfer a Cubesat satellite from a LEO orbit to a lunar orbit with the characteristic constraints of a Cubesat. A next step of this research would be to replicate this study but in three dimensions, working on the context of the *Circular and Restricted Three Body Problem* (CR3BP).

Agradecimientos

Quiero agradecer a todo el equipo de Spel, al profesor Marcos Díaz por apoyar la realización de este trabajo y a los compañeros de laboratorio: José Pedreros por toda su ayuda y compañerismo, a Javier Rojas por siempre alentarme, a Camilo Rojas por su ayuda con temas de software, a Ignacio "Viki" Maldonado por su trabajo en propulsión eléctrica que influyó en el mío y a todos quienes me brindaron consejo y ánimo, muchas gracias.

También quiero agradecer al equipo del laboratio de plasmas y fusión nuclear de la Cchen, en particular a Leopoldo Soto y Cristian Pavez por brindarme espacio en el laboratorio y por siempre compartir su conocimiento y experiencia.

Agradezco a mis padres que me apoyaron a lo largo del programa y gracias a ellos este proyecto pudo realizarse.

Y agradezco de forma muy especial el apoyo de mi compañera Adoreé. Gracias por estar siempre ahí para animarme, por tu paciencia y ser determinante para que este trabajo culminara de manera satisfactoria.

A todos, muchas gracias.

Contents

List of Tables

List of Figures

Chapter 1

Introduction

1.1. Motivation

The Moon has always been an object of admiration and astonishing for the human being, that is why it has been observed and studied in detailed[1]. In modern times landing on the Moon implied the *conquest of space* by the so called Space Race. The Apollo mission accomplished this by putting the first man on the Moon[2, 3].

Three decades ago the idea of a Moon base was a program[4] and today it has been stated the principles of a Moon base[5] and even the term of *Moon Village*, as Heinicke and Foing says in their work, it is now considered[6]:

> "... ESA has proposed the concept of the Moon Village, with the goal of a sustainable human presence and activity on the lunar surface."

Nowadays, NASA is developing the Artemis program to come back to the Moon and put the first woman on Lunar soil[7, 8, 9, 10, 11].

1.1.1. The Standard Cubesat and Its Exponential Growth

In 1999 Bob Twiggs and Jordi Puig-Suari developed the standard Cubesat as a way to put small satellites in orbit[12]. By 2009, the total number of Cubesat projects reached approximately the one hundred[13], and in 2013 only there was 80 Cubesat projects[14]. In the almost 20 years after the Cubesat development, Swartwout has published several works showing the exponential growth in the use of this technology. In the introduction of his work of 2011, Swartwout stated[15]:

> "...as in all previous years, we still confess that we have little-to-no idea what cubesats mean for the long-term future of space missions: are they just a phase, another launch option, or a fundamental change in the way that space missions are pursued? our opinions have indeed shifted: in 2004, we leaned towards short-term phase; today, we have more confidence that cubesats are a long-term trend with revolutionary implications for some sectors of space industry..."

Approximately seven years later, Swartwout said in the conclusion of his work of 2018 the next[16]:

> "... it was extremely rewarding to review the earlier papers we have published on this topic, and compare the concerns of five and ten years ago to the situation today. We can happily report that we were wrong about all of most dire predictions, and even our optimistic predictions were not optimistic enough. Ten years ago, a launch rate of 8-10 university-class missions per year was thought to be too good to be sustainable, whereas now 8 missions is the average quarterly output.".

By 2019 it was expected that the number of Cubesat launches reached the one thousand in 2021[17]. All this seems to indicate that the use of the Cubesat technology will follow growing in the near future.

1.1.2. Cubesat-Moon Projects

Even there is not record of a mission to the Moon using a cubesat, there is currently several mission proposal of these kind, mainly in the frame of the Artemis mission and the Esa SysNova competition. In the case of the Artemis, there are thirteen cubesat missions selected to go on the launcher SLS to the Moon by 2024, among them the next three cases: Mission to Earth–Moon Lagrange point by a 6u cubesat: EQUULEUS, the EQUULEUS Cubesat of six units is under development by JAXA and Tokyo University and it will fly to the Earth-Moon second Lagrange point[18]; The Lunar IceCube Mission, which is a cubesat of six units that it will prospect for water on the Moon and which is under development by NASA Goddard Space Flight Center And Purdue University[19]; The Lunar Polar Hydrogen Mapper CubeSat Mission, which it will map the hydrogen distribution on the South pole of the Moon[20].

An example of the four Cubesats related to the Esa SysNova: The LUMIO mission, a twelve units cubesats which will monitor and process meteoroids impacts[21]. Private efforts are made in this topic also, as it is the case of Busek company, which is developing its LunarCube, a cubesat of six units intended to missions beyond LEO orbit[22]; it is worth noting that the Lunar IceCube is a LunarCube.

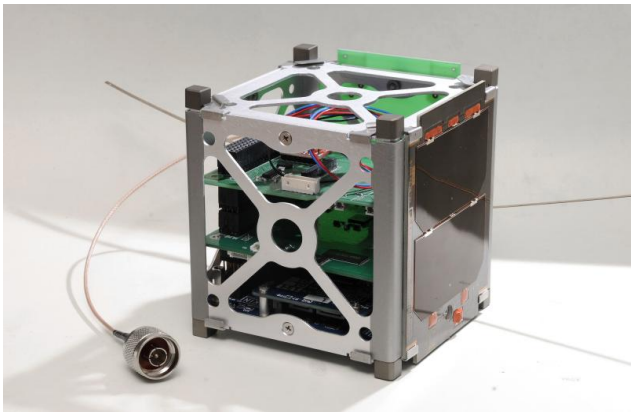

(a) Suchai 1, a satellite of standard Cubesat of one unit (1U) or 1.33 kg of mass.

(b) Artemis program from NASA seeks coming back to the Moon.

Figure 1.1: Suchai 1. Artemis program.

Our laboratory has successfully launched a Cubesat of one unit in the frame of the Suchai Project of Spel laboratory of the Universidad de Chile[23, 24].

1.1.3. The Planar and Circular Restricted Three Body Problem

Considering all of this, to understand at least some aspects of the behaviour of a cubesat satellite in orbit around the Moon seems an interesting topic to study. That is why this thesis evaluate the transfer orbit of a Cubesat of 6 units (8 kg in mass) from a LEO orbit to a lunar orbit. To do this, a special case of The Three Body Problem is solved, the Planar and Circular Restricted Three Body Problem (PCR3BP).

The PCR3BP is the three body problem but one of the bodies has a negligible mass (the satellite), which is called *secondary*, compared with the other two bodies (The Earth and the Moon), which are called primaries. The PCR3BP is determined by only one factor called μ which in the case of the Earth-Moon System is approximately equal to 0.012. In this work, the equations of motion in the context of the PCR3BP of the satellite are solved numerically by the Runge-Kutta method of fourth order.

1.2. Hypothesis

The hypothesis proposed by this work is the following: It is possible for a satellite of standard Cubesat of six units (6U) makes a transfer orbit from a LEO orbit to a lunar orbit in the context of the Planar and Circular Resctricted Three Body Problem (PCR3BP). We consider the use of a thruster under development by Spel laboratory in collaboration with the Laboratorio de Plasmas y Fusión Nuclear of Comisión Chilena de Energía Nuclear (Cchen), the nano Pulsed Plasma Thruster (nPPT). The nPPT has theoretical values of specific impulse approximately of 10000 seconds and a thrust force of the order of 0.1 μN, in contrast with commercial PPT thruster with specific impulse of approximately 5000-6000 seconds and thrust force of the order of 1 μN. The next general objective is established to prove this hypothesis.

1.3. General Objective

The general objective of this thesis is to find at least one transfer orbit from a LEO orbit to a lunar orbit by numerically solving the equations of the PCR3BP. This computation considers the restrictions associated to a Cubesat satellite of six units (6U) or 8 kg its equivalent in mass and the the use of the nPPT thruster for propulsion.

1.4. Specific Objectives

To accomplish the General Objective the following specific objectives are proposed:

- Solve the equations of motion of the satellite in the context of the Planar and Circular Restricted Three Body Problem (PCR3BP).
- Estimate the fuel mass needed by the satellite to orbit all the path from a LEO orbit until a lunar orbit.

- Estimate the total time of flight for every orbit computed.
- Estimate the total energy consumed along the orbit.

1.5. Thesis Structure

This thesis has the following structure:

- Chapter 2, Theoretical Framework, introduces the PCR3BP problem and its equations of motion. Presents the Jacobi constant C and it also describes three perturbations on the satellite dynamics: the effect of oblate Earth ($J2$ factor), atmospheric drag and Sun gravity.
- Chapter 3, Electrical Propulsion: The Nano Pulsed Plasma Thruster, describes the propulsion model proposed in this work. The thrust force is a mean value over a time interval which depends on the operation frequency of the thruster and always aims in the movement direction $\hat{v}$.
- Chapter 4, Results, displays the results obtained in this work. It is obtained regular orbits for the case of LEO, GEO and lunar orbits without thrust as it might be expected. A comparison among perturbations is presented. It is presented transfer orbits from LEO to lunar orbits, landing orbits and stationary orbits. Transfer orbits from GEO orbit are presented. Transfer orbits from LEO orbit to a lunar orbit with a 10 % reduction in the ejected mass Δm and the velocity of the ejected mass c are presented.
- Chapter 5 presents the conclusions of this thesis. It was possible for a satellite of standard Cubesat of six units to transfer from a LEO orbit to a lunar orbit, using the nanoPPT proposed here, in the context of the PCR3BP. The mass of fuel needed to make this transition orbit was around one half of a kilogram and the time of flight depended on the operation frequency of the thruster, being 4, 8 and 16 periods (with 1 period approximately equal to 27.3 days) the time it took for the satellite to reach an altitude of $160k$ km approximately, with operation frequencies of 20, 10 and 5 Hz, respectively. After that, the satellite took between 1 and 2 periods to transit from an orbit around Earth to an orbit around the Moon. For the case of initial GEO orbit, the transfer orbit required one third of the propeller mass of the LEO case (160 gr approximately) and one quarter of the time to reach an altitude of $160k$ km (1, 2 and 4 periods for 20, 10 and 5 Hz of operation frequency of the thruster, respectively). Orbits with a 10 % reduction on Δm and c are presented. Orbits with a 10 % reduction only on Δm increased the time to reach an altitude of $160k$ km and the total energy used in around a 10 %. For the case in a 10 % reduction on c, the time of flight to the $160k$ km of altitude, the propeller mass and the total energy increased in a 10 % approximately. For the case both parameters were decreased in a 10 %, the time to reach $160k$ km of altitude increased in 22.5 %, the propeller mass increased in a 10 % and the total energy increased in a 20 % approximately. This chapter also proposes a future work which considers that the next step it is to replicate the results obtained in this work but working in three dimensions, or on the so called Circular Restricted 3 Body Problem (CR3BP).

Chapter 2

Theoretical Framework

In this chapter the theoretical framework is presented. The equations of motion of the satellite in PCR3BP are introduced. The frames of reference are explained with its respective transformation from the non inertial frame to the inertial one (inertial frame is centered at the barycenter, or center of mass, of the Earth-Moon system and the non inertial rotating frame which is also centered at the barycenter of the Earth-Moon system but it rotates such that the Earth and the Moon appear fixed in it). The Jacobi constant C is introduce with the forbidden zones for the satellite, or the so called Hill's regions. Also, three perturbations are introduce, in this case, the perturbations considered are the atmospheric drag, the oblate Earth ($J2$ factor) and Sun gravity.

2.1. Equations of Motion

To describe the motion of the satellite under the gravity effects of the primaries, the Earth and the Moon, the equations of motion of the Planar Circular Restricted 3 Body Problem (PCR3BP) can be used[1].

$$\begin{aligned} \ddot{x} &= 2\dot{y} + \frac{\partial \Omega}{\partial x} \\ \ddot{y} &= -2\dot{x} + \frac{\partial \Omega}{\partial y} \end{aligned} \tag{2.1}$$

Where (x, y) are the coordinates of the satellite and Ω is an effective potential given by equation (2.2).

$$\begin{aligned} \Omega &= \frac{x^2 + y^2}{2} + \frac{1-\mu}{r_1} + \frac{\mu}{r_2} \\ r_1 &= \sqrt{(x+\mu)^2 + y^2} \\ r_2 &= \sqrt{(x+\mu-1)^2 + y^2} \end{aligned} \tag{2.2}$$

All units are normalized by the factors D, n, and M; the mean distance between the primaries, the mean motion of the primaries around the center of mass and the total mass of both

[1] For a Newtonian, Hamiltonian and Lagrangian formulation, please consult chapter 2.12 of Curtis[25], chapter 5 of Valtonen[26] and chapter 12 of Rajeev[27], respectively.

primaries, respectively. The terms r_1 and r_2 are the distances from the Earth and from the Moon to the satellite, respectively (see figure 2.1).
The PCR3BP is determined by the dimensionless factor μ, which in the case of the Earth-Moon system is approximately 0.012. The μ factor represents both, the distance of the center of the Earth to the center of mass, also called barycenter, and the dimensionless mass of the Moon. For a derivation of the μ factor and a derivation of equations of motion, the reader may refer to the the appendix B and C, respectively.

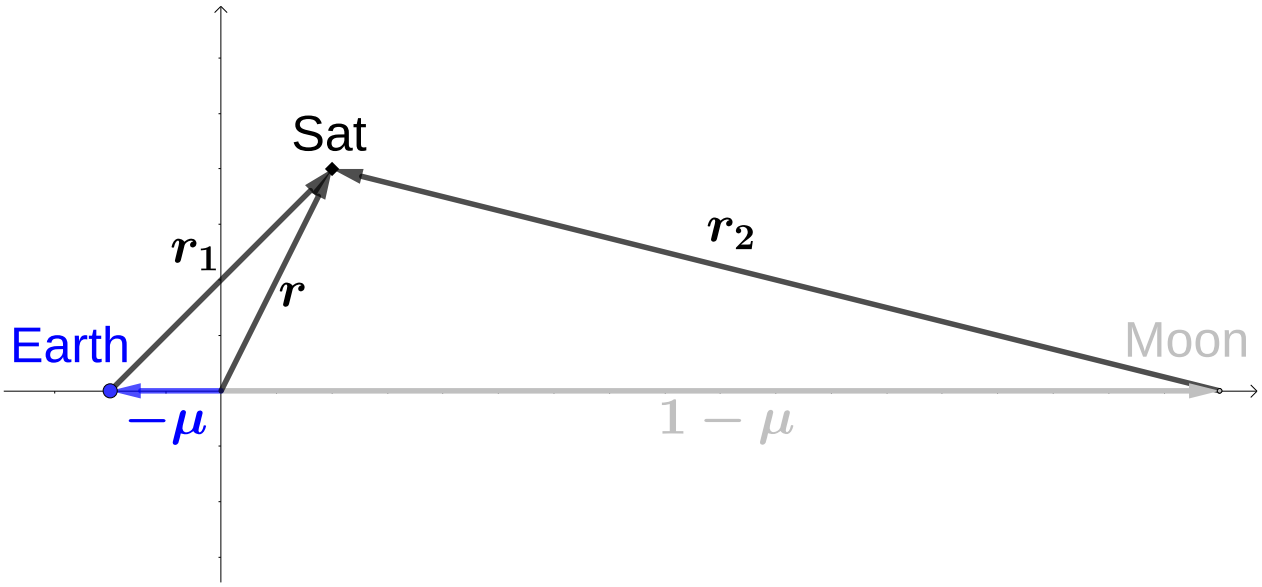

Figure 2.1: PCR3BP scheme. The frame of reference rotates such that both Earth and the Moon are fixed. This image is not at scale.

Equations (2.1) can be written explicitly as below

$$\begin{aligned} \ddot{x} &= 2\dot{y} + x - \frac{(1-\mu)(x+\mu)}{r_1^3} - \frac{\mu(x+\mu-1)}{r_2^3} \\ \ddot{y} &= -2\dot{x} + y - \frac{(1-\mu)y}{r_1^3} - \frac{\mu y}{r_2^3} \end{aligned} \tag{2.3}$$

2.1.1. Frames of Reference

The equations (2.1) are written in a frame of reference where the primaries are fixed. To transform the coordinates from this rotating frame of reference to an inertial frame of reference, we use equations (2.4)[26].

$$\begin{aligned} \xi &= x\cos t - y\sin t \\ \eta &= x\sin t + y\cos t \end{aligned} \tag{2.4}$$

The initial position is taken of the form $(x, y) = (x_0, 0)$, and the initial velocity is of the form $(\dot{x}, \dot{y}) = (0, \dot{y}_0)$. This shape for the initial condition is used in periodic orbits [28, 29]. It can be considered that a satellite follows a periodic orbit in LEO regime. In this case, the

initial normalized velocity of the satellite can be computed as below.

$$v_0 = \frac{1}{nD}\sqrt{\frac{GM_e}{R_e + H_0}} \tag{2.5}$$

The factor nD normalizes the initial velocity. The velocity of expression (2.5) needs to be transformed to the rotating frame of PCR3BP. Defining the initial position x_0 and initial velocity $\dot{y}_0$ as:

$$\begin{aligned} x_0 &= \frac{R_e + H_0}{D} - \mu \\ \dot{y}_0 &= v_0 - \mu - x_0 \end{aligned} \tag{2.6}$$

The relations (2.6) can be used to compute orbits in PCR3BP knowing the initial conditions in a LEO orbit. For a derivation of initial conditions and more details on the frames of reference mentioned here, the reader may refer to the the appendix D.

2.1.2. Jacobi Constant C

The Jacobi constant can be derived from the equations of motion. This constant is given by equation (2.7).

$$C = 2\Omega - v^2 \tag{2.7}$$

This constant defines the Hill's regions. These regions are forbidden zones for the satellite movement [30]. Some examples of Hill's regions for the case of $\mu \approx 0.012$ (Earth-Moon system) can be seen at figure (4.14). In the appendix E the reader may see a derivation of the Jacobi constant C.

2.1.3. Euler-Lagrange Points

In every PCR3BP there are five points where the forces cancel out each other and any satellite put in any of these five points will remain there at rest. Even though these points are widely known as Lagrange points, Euler found the three collinear points, usually represented as L_1, L_2, L_3 and Lagrange found later the two lateral L_4, L_5. The coordinates of the L points can be calculated by equations 2.8 and visulized at figure 2.2:

$$
\begin{aligned}
L_1 &= 1 - \left(\frac{\mu}{3}\right)^{\frac{1}{3}} \\
L_2 &= 1 + \left(\frac{\mu}{3}\right)^{\frac{1}{3}} \\
L_3 &= -\left(1 + \frac{5\mu}{12}\right) \\
L_4 &= \left[\frac{1}{2} - \mu, \frac{\sqrt{3}}{2}\right] \\
L_5 &= \left[\frac{1}{2} - \mu, -\frac{\sqrt{3}}{2}\right]
\end{aligned}
\tag{2.8}
$$

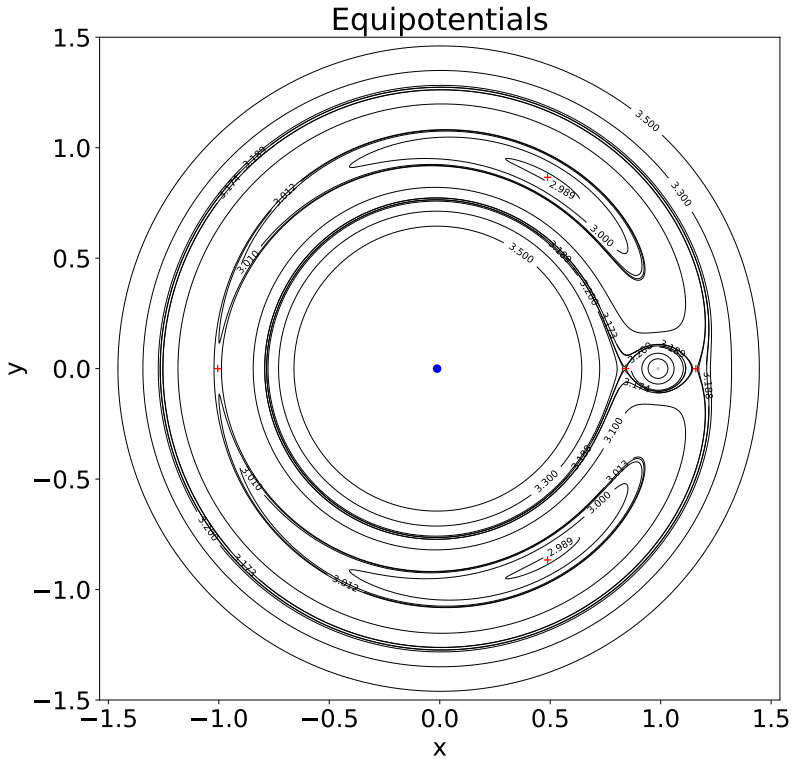

Figure 2.2: Euler-Lagrange points or L points represented by red crosses. The Earth is approximately at the center. The Moon is approximately at $x = 1$. At the L points the gravitational forces from the primaries cancel out.

For a derivation of the L-points, the reader may refer to Valtonen, chapter 5[26]. Valtonen gives the expressions for L_4 and L_5, but not for L_1, L_2 nor L_3. Nevertheless, it gives the expressions that must be solved to obtain the results of equations (2.8). The value of the collinear L-points are extracted from the MIT lecture on Dynamics number 18 by Widnall[30].

2.2. Perturbations

There are forces on the satellite that can be considered as perturbations such as the accelerations due to the non perfect spherical shape of the Earth ($J2$ factor), atmospheric drag and Sun gravity. In this section these accelerations are described.

2.2.1. Atmospheric Drag

In Curtis chapter 12.4 "Atmospheric Drag"[25], it is proposed a model for the perturbing acceleration due to atmospheric drag as shown below.

$$\mathbf{a_D} = -\frac{1}{2}\frac{c_D A}{m}\rho v \mathbf{v} \tag{2.9}$$

Where c_D is the drag coefficient, A is the area of the satellite normal to the movement direction, m is the mass of the satellite, ρ is the atmospheric density and $\mathbf{v}$ is the velocity vector with its modulus v.

The atmospheric density can be described by equation (2.10)[31].

$$\rho = \rho_0 e^{-\frac{h-h_0}{H}} \tag{2.10}$$

Where ρ_0 is the atmospheric density at some given height h_0 and H is the scale factor, which depends on the altitude. The value of these three last parameters are extracted from Rocket and Space Technology Web Page[31].

By other side, Murray proposes a model drag for the case of the restricted three body problem[32]. Murray drag force per unit mass has the next form:

$$\begin{aligned} \mathbf{F_i} &= k\mathbf{v}g\left(x, y, \dot{x}, \dot{y}\right) \\ \mathbf{v} &= \left(\dot{x} - y, \dot{y} + x\right) \end{aligned} \tag{2.11}$$

The model proposed by Murray is not detailed because it does not give a value for the constant k nor the scalar function g, but, comparing the model drag proposed by Murray with the expression for the drag given by equation (2.9), it is seemed reasonable to make the next assumptions:

$$\begin{aligned} k &= -\frac{c_D A}{2m} \\ g\left(x, y, \dot{x}, \dot{y}\right) &= \rho v \end{aligned} \tag{2.12}$$

Please note that the function ρ is a function of the position because $h = r_1 - r_e$, where r_1 is the same as in equation (2.2) and it is a function of x and y. The factor r_e is the normalized Earth radius $r_e = R_e/D$. Because the shape of the velocity by Murray given in equation (2.11), the function v will depend on the components of position and velocity as below

$$\begin{aligned} h &= r_1 - r_e \\ v &= \sqrt{\left(\dot{x} - y\right)^2 + \left(\dot{y} + x\right)^2} \end{aligned} \tag{2.13}$$

In general, the drag coefficient c_D is an elaborated function of temperature and the angle

between the normal to the surface of the satellite and the direction of movement and it is computed in the theoretical framework of Free Molecular Flow[33]. The work by Kato[34] proposes a model for c_D which has a normal component and a tangential component, respect to the surface of attack of the satellite. Because in this thesis work it is assumed that the satellite moves always in an orthogonal way to the displacement direction, the angle between the normal to the surface and the movement direction is zero, so it is the tangential component of the drag coefficient by Kato. The normal component can be considered as the c_D, says Kato, and can be approximated to 2.2. Also the work of Oltrogge[35] proposes the value of 2.2 as a first approximation for drag coefficient. Hence in this work it will be considered that $c_D = 2.2$.

It is also necessary to consider some aspects of the orientation of the satellite to choose an appropriate value for the area of attack A. For a satellite of standard Cubesats of six units, it is intuitive that its orbit will no be along its larger axis. This can be seen noting that the larger axis of the satellite will be aligned with the local vertical, the line from the center of the Earth to center of gravity of the satellite[36]. To find if the satellite align its shorter or mid axis along the orbit, it is necessary to develop a more complicated analysis. This is done using "Gravity-gradient stabilization", and it is left at the appendix F. In this case, it is concluded that the satellite will orbit along its mid axis, with the larger axis aligned with the local vertical and the shorter axis aligned with the normal axis of the orbit, or the direction of displacement. In consequence, $A = 3 \cdot 10$ cm$\cdot 10$ cm. Please note that this area A must be normalized by D^2.

2.2.2. Oblate Earth: J2 factor

Because Earth is not a perfect sphere, its gravity potential can be corrected to obtain a better approximation. Equation (2.14) shows the change in the gravity potential of Earth for the PCR3BP case.

$$U_e = -\frac{1-\mu}{r_1} \rightarrow U_e = -\frac{1-\mu}{r_1} + \Phi\left(r_1, \phi = \frac{\pi}{2}\right) \tag{2.14}$$

The correction to the gravity potential can be written as a power series on r_1 as displayed in equation (2.15).

$$\Phi\left(r_1, \phi\right) = \frac{1-\mu}{r_1} \sum_{k=2}^{\infty} J_k \left(\frac{r_e}{r_1}\right)^k P_k\left(\cos\phi\right) \tag{2.15}$$

Where ϕ is the polar angle, measured from z-axis to the radial. For PCR3BP $\phi = \frac{\pi}{2}$. The change in acceleration due to Earth potential gravity is shown in equation (2.16). This expansion is considered until $J2$ because is the major contribution to the perturbation (the first factors of order superior to $J2$ are approximately three orders of magnitude smaller). For more details, the reader is referred to the appendix G.

$$\begin{aligned} -(1-\mu)\frac{(x+\mu)}{r_1^3} &\rightarrow -(1-\mu)\frac{(x+\mu)}{r_1^3}\left[1 + \frac{3}{2}J_2\left(\frac{r_e}{r_1}\right)^2\right] \\ -(1-\mu)\frac{y}{r_1^3} &\rightarrow -(1-\mu)\frac{y}{r_1^3}\left[1 + \frac{3}{2}J_2\left(\frac{r_e}{r_1}\right)^2\right] \end{aligned} \tag{2.16}$$

2.2.3. Sun Gravity

To take into account the effect of the Sun's gravity, the Bicircular Model (BCM) can be used. Figure 2.3 shows an schematic of the BCM proposed by Koon et al.[37].

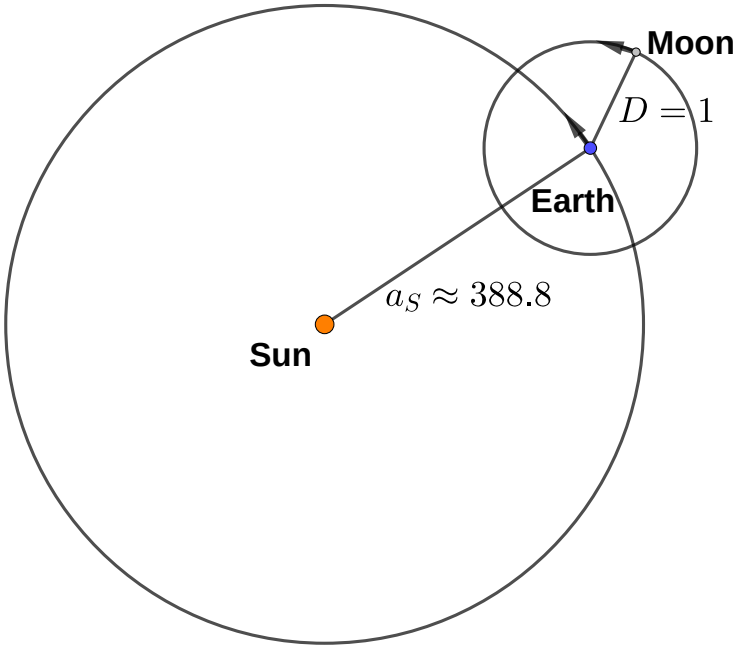

Figure 2.3: Bicircular Model (BCM). The Earth describes a circular orbit around the Sun and the Moon describes also a circular orbit but around the Earth. This image is not at scale.

To the equations of motion of equation (2.1) are added the next terms in the right side of the equations

$$\begin{aligned} &-\frac{\mu_S}{r_S^3}(x - x_S) - \frac{\mu_S}{a_S^3}x_S \\ &-\frac{\mu_S}{r_S^3}(y - y_S) - \frac{\mu_S}{a_S^3}y_S \end{aligned} \tag{2.17}$$

Where μ_S is the normalized mass of the Sun, x_S and y_S are the coordinates of the position of the Sun and a_S is the distance from the Sun to the barycenter of the Earth-Moon system. The value of these parameter are given in equations (2.18).

$$\begin{aligned} \mu_S &= 328900.54 \\ a_S &= 388.81114 \\ \omega_S &= 0.925195985520347 \end{aligned} \tag{2.18}$$

The coordinates of the Sun can be computed using equations (2.19). The initial angular

position of the Sun will be considered zero $\theta_0 = 0$. This last will be true if $t = 0$; if a computation is made such that $t > 0$ then the value of $\theta_0 = 0$ must be computed using equation of θ_S in equations (2.19) using the appropriate value of the variable time t.

$$\begin{aligned} x_S &= a_S \cos(\theta_S) \\ y_S &= a_S \sin(\theta_S) \\ \theta_S &= -\omega_S t + \theta_0 \end{aligned} \tag{2.19}$$

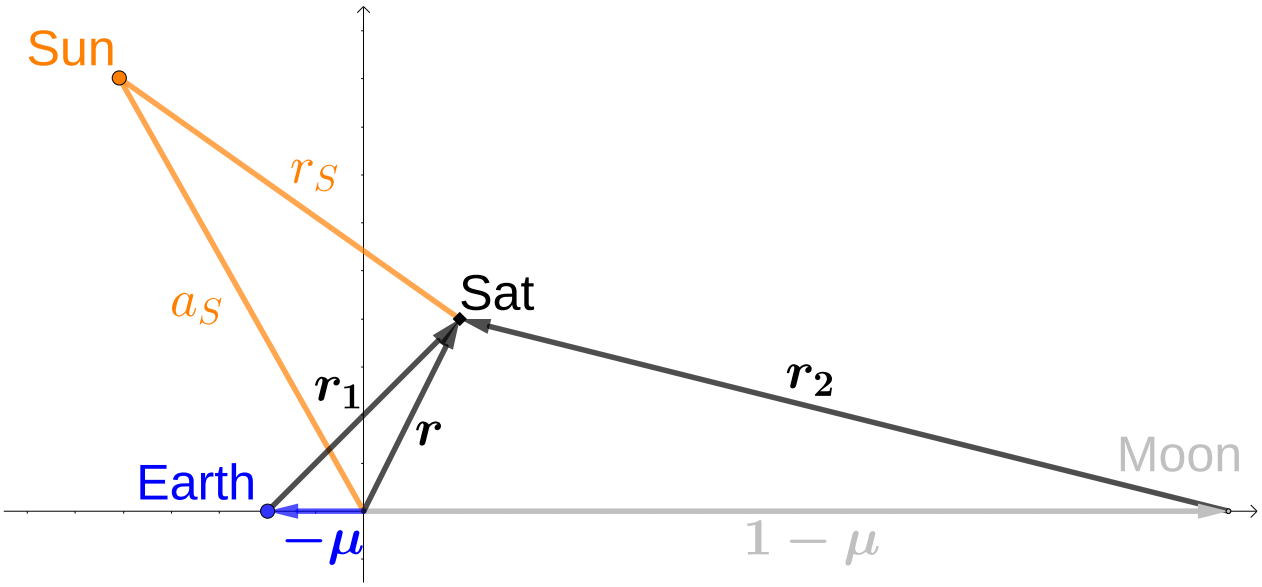

Figure 2.4: The BCM in the PCR3BP reference. The Sun rotates around the barycenter of the Earth-Moon system in a clockwise sense (with a negative angular velocity). This image is not at scale.

Chapter 3

Electrical Propulsion: The Nano Pulsed Plasma Thruster

In this chapter the general concepts of electrical propulsion are presented. A simple thruster model is proposed. The nanoPPT is introduced.

3.1. Space propulsion

To make a satellite change its orbit from a LEO orbit to a lunar orbit, it is necessary to use some propulsion mechanism[38, 39] to exert a force on the satellite and change its state, to use a thrust.

The thrust is the force that acts on the satellite and change its velocity, allowing the satellite to accelerate and consequently change its orbit. The thrust is given by equation 3.1.

$$F = \dot{m}c \tag{3.1}$$

Where $\dot{m}$ is the rate of change of the mass of the satellite over time and c is the velocity of the mass ejected from the satellite. As it can be seen from equation (3.1) the thrust force is obtained by leaving mass behind the satellite. Ideally, a tiny mass is ejected at a high speed from the satellite in the opposite direction of movement of the satellite. This thrust is delivered by a thruster.

To measure the efficiency of a thruster, the specific impulse (I_{sp}) can be computed as shown in equation (3.2).

$$I_{sp} = \frac{c}{g_0} \tag{3.2}$$

Where g_0 is the gravity acceleration at sea level.

Also, it can be defined the variation on velocity or the so called velocity budget given by equation (3.3).

$$\Delta v = c \ln\left(\frac{m_0}{m}\right) \tag{3.3}$$

Where m_0 is the total initial mass of the satellite and m the final mass of the satellite after the thruster has used all its fuel or the also called propeller. If the propeller mass is defined as m_p then $m_0 = m_p + m$. In general, it can be assumed that $m_p \ll m$ and because

$\ln(1+x) \approx x$ when $x \ll 1$ then the factor of the natural logarithm in equation 3.3 can be written as

$$\ln\left(\frac{m_0}{m}\right) = \ln\left(\frac{m_p + m}{m}\right) = \ln\left(1 + \frac{m_p}{m}\right) \approx \frac{m_p}{m} \tag{3.4}$$

Then, equation (3.3) can be written as shown below

$$\Delta v = \frac{m_p}{m} c \tag{3.5}$$

3.1.1. Thruster: Categories and Examples

Propulsion systems can be classified in two general categories: chemical and electric. Chemical propulsion is characterized for its huge thrust and its low specific impulse. The electric propulsion is just the opposite, low thrust and high specific impulse[40, 41]. Electric propulsion has three categories: electrothermal, electrostatic and electromagnetic. Electrothermal thruster heat up some gas or liquid which expand through a nozzle and produce thrust; an example of this technology is the *Resistojet*[40, 41]. Electrostatic thruster accelerate particles using a high voltage electric field. These particles leave the satellite and produce thrust; an example of this technology is the Electro-Spray[42, 43]. Electromagnetic thruster uses electric and magnetic fields to accelerate particles that leave the satellite and produce thrust. An example of this technology is the Pulsed Plasma Thruster (PPT)[44, 45].

3.2. Plasma Focus and its Miniaturization

A technology to produce plasma is the Plasma Focus (PF)[46]. Figure 3.1 shows an schematic of a PF; note the resemblance with figure 3.2 of the schematic of a PPT. It is of interest of this work the Plasma Focus technology because it has been proposed as a pulsed plasma thruster[47, 48, 49, 50, 51, 52].

At Comisión Chilena de Energía Nuclear (Cchen) the research group Laboratorio de Plasma y Fusión Nuclear has developed the smallest PF device ever made, the Plasma Nanofocus[53].

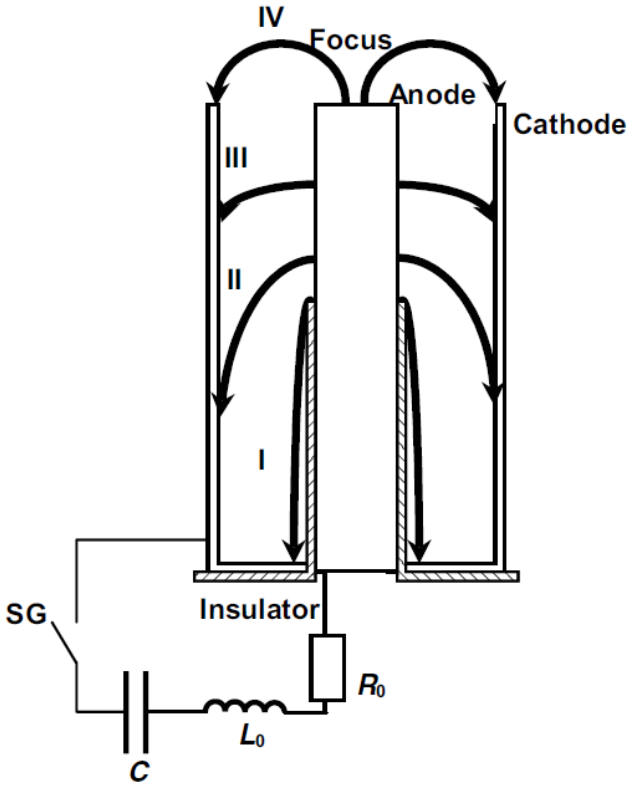

Figure 3.1: Plasma Focus PF schematic. The numbers indicate the evolution of the plasma dynamics. Extracted from Soto, 2005[46].

Because the miniaturization achieved in the Nanofocus device and the work that proposed the use of PF as a PPT, it is seems plausible to evaluate the Nanofocus as a PPT; this will be called nanoPPT (nPPT).

3.2.1. The Nano Pulsed Plasma Thruster nPPT

The electrical propulsion systems [39, 38, 54, 55] and their different types of thrusters [56, 57, 40, 58] are well studied. This work focus on the Pulsed Plasma Thruster (PPT)[44, 45, 59], particularly in one type of PPT proposed by us which we call nanoPPT(nPPT). The nPPT is a proposal of electrical thruster from the Pulsed Plasma Focus(PPF)

3.3. Pulsed Plasma Thruster PPT

The interest of this work is the PPT, this is detailed in this section. Pulsed plasma thruster (PPT) is a space propulsion technology developed since around the 60's[44]. It consists in applying a high voltage in a vacuum to a block of teflon (PTFE). This teflon is eroded or ablated and turned into plasma. When the current flows through the plasma, a magnetic field is induced and a Lorentz force $\mathbf{J} \times \mathbf{B}$ is applied on the plasma, accelerating it and making it to leave the PPT as a plasma sheet, consequently producing a thrust. Figure 3.2 shows an schematic of a PPT of cylindrical geometry[1].

[1] Although parallel plates PPT could be considered as the standard PPT, the attention of this this work will be on the concentric cylindrical plates PPT, because the similarity of the geometry of the plasma focus.

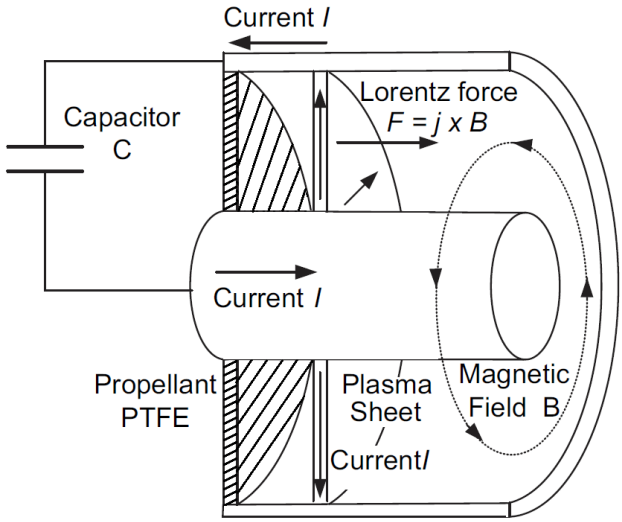

Figure 3.2: Pulsed Plasma Thruster PPT schematic. The plasma sheet is accelerated by a Lorentz force, leaving the satellite and exerting a thrust on it. Extracted from Krejci et al., 2013[60]. The hatched pattern has been added to the original image.

3.4. The Thruster Model

To consider a thruster force in the equations (2.3), a mean thrust is proposed to be used as the propulsion force.

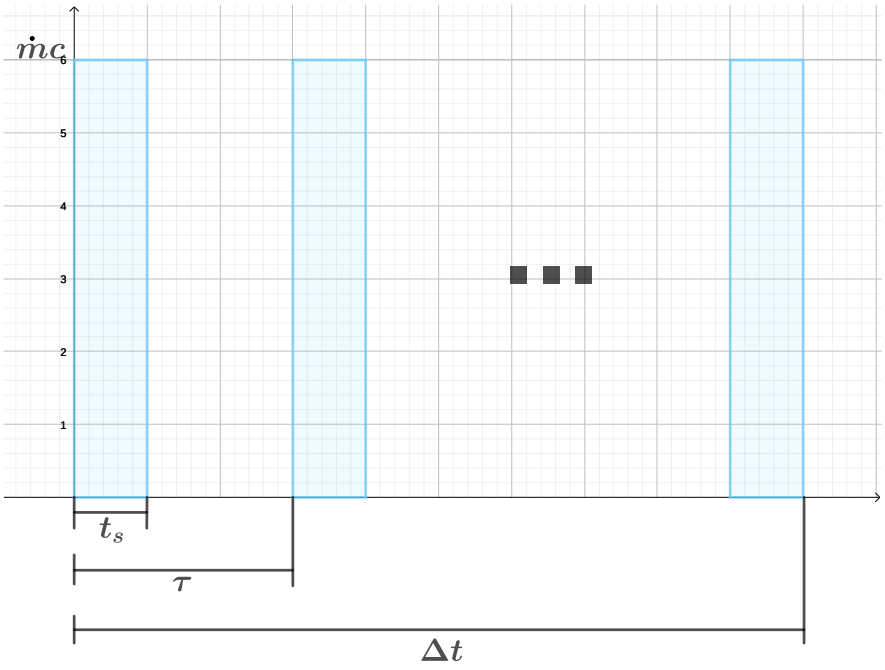

Figure 3.3: Mean thrust. The period of one shot is $\tau = 1/f$. The mean thrust is equal to Δmfc.

$$\bar{F} = \frac{1}{\tau}\int_0^{\tau} F dt \tag{3.6}$$

If $F = \dot{m}c$, $\dot{m} = -\dfrac{dm}{dt}$ and $\frac{1}{\tau} = f$, then the mean force over one period of the thrust force τ will be

$$\begin{aligned}
\bar{F} &= -f\int_0^{t_s} \dot{m}c dt + f\int_{t_s}^{\tau} 0 dt \\
&= -fc\int_0^{t_s} \frac{dm}{dt} dt \\
&= -fc\int_{m(0)}^{m(t_s)} dm \\
&= -fc\,(m(t_s) - m(0))
\end{aligned}$$

Notice that $|m(t_s) - m(0)|$ is equal to the ejected mass in one shot Δm. Also, observe that $(m(t_s) - m(0)) < 0$, because the total mass decreases in every ejection or shot. Consequently $m(t_s) - m(0) = -fc\,(-\Delta m)$. Thus, the mean thrust is equal to:

$$\bar{F} = \Delta m f c \tag{3.7}$$

This method proposes the direction of the thrust force is the movement direction, this is $\hat{v} = \dfrac{\mathbf{v}}{v}$, then the mean force is:

$$\bar{\mathbf{F}} = \Delta m f c \frac{\mathbf{v}}{v} \tag{3.8}$$

In general, it will be necessary to use more than one thruster on the satellite at the same time. If N_{Th} is the number of thrusters used on the satellite at the same time, then the mean thrust force will be:

$$\bar{\mathbf{F}} = N_{\text{Th}} \Delta m f c \frac{\mathbf{v}}{v} \tag{3.9}$$

The number of thrusters

Using more than one thruster avoids any internal torque around the center of mass of the satellite by the thrust force, as long as the thrusters work in a symmetrical fashion and at the same time. Considering this, the minimum value for N_{Th} is four, then $N_{\text{Th}} = 4$. Figure 3.4 shows a plasma gun of the nPPT and an schematic of it; figure 3.4 also displays an schematic of an array of guns. The electrodes or guns are made of copper while the dielectric, which is used as propeller, is made of Teflon (PTFE). The number of thruster needed in the satellite can be estimated accordingly to the propeller mass. Observe that the Teflon area of one thruster is $A = \pi\,(0.85^2 - 0.25^2)$ mm^2 $= 0.66\pi$ mm^2. If the length of one gun is 100 mm and considering that the density of the Teflon is $\rho = 2.2$ mg/mm^2, then the mass per gun is equal to $m_g = 2.2 \cdot 0.66\pi \cdot 100$ mg ≈ 456.16 mg. In this work it has been found that the satellite will need around half of a kilogram of propeller to orbit from LEO to a lunar orbit. Considering this, if the propeller mass is 0.55 kg, the number of guns needed will be $550000/456.16 \approx 1205$. If the array of guns has an square shape, then the number of guns

per arrow will be $N_a \approx \sqrt{1205} \approx 34.7 < 35$. Then, the number of thrusters per arrow could be chosen as $N_a = 35$. If there are 35 guns and each of them occupies an square of length side of 2.8 mm, then the total length of an arrow of these guns will occupy 98 mm, which is 2 mm shorter than the length of a face of one unit Cubesat.

The ablated mass

To compute a value for the thrust, it is necessary to have a value for the ablated mass from the thruster Δm. In general, the ablated mass depends on the energy at the capacitor. If we consider the capacitor of the nPPT as $C = 3.3$ nF, the energy at the capacitor can be computed as $E_0 = \frac{1}{2}CV^2$. Considering a voltage range of $[0.5 - 5.0]$ kV, then the energy will range $[0.41 - 41.25]$ mJ approximately.

To estimate the ablated mass from a PPT, we can use Zeng's work[61]. In figure 3.5 the ablated mass from the nanofocus using Zeng's method is plotted. The energy E_0 is stored at the capacitor of the Nanofocus. Zeng proposes that the energy used to ablate the PTFE is between 3 % and 4 % of E_0. More details of Zeng's method can be found at the appendix H.

Wagner proposes the next equation to estimate the ablated mass from a PPT[62][2]: $\Delta m = 1.32 \cdot 10^{-6} A_p^{0.65} E_0^{0.35}$ kg; where A_p is the ablated area in square meters and E_0 is the energy in the capacitor in Joules. The figure 3.6 shows the ablated mass from the Nanofocus using Wagner's equation. Considering both estimations, if the voltage used is $V = 5$ kV, then $\Delta m = 10^{-10}$ kg, approximately. This value for Δm is used in the simulations of this work.

To produce Δm it is necessary to use a high voltage in the thruster. This high voltage needs to be high enough to produce a breakdown voltage but can not be too high so the satellite will not be able to produce it. In general, a breakdown voltage in vacuum is in the order of kilovolts and a value of 5 kV seems a reasonable low value in this range for a gap of 0.6 mm which is the case of the Nanofocus[64, 65][3].

Range of operation frequencies of the thruster

Respect to the operation frequency of the thruster, Keidar[69] describes its PPT thruster called μCAT that can operate with pulse frequencies between 1 and 50 Hz[4]. It is also expected that the Nanofocus can operate in this range of frequencies[53].

Range of the thrust force magnitude

Considering all the values for every parameter for the thrust force, this will deliver a force of 40 μN for an operation frequency of 1 Hz. In this work the maximum operation frequency is considered as 20 Hz and the frequency to stop around the Moon is considered 25 Hz as a maximum; these two conditions give values for the thrust of 800 μN and 1 mN, respectively.

[2] Wagner's equation has an experimental base from Igarashi's work[63]

[3] High voltage in vacuum is an area of intense research and a detailed description of it goes beyond the scope of this work. The interested reader in this topic is referred to specialized literature[66, 67, 68].

[4] Part of Keidar's work can be found on his book on plasma engineering [59].

(a) Gun electrode upper view.

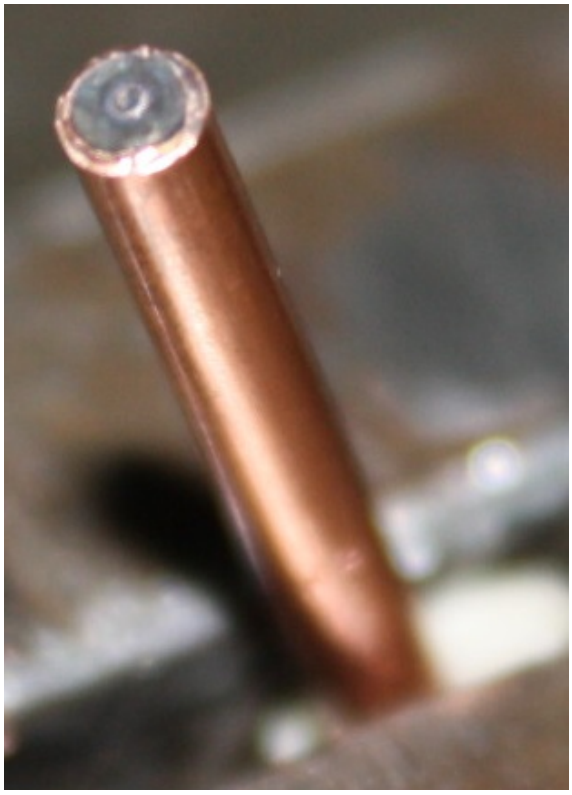

(b) Gun electrode.

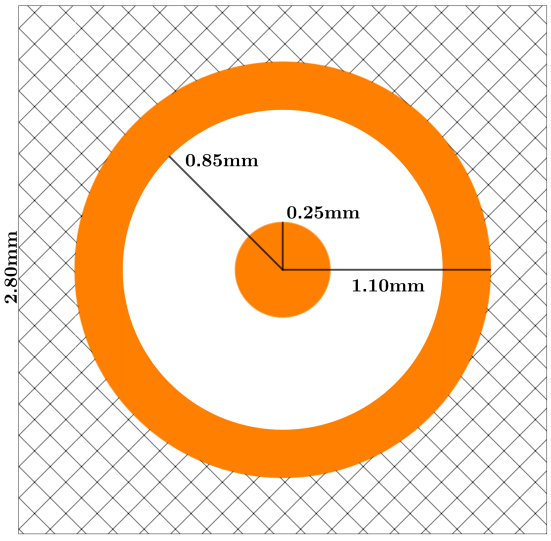

(c) Gun electrode schematic.

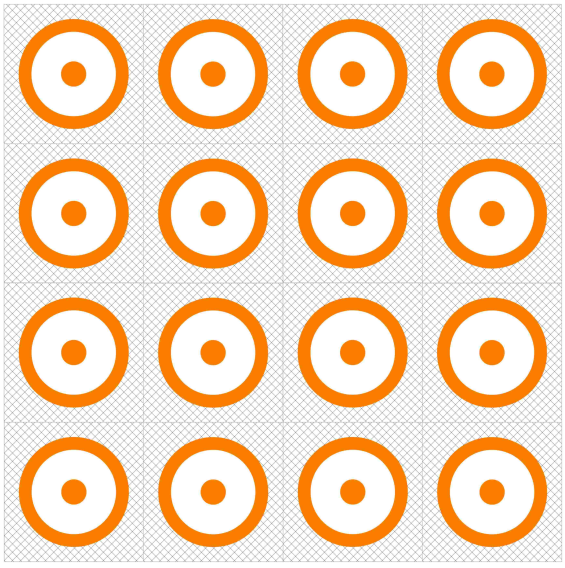

(d) Array of guns or thrusters.

Figure 3.4: Gun used as a thruster and array of guns of thruster. The thruster occupies an square of 2.8 mm of size. One face of one unit of the cubesat could be covered by these guns, with a maximum of 1225 guns in a 35X35 square shape array.

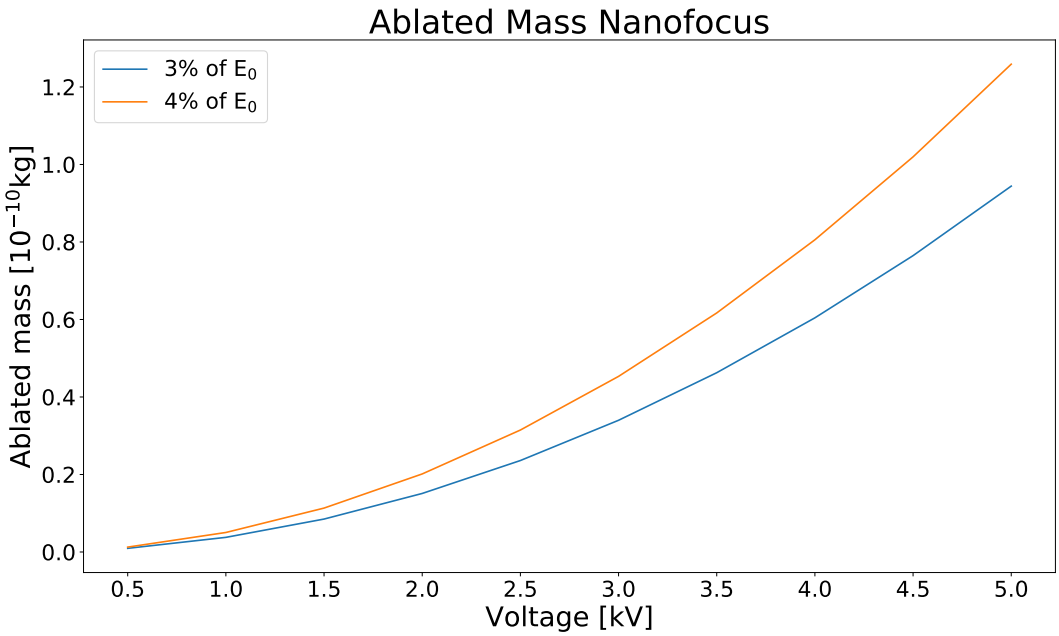

Figure 3.5: Ablated mass from the Nanofocus using Zeng's model. At 5 kV the ablated mass is approximately $1 \cdot 10^{-10}$ kg.

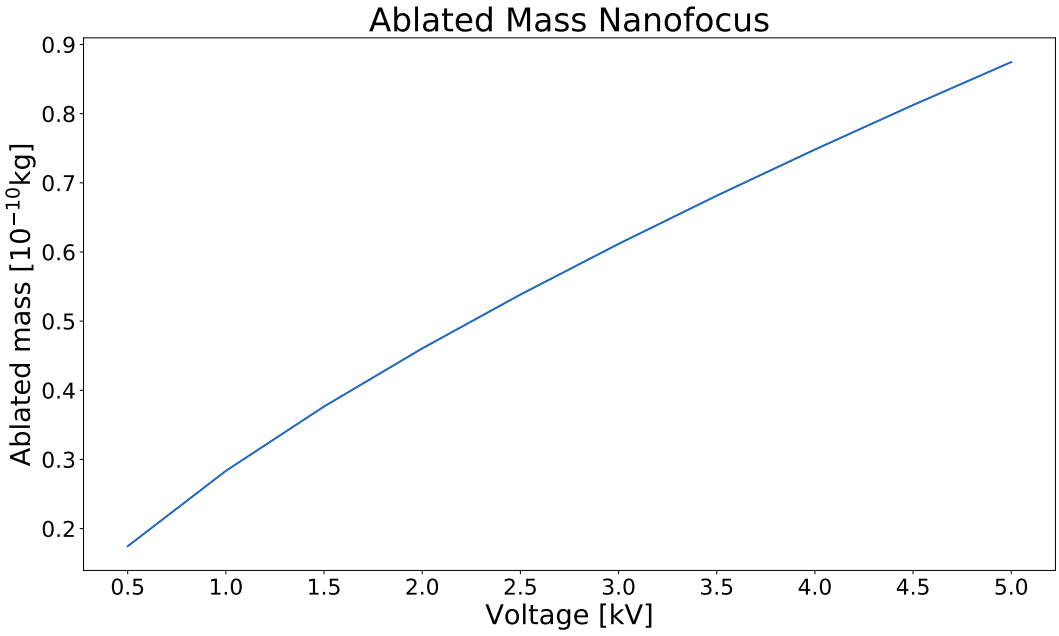

Figure 3.6: Ablated mass from the Nanofocus using Wagner's equation. At 5 kV the ablated mass is approximately $0.9 \cdot 10^{-10}$ kg.

Chapter 4

Results

In this section the results of the implementation of the equations of PCR3BP subject to three perturbations and a thrust force are presented. Orbits with no thrust are presented with the expected results. The perturbations are compared to each other; it is found that the perturbation due to $J2$ is dominant over the drag and Sun gravity accelerations along almost the whole orbit. Drag acceleration is considered null over 1000 km of height and the $J2$ perturbation it is practically zero when the satellite orbits the Moon, where Sun gravity acceleration dominates. Transfer orbits are presented for the cases of operation frequency of the thruster f is 5, 10 and 20 Hz in the ascending part of the orbit with the thruster always aiming to the direction of movement ($\hat{v}$ direction in the rotating frame of reference). In general, the frequency to stop the satellite f_S and make it to orbit the Moon needs to be high (from 15 to 25 Hz). Landing and stationary orbits are presented. Transfer orbits from a geostationary orbit are presented too. Transfer orbits are presented where the ejected mass is reduced in a 10 %, the velocity of the ejected mass is reduced in a 10 % and both cases at the same time. The time of flight, fuel and total energy used for the satellite in these orbits are presented at the end of every section.

4.1. Circular Orbits

In this section results about circular orbits are presented. These orbits do not have thrust. Consider some initial altitude for the satellite as H_0, initial velocity is georeferenced and can be computed using equation (2.5). Then, the initial condition is obtained using equation (2.6).

Figure 4.1 shows LEO orbits in rotating frame for fractions of the period and a whole period. As it may be expected, the orbits around Earth are circular. Please note this result is saying that the satellite makes a circle centered at Earth, but the zero of the axes is not at the center of the Earth, in other words, the satellite is not making a circle around the origin of the axes, but at the center of Earth (see figure 2.1).

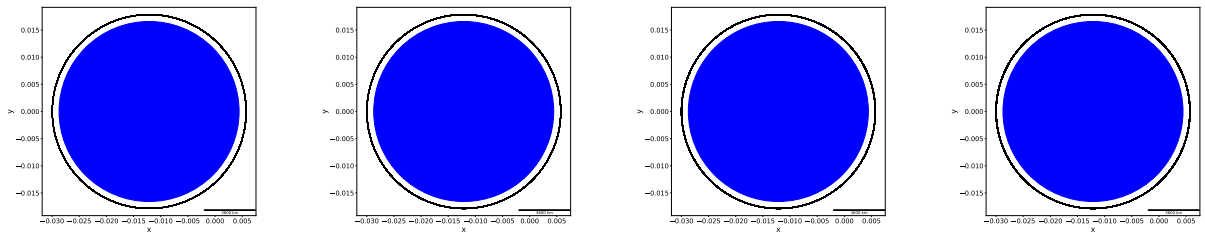

(a) $t = 1/4\mathrm{T}$ (b) $t = 1/2\mathrm{T}$ (c) $t = 3/4\mathrm{T}$ (d) $t = 1\mathrm{T}$

Figure 4.1: LEO orbit in rotating frame. The orbit remains circular over all the time, as it is expected for a LEO orbit.

The results of figure 4.1 can be plotted in the inertial frame of reference using the transformation given by equation (2.4). Figure 4.2 shows the LEO orbit in the inertial frame of reference. The blue orbit represents the orbit of the center of the Earth around the barycenter. The black orbit represents the satellite orbit "following" the center of the Earth. We plot a fraction of the total satellite orbit, if it were plotted completely, it would not visible Earth's orbit.

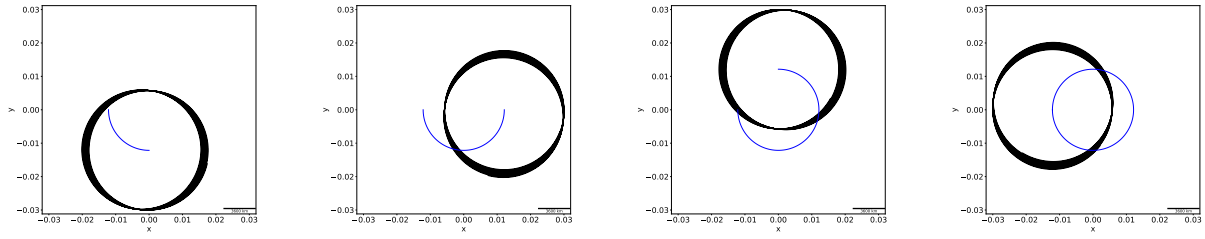

(a) $t = 1/4\mathrm{T}$ (b) $t = 1/2\mathrm{T}$ (c) $t = 3/4\mathrm{T}$ (d) $t = 1\mathrm{T}$

Figure 4.2: LEO orbit in the inertial frame of reference. The blue orbit represents the center of the Earth around the barycenter. The satellite orbit "follows" the center of the Earth. For simplicity, a fraction of the satellite orbit is plotted in each case.

A similar result can be obtained for the case of a geostationary orbit (GEO). Figure 4.3 shows a GEO orbit in rotating frame. As it may be expected, this orbit is a circular one centered on Earth. The orbit remains circular along full simulation.

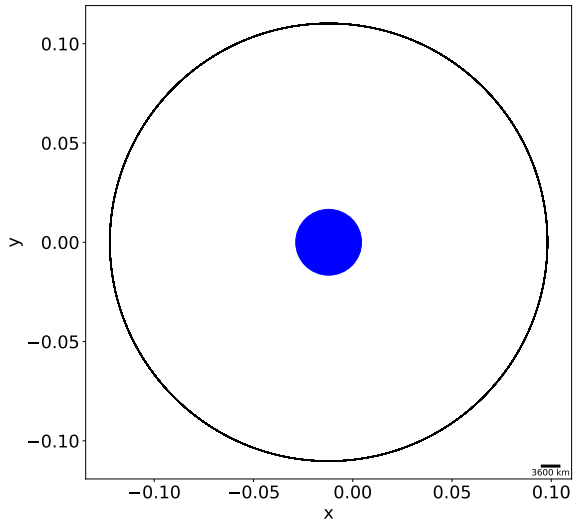

Figure 4.3: GEO orbit in rotating frame. The orbit remains circular centered at Earth as it may be expected.

Figure 4.4 shows the GEO orbit in the inertial frame of reference. This orbit is for one period of the system (27 days approximately). The blue circle is the orbit of the center of the Earth around the barycenter in a total period. The black strip shape is the the full orbit of the satellite along a whole period. This is the shape of the orbit "following" the center of the Earth.

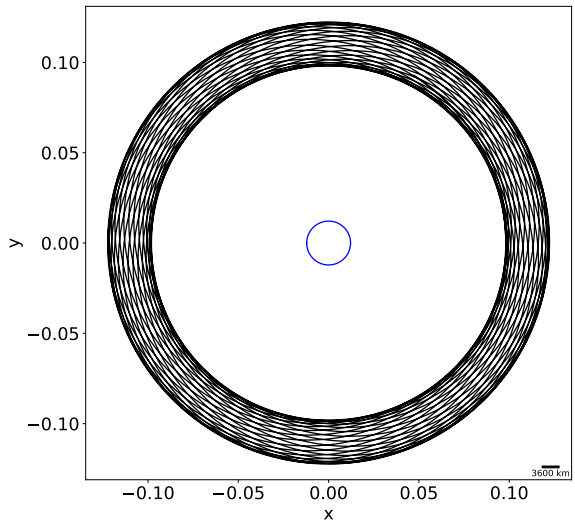

Figure 4.4: GEO orbit in the inertial frame of reference. The blue circle is the center of the Earth orbiting the barycenter. The black strip is the satellite orbit making circles around and "following" the center of the Earth.

HEO orbits can be obtained as shown in Figure 4.5; the initial altitude of the satellite is

represented as a percentage of D, the mean distance between Earth and Moon centers. As it can be seen, orbits remain circular until around one half the distance between the Earth and the Moon (distance $D \approx 380k$ km), where orbits become to loose their regular circular shape at lower altitudes. The satellite will remain orbiting around Earth until 80 % of D approximately, or equivalently until $300k$ km. Beyond that, the satellite will escape of Earth attraction. In this case the satellite will orbit in the exterior of the Earth-Moon system, as shown in last picture in figure 4.5. Figure 4.6 shows the same orbits as figure 4.5 in the inertial frame of reference.

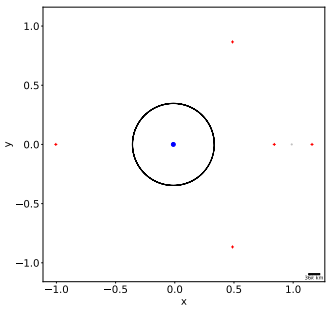

(a) 33 %D

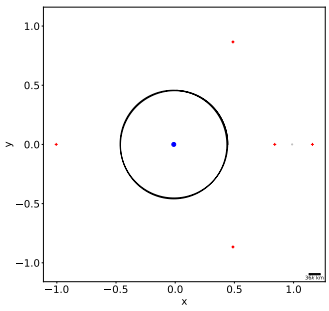

(b) 44 %D

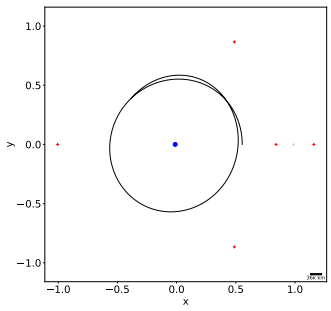

(c) 55 %D

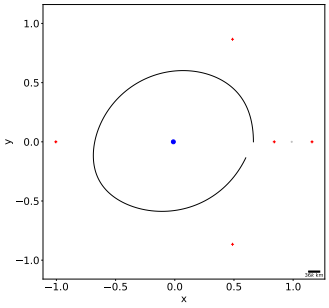

(d) 66 %D

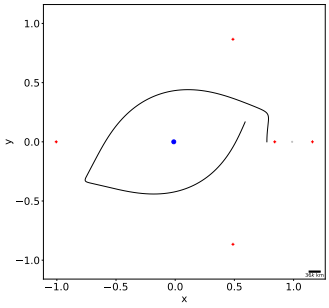

(e) 77 %D

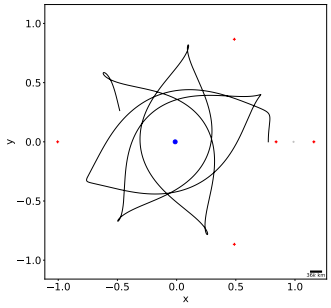

(f) 77 %D and $t = 3$T

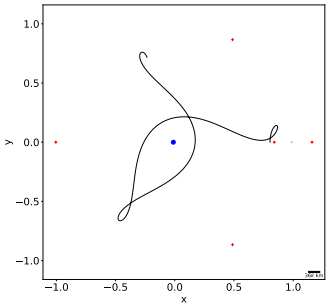

(g) 80 %D and $t = 3$T

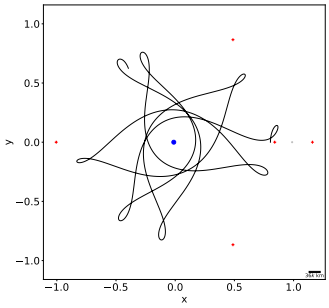

(h) 80 %D and $t = 3$T

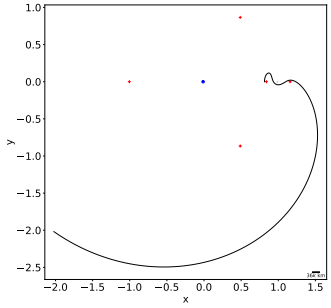

(i) 81 %D

Figure 4.5: HEO orbits in rotating frame. The percentages of D indicates the initial altitude of the satellite. All orbits are plot for $t = 1$ T. The cases 77 %D and 80 %D are plot also for $t = 3$T. The last case for 81 %D, the satellite escapes from the interior of the Earth-Moon system.

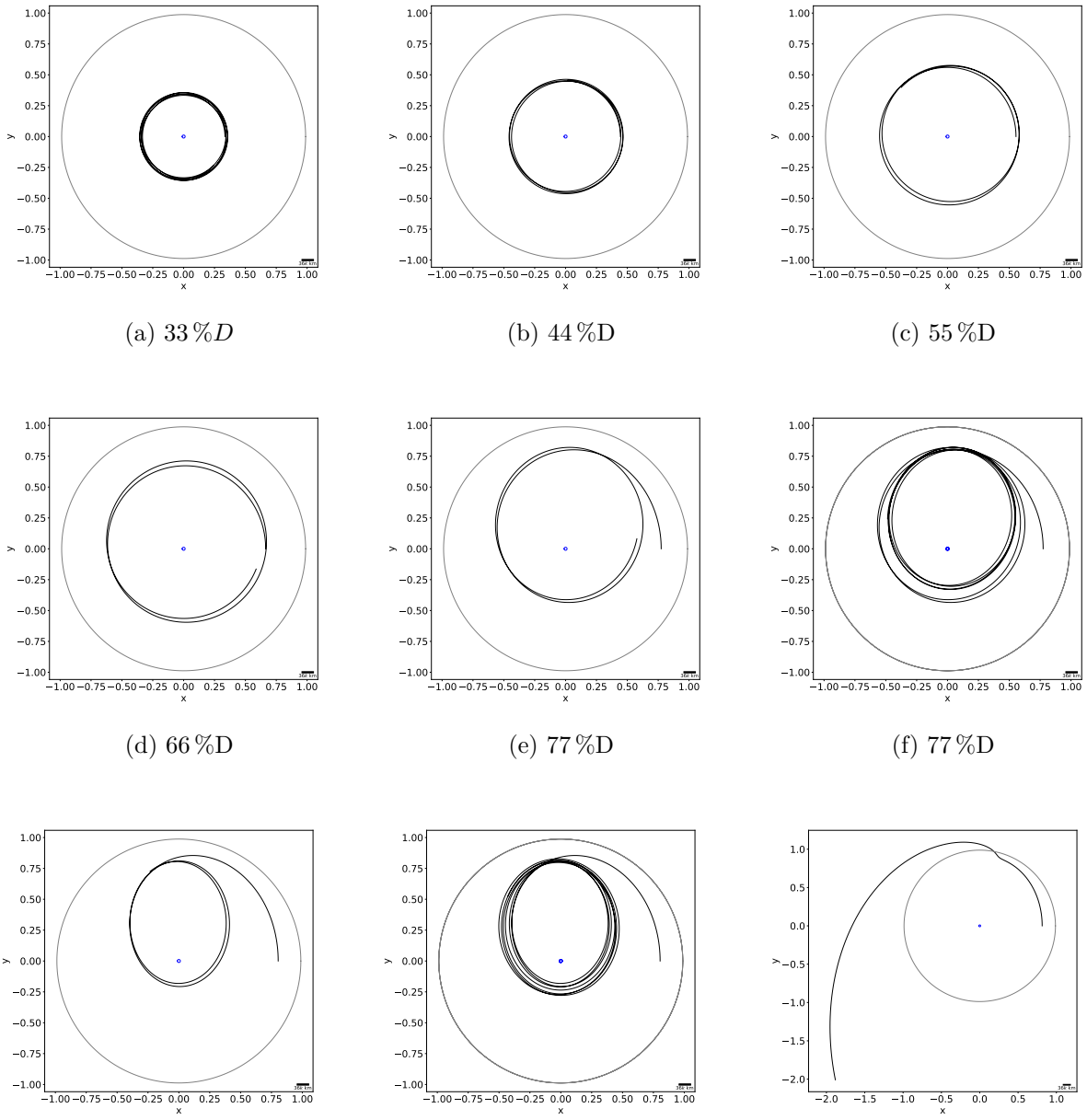

(a) 33 %D (b) 44 %D (c) 55 %D

(d) 66 %D (e) 77 %D (f) 77 %D

(g) 80 %D (h) 80 %D and $t = 3$T (i) 81 %D

Figure 4.6: HEO orbits in inertial frame, the percentage of D is the initial altitude of the satellite. All orbits are plot for $t = 1$ T, except the cases 77 %D and 80 %D, where they are plotted also for $t = 3$ T. The last case for 81 %D the satellite escapes from the interior of the Eart-Moon system.

To obtain the result in figure 4.7, initial conditions proposed by Ugai are used[29]. It is interesting to note that the same result is obtained with the methodology proposed here as the methodology proposed by Ugai, using its initial condition $(x_0, y_0, \dot{x}_0, \dot{y}_0) = (0.152125, 0, 0, 3.16077)$. One interesting point of this orbit is that has a close point near to the Earth and a far one, beyond the orbit of the Moon. This scenario would allow to make observations from outside the Earth-Moon systems, in the far point or apogee, and download data at the closest point, when it is near Earth (around $50k$ km of height) in the perigee of the orbit.

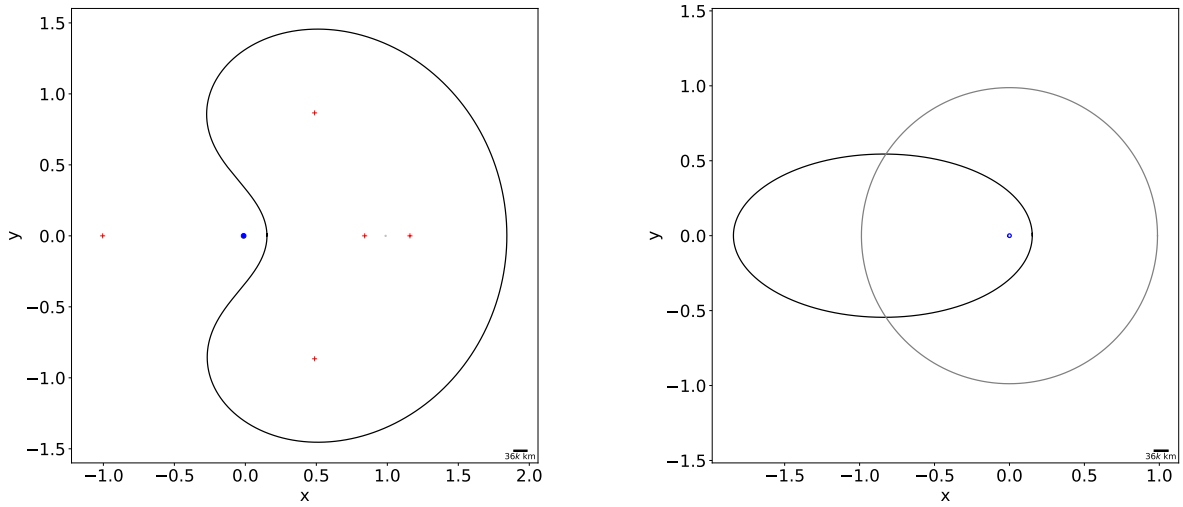

(a) Rotating frame.

(b) Inertial frame.

Figure 4.7: Orbit proposed by Ugai[29]. This methodology replicates results of Ugai's work using its initial conditions.

Similar results as figure 4.5 can be obtained for the lunar case, as shown in figure 4.8. Note the orbits are also circular as the case of Earth. Thus will be until the height is approximately $20k$ km. When the height is 16 % of D,the satellite will not longer remain orbiting the Moon and it will go inside the system Earth-Moon, as shown in the last image in figure 4.8.

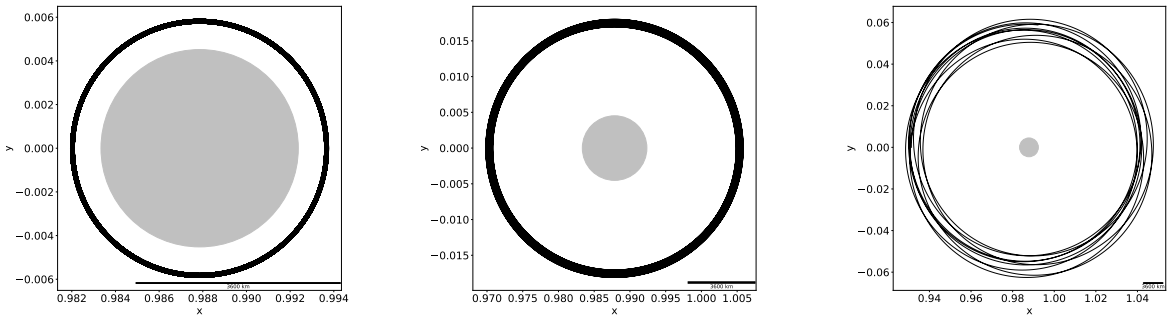

(a) 500 km (b) 5 (c)

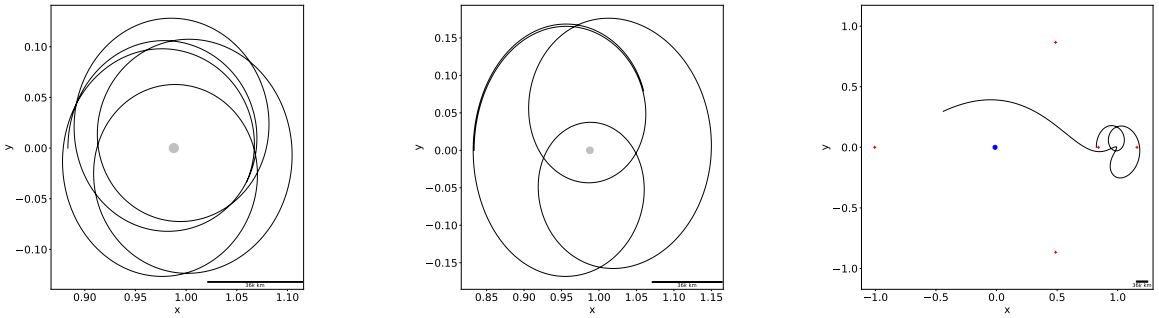

(d) (e) (f)

Figure 4.8: Lunar orbits in rotating frame of reference. These orbits remain almost circular until height is around $20k$ km. When height is $16\,\%$ of D, the satellite will not longer orbit around the Moon and it will move inside the sysmtem Earth-Moon.

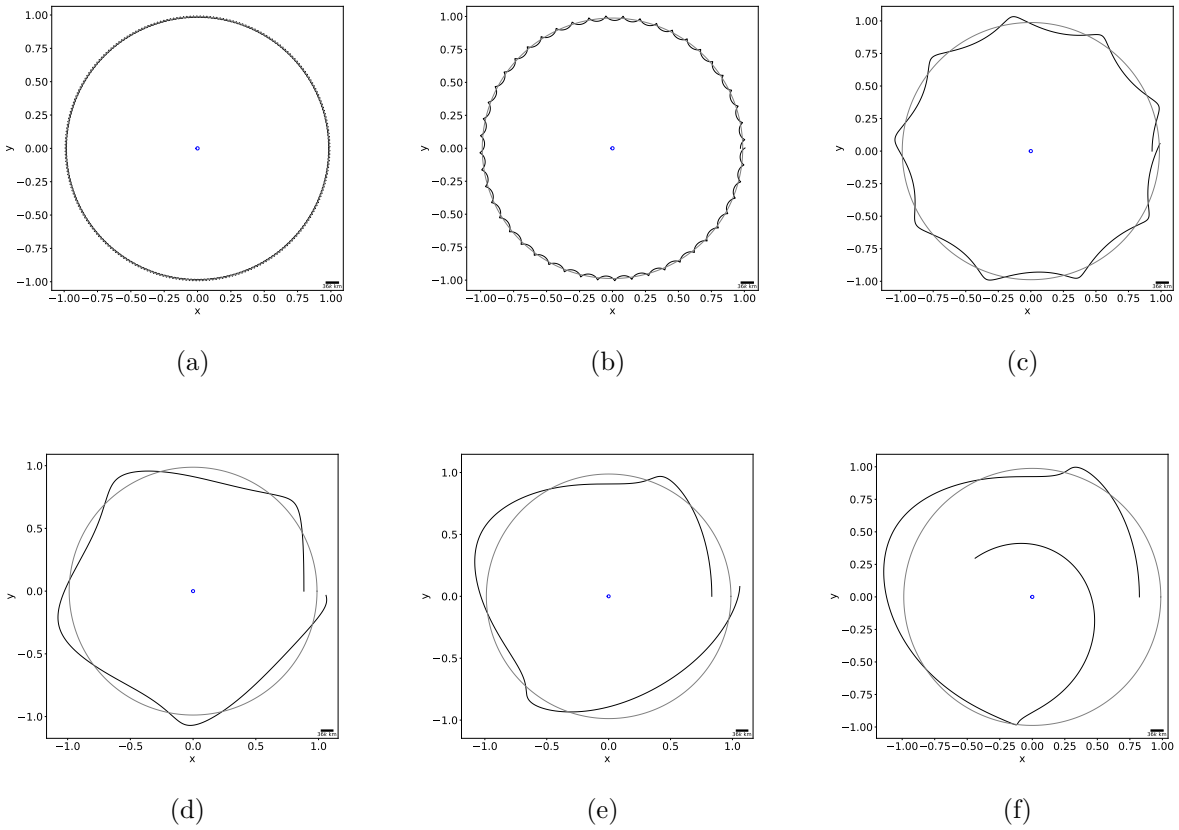

(a) (b) (c)

(d) (e) (f)

Figure 4.9: Lunar orbits in inertial frame of reference. The blue circle at the center is the orbit of the center of the Earth. The big grey circle is the orbit of the center of the Moon around the barycenter. The ripples in the satellite orbit are because it is "following" the center of the Moon.

4.2. Comparison Among Perturbations

Figure 4.10 shows the accelerations due to the: atmospheric drag, $J2$ factor and the Sun gravity; in function of the time and in function of the height, with T the period of the Moon around the center of mass (also the period of the Earth around the center of mass) and being approximately equal to 27.3 days, and $k = 1000$. These plots corresponds to the case of $f_1 = 20$ Hz, $t_1 = 4$ T, $f_2 = 8$ Hz and $t_2 = 4$ T. The meaning of these frequencies f and times t is explained in the next section. The plots are sketched until time $t = 0.25$ T with initial time $t_0 = 0$ or equivalently, with initial altitude $H_0 = 0.5k$ km until the height is $H \approx 1.2k$ km. In this range, the acceleration on the satellite due to the $J2$ factor is dominant, with an acceleration ~ 10 mm/s^2, over the the acceleration due to the atmospheric drag $\sim 0.1\mu$m/s^2 and the Sun gravity acceleration oscillating between 0.1 μm/s^2 and 0.9 μm/s^2. At the end of this range, at $1.2k$ km of height, the acceleration due to the atmospheric drag is approximately zero.

Figure 4.11 shows accelerations due to the $J2$ factor and the Sun gravity. In this case the initial time is $t_0 = 0.25$ T, until $t = 1$ T. Equivalently in height $H_0 = 1.2k$ km until height $H = 4.2k$ km. In this second range, the acceleration due to factor $J2$, with values from 8

mm/s^2 to 2 mm/s^2, is still dominant over the acceleration due to the Sun gravity, this last one with maximum value around 1 μm/s^2.

Figure 4.12 shows a third range of accelerations due to $J2$ factor and Sun gravity. In this case, the initial time is $t_0 = 1$ T until $t = 4$ T and, equivalently, initial altitude $H_0 = 4.2k$ km until $H = 166.2k$ km. In this range, the acceleration due to the $J2$ factor dominates but drops almost to zero while the acceleration due to the Sun gravity increases to around 10μm/s^2, being the dominant perturbation in the heights over $100k$ km.

Figure 4.13 shows a fourth range with the accelerations due to factor $J2$ and Sun gravity. In this range the initial time is $t_0 = 4$ T until $t = 8$ T, equivalently, $H_0 = 166.2$k km until $H = 423.7$k km (satellite orbiting the Moon). The acceleration due to Sun gravity is around 10 μm/s^2 and dominates over the acceleration due to the $J2$ factor which is approximately zero.

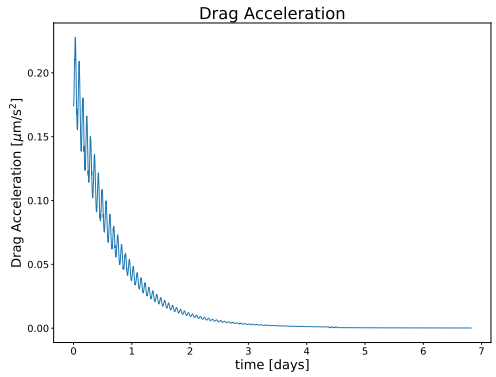

(a)

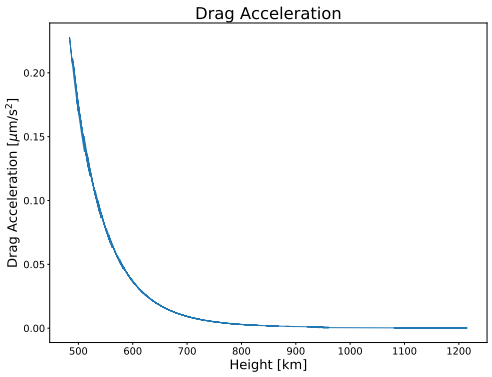

(b)

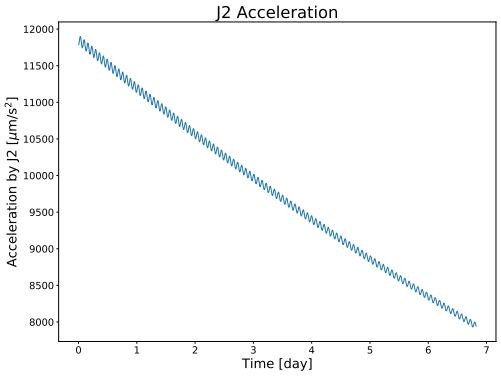

(c)

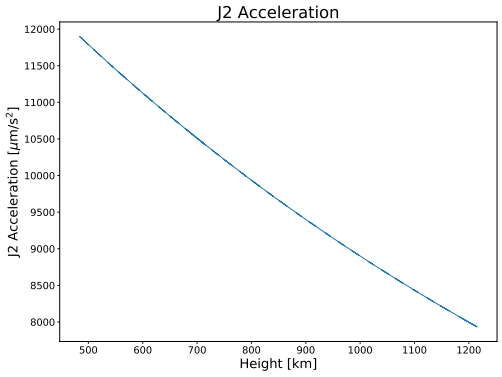

(d)

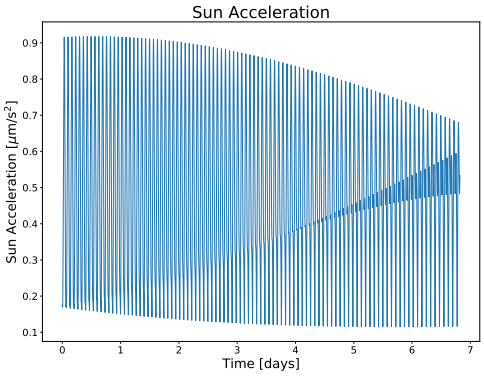

(e)

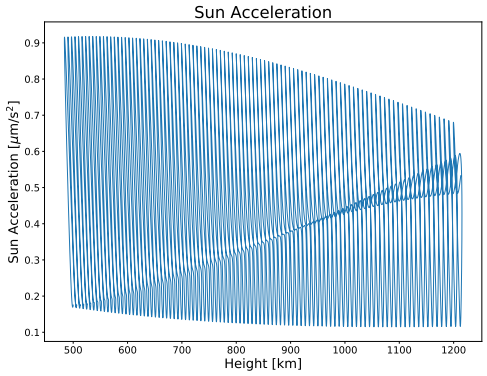

(f)

Figure 4.10: Perturbations between initial altitude $H_0 = 500$ km and final height $H = 1.2k$ km. The initial time and final time are $t_0 = 0$ and $t = 0.25$ T, respectively. At this range of heights the $J2$ factor acceleration dominates over the drag and Sun gravity accelerations. At approximately 1000 km of height the drag acceleration is zero.

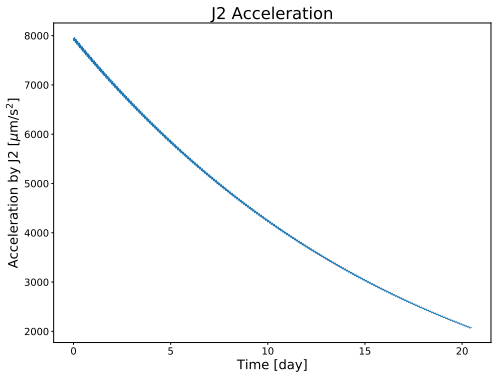

(a)

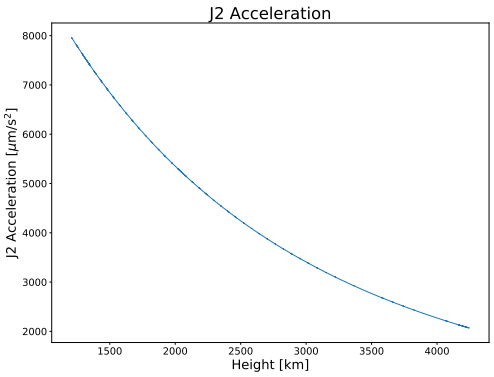

(b)

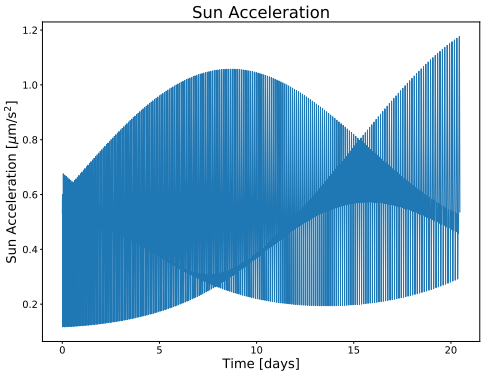

(c)

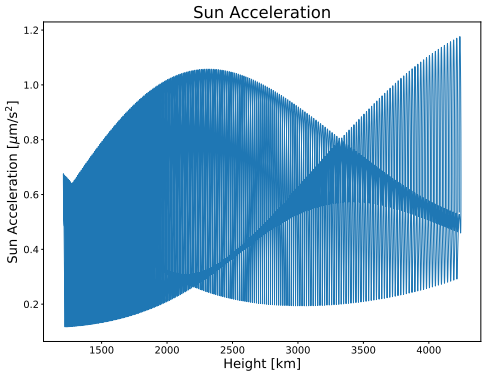

(d)

Figure 4.11: Perturbations between $H_0 = 1.2k$ km and $H = 4.2k$ km. The acceleration due to the J2 factor is still dominant over Sun gravity acceleration.

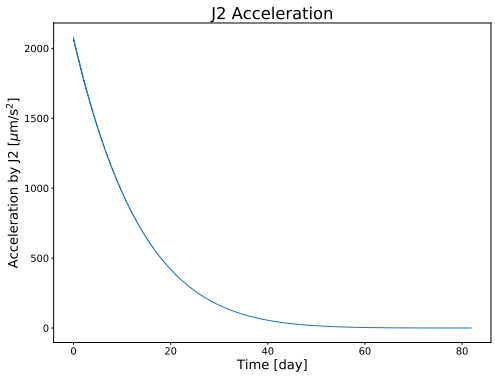

(a)

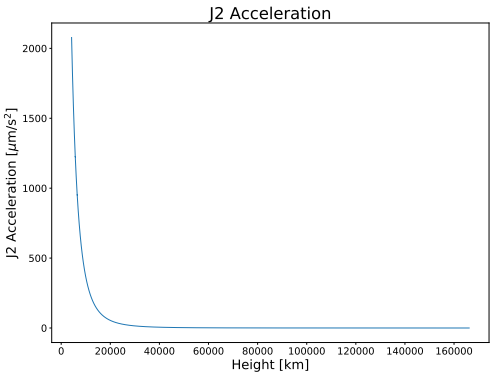

(b)

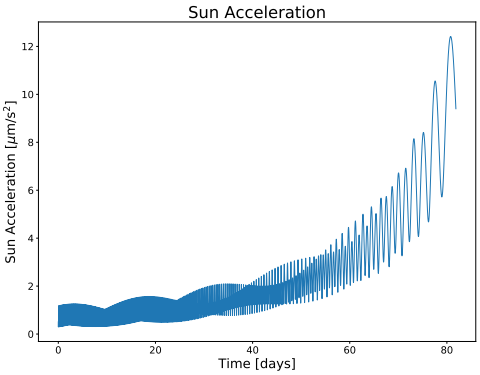

(c)

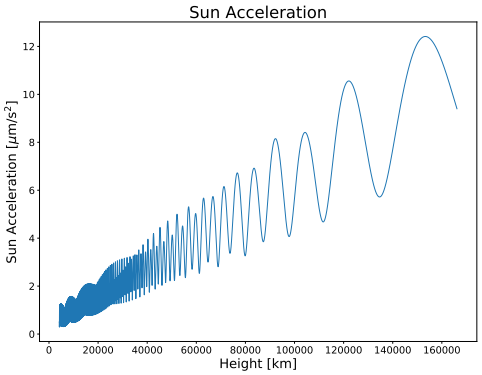

(d)

Figure 4.12: Perturbations between $H_0 = 4.2k$ km and $H = 166.2k$ km. The acceleration due to $J2$ factor drops to almost zero at heights over $100k$ km. The acceleration due to Sun Gravity is around 10 μm/s^2 at a height of $166k$ km.

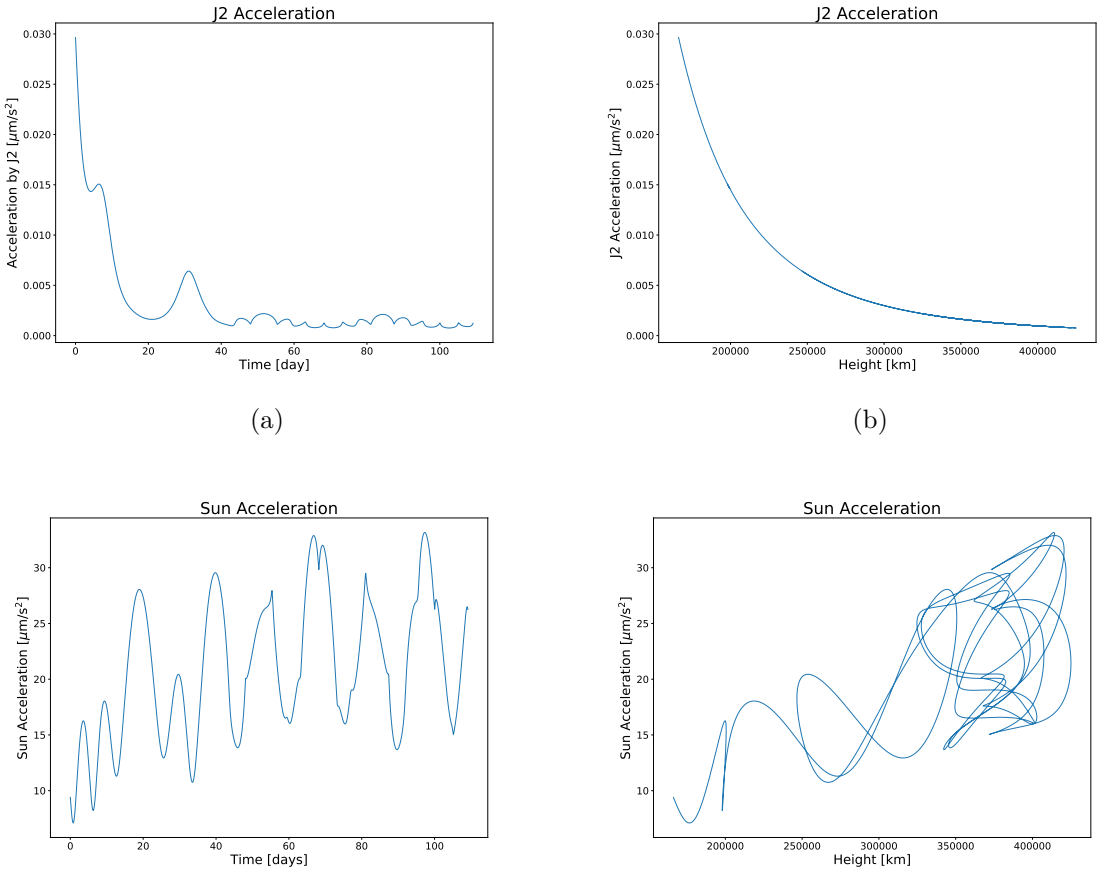

(a) (b)

(c) (d)

Figure 4.13: Perturbations between $H_0 = 166.2k$ km and $H = 423.7k$ km. The acceleration due to factor $J2$ is approximately zero. At this height the sun gravity acceleration dominates over the acceleration by $J2$.

4.3. Transfer Orbits

To find a transfer orbit, the Jacobi constant is helpful to determine a possible orbit so the satellite goes from a LEO orbit to a lunar orbit. Figure 4.14 shows the Hill's regions for different values of the Jacobi Constant C, which are forbidden zones for the satellite to be and in consequence to orbit through. For $C = 3.2$ can be defined 3 possibles zones for the satellite to orbit: around Earth, around the Moon and around the Earth-Moon system. If C decreases to $C = 3.188$, the Hill's zone "opens" around the point $L1$, and the zone around the Earth and around the Moon connects to each other. For $C = 3.173$ the Hill's region "opens" again, but this time around the point $L2$, so the inside zone connects to the outside zone. For $C = 3.013$ the Hill's region has a "C" shape and opens around point $L3$ as C decreases. For smaller C the Hill's region vanishes around points $L4$ and $L5$, as "island" of forbidden zones. For a LEO orbit $C \approx 55$.

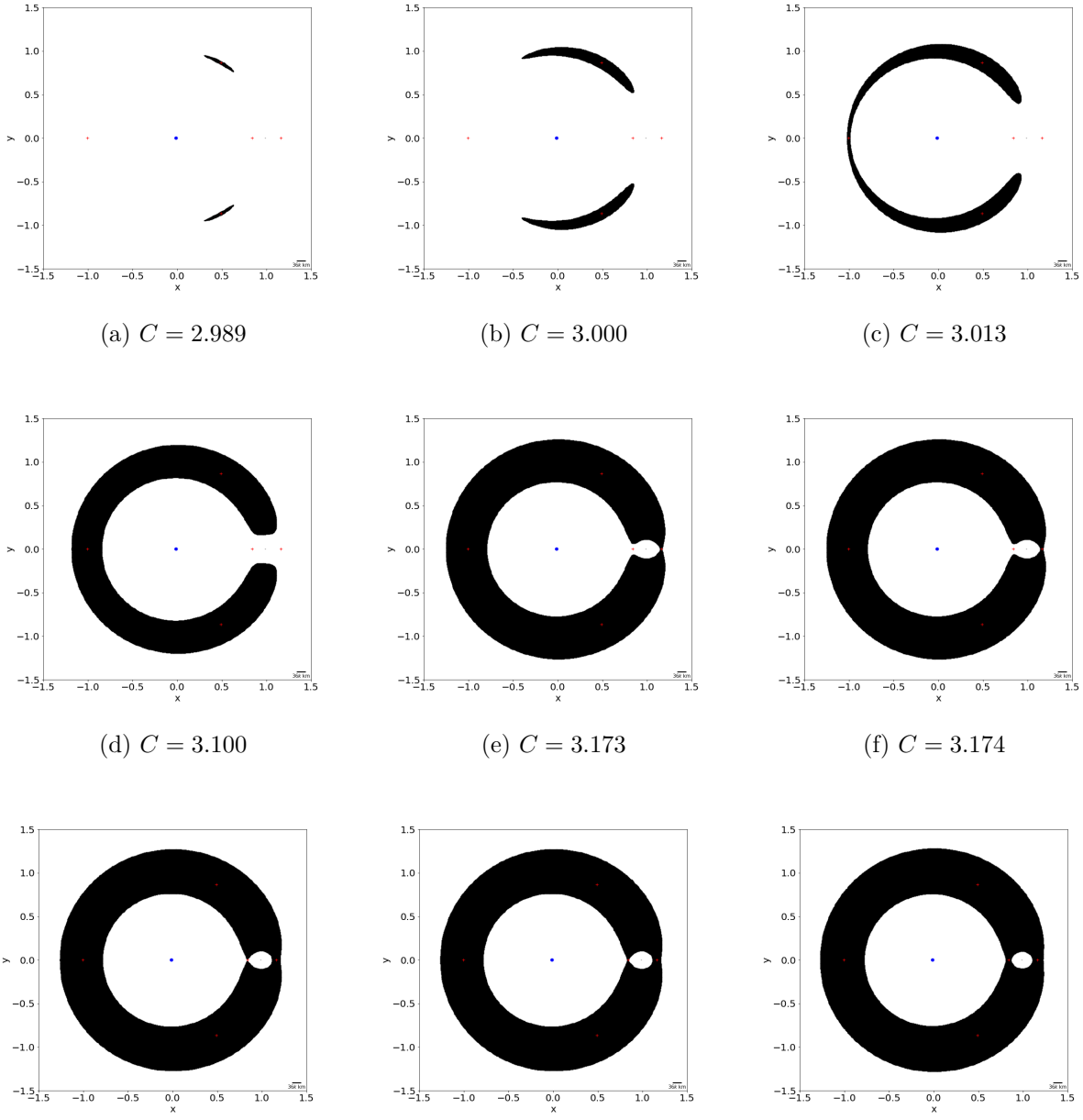

(a) $C = 2.989$ (b) $C = 3.000$ (c) $C = 3.013$

(d) $C = 3.100$ (e) $C = 3.173$ (f) $C = 3.174$

(g) $C = 3.188$ (h) $C = 3.189$ (i) $C = 3.200$

Figure 4.14: Hill's regions. The shaded area are forbidden zones for the satellite to be and consequently, forbidden zones to orbit through. As the value of the constant Jacobi C decreases, the forbidden zones start to vanish around Euler-Lagrange points. For a satellite in the Earth-Moon system in LEO orbit $C \approx 55$, and for $C < 2.989$ there are not forbidden zones.

In order to the satellite escapes from Earth and transit to the Moon, the value of the Jacobi constant C has to decrease and for this propulsion can be used. It can be choose a value of C small enough so the satellite can transit to the Moon from Earth, as $C < 3.2$ but high enough so the satellite transits to the Moon and not escapes by the $L3$ point, as $C > 3$. The value of $C = 3.015$ is low enough to let the satellite transit to the zone around the Moon and it is high enough to not let the it escape by the point $L3$. These conditions are not enough to ensure the satellite orbits the Moon. While the satellite approaches to the

Moon, once has escaped from Earth, the value of C has to increase so the Hill's zone "closes" when the satellite is near to the Moon. A value of $C = 3.189$ is high enough to close the Hill's zone so the satellite can be bounded to the Moon gravity. The propulsion will be defined by the frequency of shoots of the thruster f.

To gain some insight of the change of the orbit as the satellite ascends see Figure 4.15. These "ascending" orbits are obtained for a time lapse of $t = 4$ T. The orbit reaches a higher final altitude as the frequency of the thruster increases, as can be expected.

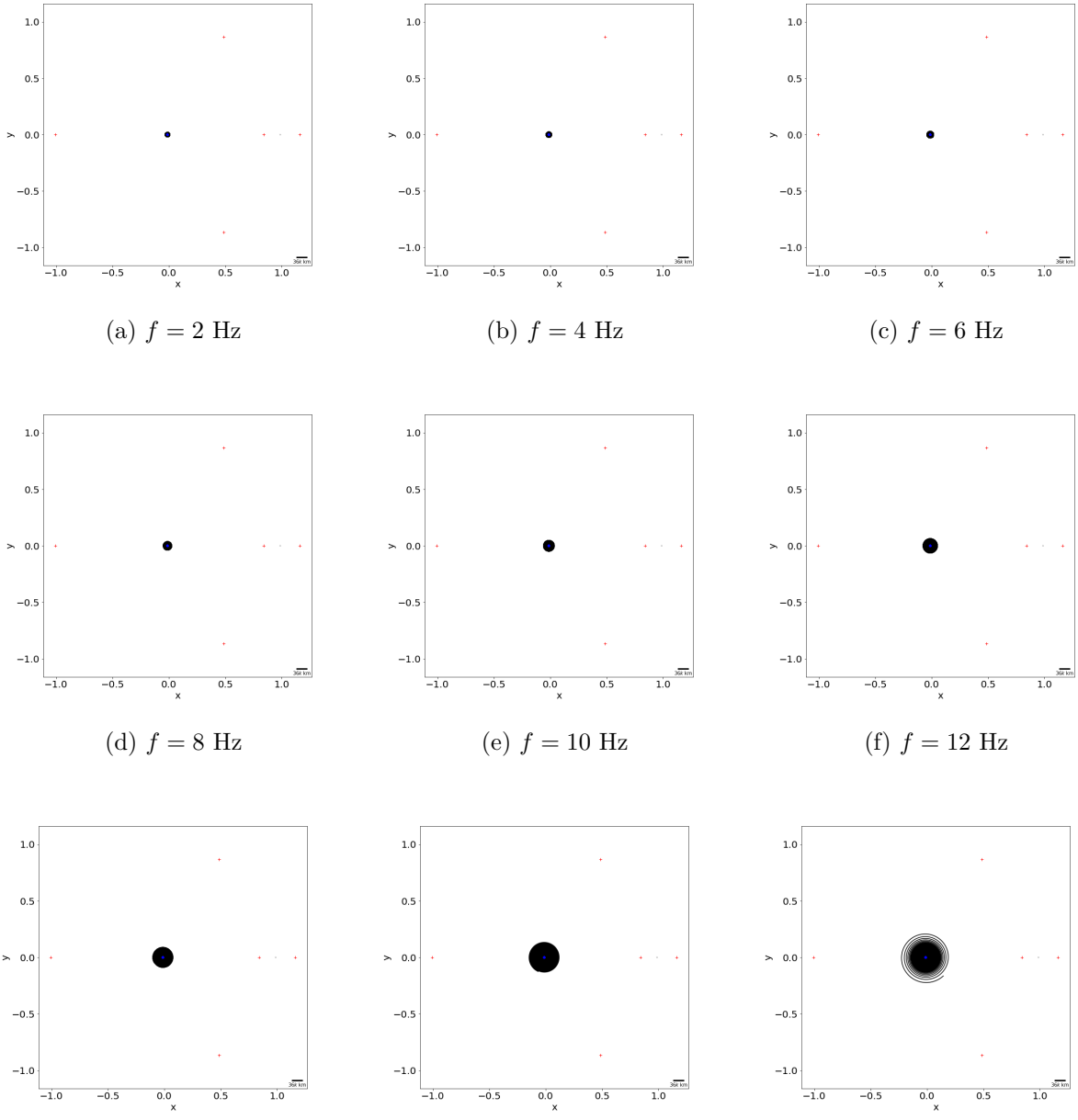

(a) $f = 2$ Hz (b) $f = 4$ Hz (c) $f = 6$ Hz

(d) $f = 8$ Hz (e) $f = 10$ Hz (f) $f = 12$ Hz

(g) $f = 14$ Hz (h) $f = 16$Hz (i) $f = 18$ Hz

Figure 4.15: Ascending orbits in rotating frame of reference for $t = 4$ T. As can be expected, the higher the operation frequency of the thruster, the higher the final altitude reached by the satellite.

Figure 4.16 shows the high reached in every case of figure 4.15. Also shows the total mass

propelled and the total energy used along the ascending orbit.

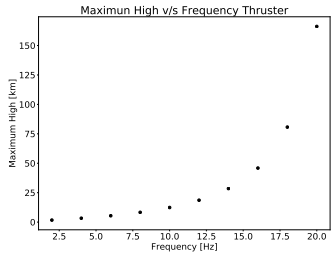

(a) Final altitude reached versus the frequency of the thruster.

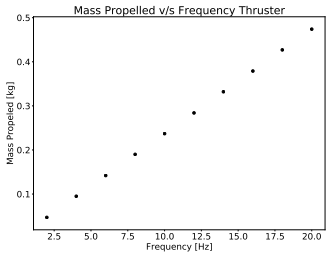

(b) Total mass propelled versus the frequency of the thruster.

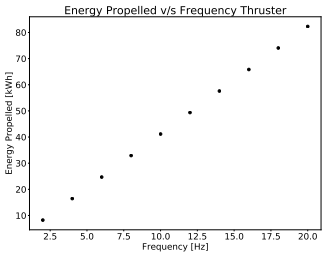

(c) Total energy used in propulsion versus the frequency of the thruster.

Figure 4.16: Final altitude reached for the satellite in orbits of figure 4.15

For the ascending part of the orbit it will be considered three cases for the operation frequency f of the thruster, f equal to 5, 10 and 20 Hz. Figure 4.17 shows these three cases. These three orbits reach approximately the same altitude of $160k$ km, but the times of flight are different, being 16, 8 and 4 periods of time T, for 5, 10 and 20 Hz of operation frequency of the thruster, respectively.

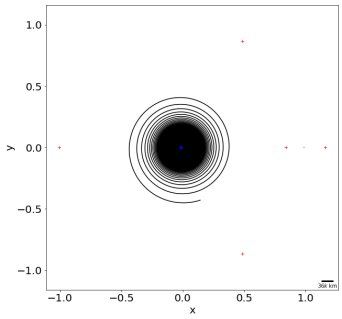

(a) Ascending orbit for $f = 5$ Hz and $t = 16$ T.

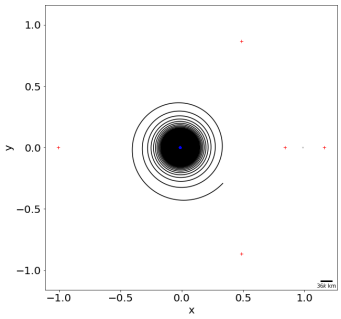

(b) Ascending orbit for $f = 10$ Hz and $t = 8$ T.

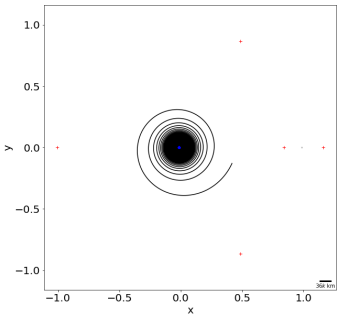

(c) Ascending orbit for $f = 20$ Hz and $t = 4$ T.

Figure 4.17: Ascending orbits for 5, 10 and 20 Hz of operation frequency of the thruster, each case takes 16, 8 and 4 periods of time T, respectively, to reach an altitude of $160k$ km approximately.

From these 3 cases of operation frequency, it is possible to obtain orbits to the Moon. An orbit from Earth to the Moon can be thought as a three stages process. First, the satellite ascends from a LEO orbit to a HEO orbit, using a frequency f_1 of thruster operation and a time t_1. Second, the satellite transits from a HEO orbit through a path where goes to the Moon and reaches a lunar orbit. This can be done using a frequency f_2 of thruster operation along a time t_2. Finally, the satellite needs to be decelerated to orbit the Moon, using a frequency f_S of thruster operation. This last frequency f_S usually needs to be the highest of the operation frequencies of the thruster to obtain a lunar orbit. The frequency f_2 will be chosen such that is less, equal or slightly higher than the frequency f_1.

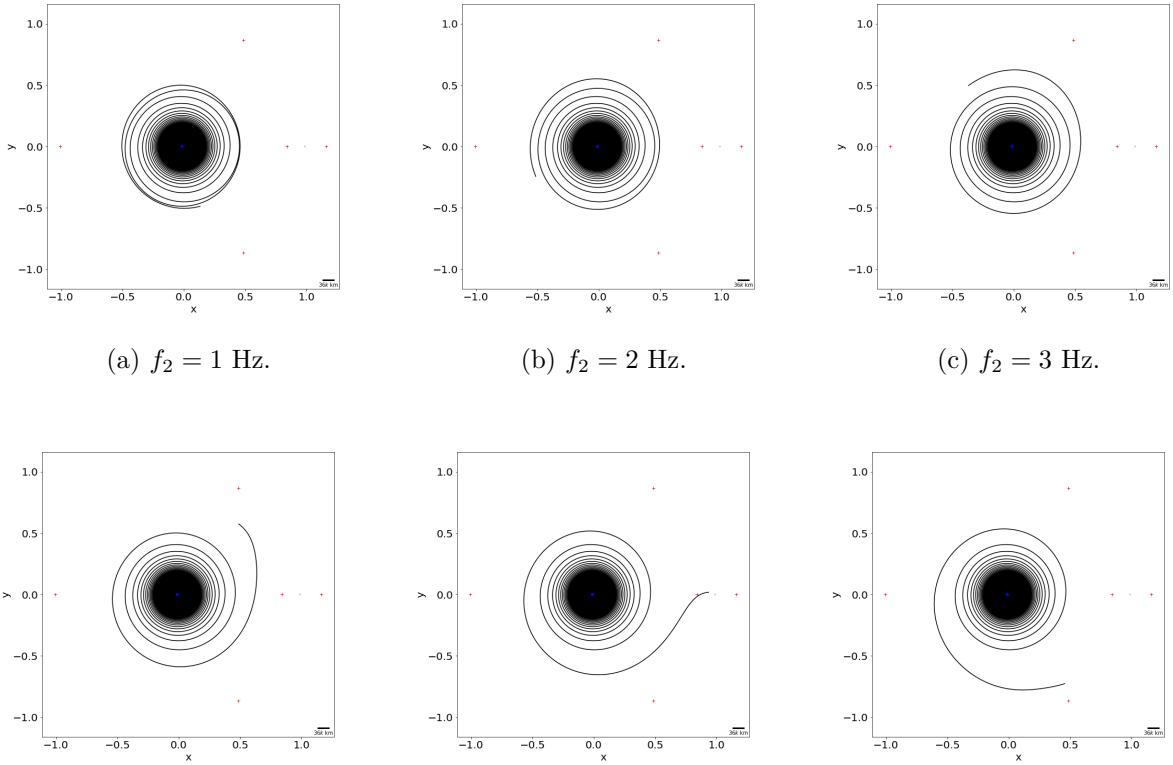

(a) $f_2 = 1$ Hz. (b) $f_2 = 2$ Hz. (c) $f_2 = 3$ Hz.

(d) $f_2 = 4$ Hz. (e) $f_2 = 5$ Hz. (f) $f_2 = 6$ Hz.

Figure 4.18: Transfer orbits sweeping on f_2 for $f_1 = 5$ Hz and $t_1 = 16$ T. Frequency f_2 is swept from 1 to 6 Hz. Frequency $f_2 = 6$ Hz seems a suitable choice for a transfer orbit to the Moon in this range of values for f_2.

For the case of $f_1 = 5$ Hz and $t_1 = 16$ T, figure 4.18 shows transfer orbits sweeping on f_2, from 1 to 6 Hz with $t_2 = 1$ T. It can be seen that for frequencies 1, 2, 3 and 4 Hz the final point of the orbit does not come close to the Moon. By the other hand, frequencies $f_2 = 5$ Hz and $f_2 = 6$ Hz could be appropriate choices to try a transfer orbit to the Moon, because the final point of the orbit come close to the Moon for $f = 5$, and the for the case of $f = 6$ Hz at the final point of the orbit, the satellite seems to go to the Moon.

Figure 4.19 shows transfer orbits for the case $f_1 = 5$ Hz, $t_1 = 16$ T, $f_2 = 6$ Hz, $t_2 = 4$ T, with f_S 20 and 25 Hz. At the left, the images from the rotating frame. At the center, zoom in centered at the Moon, it can be seen as the satellite orbits around the Moon. At the right, the whole orbit of the satellite in the non rotating frame of reference (NRF).

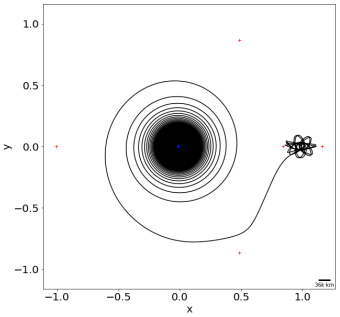

(a) $f_S = 20$ Hz.

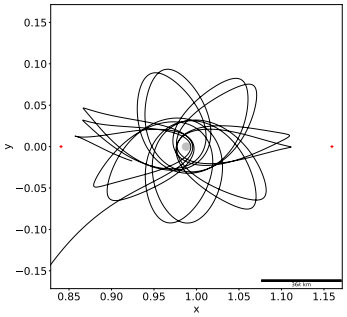

(b) Zoom in centered at the Moon for $f_S = 20$ Hz.

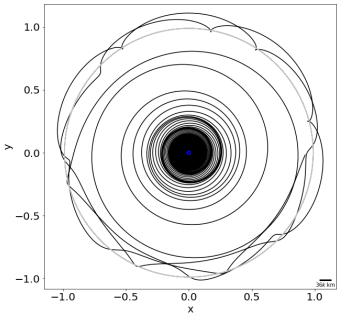

(c) Non rotating frame for $f_S = 20$ Hz.

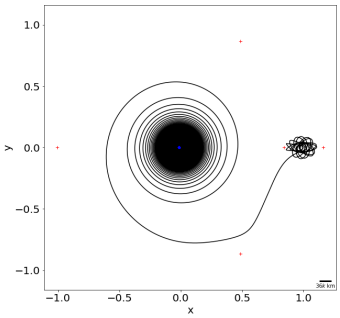

(d) $f_S = 25$ Hz.

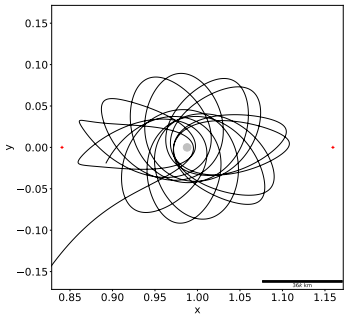

(e) Zoom in centered at the Moon for $f_S = 25$ Hz.

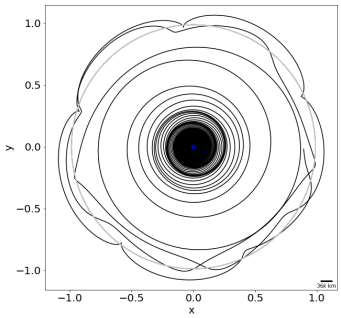

(f) Non rotating frame for $f_S = 25$ Hz.

Figure 4.19: Transfer orbits for $f_1 = 5$ Hz, $t_1 = 16$ T, $f_2 = 6$ Hz, $t_2 = 4$ T, with $f_S = 20$ Hz and $f_S = 25$ Hz.

This approach can be repeated for the case of $f_1 = 10$ Hz and $t_1 = 8$ T. Figure 4.20 shows transfer orbits sweeping on f_2, from 2 to 10 Hz. This suggest that $f_2 = 5$ Hz and over could be appropriate frequencies to try a transfer orbit to the Moon.

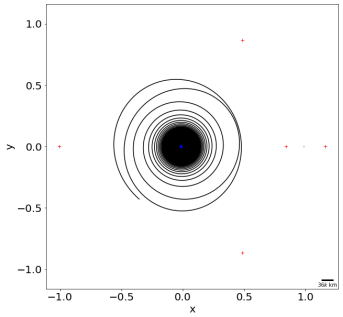

(a) $f_2 = 2$ Hz.

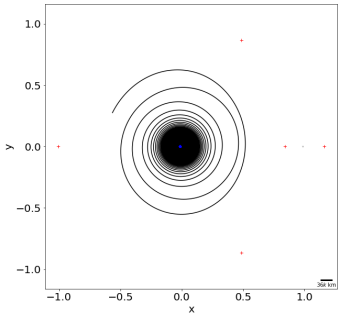

(b) $f_2 = 3$ Hz.

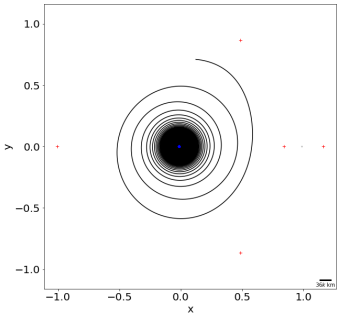

(c) $f_2 = 4$ Hz.

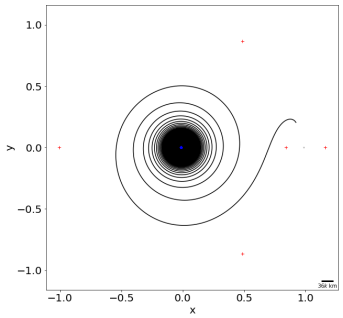

(d) $f_2 = 5$ Hz.

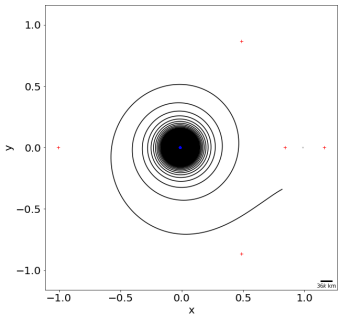

(e) $f_2 = 6$ Hz.

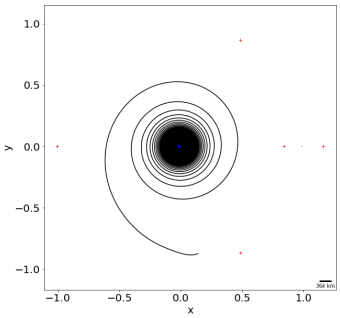

(f) $f_2 = 7$ Hz.

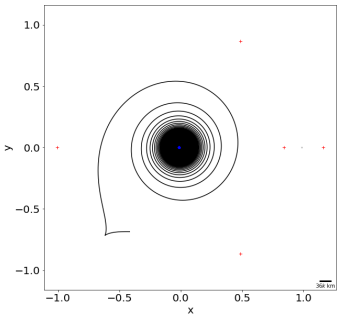

(g) $f_2 = 8$ Hz.

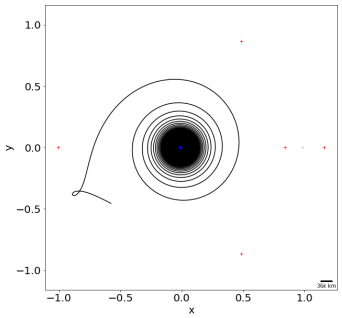

(h) $f_2 = 9$ Hz.

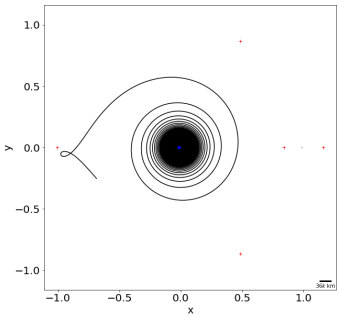

(i) $f_2 = 10$ Hz.

Figure 4.20: Transfer orbits sweeping on f_2 for $f_1 = 10$ Hz and $t_1 = 8$ T. Frequency f_2 is swept from 2 to 10 Hz. Frequency $f_2 = 5$ Hz and over seems suitable choices for a transfer orbit to the Moon in this range of values for f_2.

Figure 4.21 shows transfer orbits for $f_1 = 10$ Hz, $t_1 = 8$ T, $f_2 = 6$ Hz, $t_2 = 4$ T, with $f_S = 11$ Hz, $f_S = 12$ Hz and $f_S = 13$ Hz.

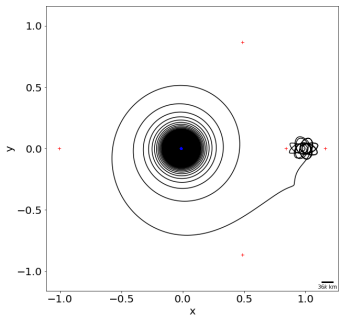

(a) $f_S = 11$ Hz.

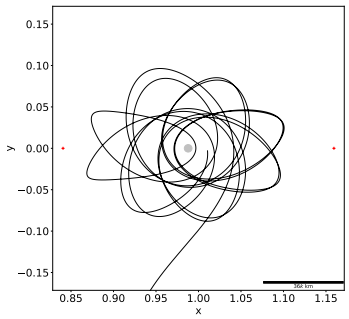

(b) Zoom in centered at the Moon for $f_S = 11$ Hz.

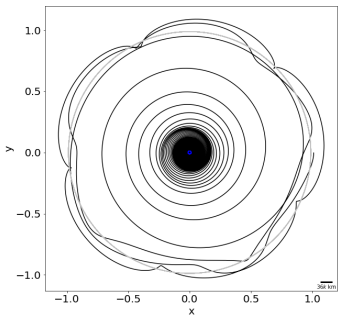

(c) Non rotating frame for $f_S = 11$ Hz.

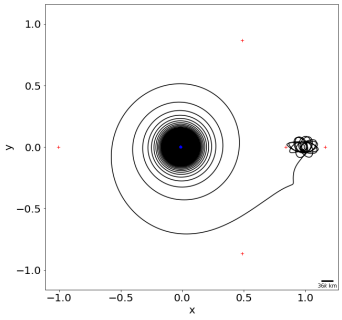

(d) $f_S = 12$ Hz.

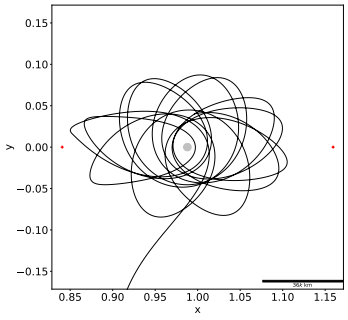

(e) Zoom in centered at the Moon for $f_S = 12$ Hz.

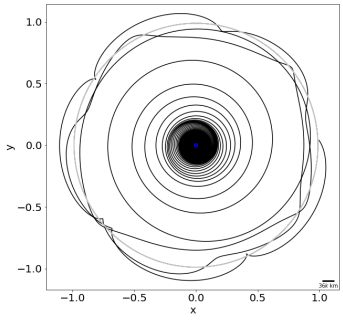

(f) Non rotating frame for $f_S = 12$ Hz.

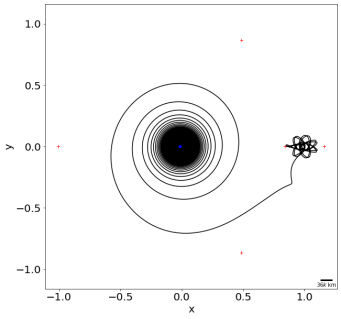

(g) $f_S = 13$ Hz.

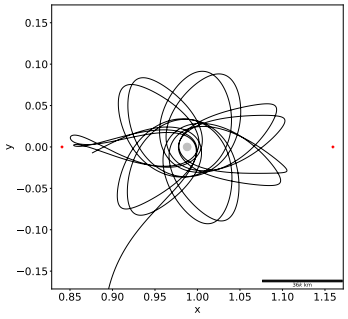

(h) Zoom in centered at the Moon for $f_S = 13$ Hz.

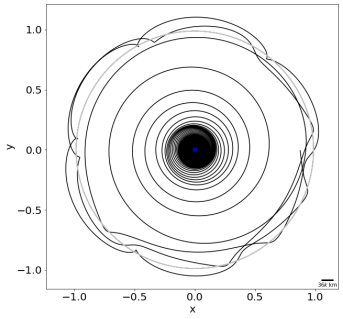

(i) Non rotating frame for $f_S = 13$ Hz.

Figure 4.21: Transfer orbits for $f_1 = 10$ Hz, $t_1 = 8$ T, $f_2 = 6$ Hz, $t_2 = 4$ T, with $f_S = 11$ Hz, $f_S = 12$ Hz and $f_S = 13$ Hz.

Figure 4.22 shows transfer orbits for $f_1 = 10$ Hz $t_1 = 8$ T, $f_2 = 7$ Hz, $t_2 = 4$ T and $f_S = 20$ Hz and $f_S = 25$ Hz.

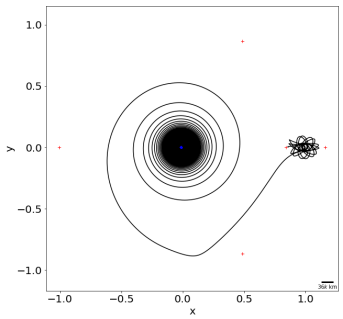

(a) $f_S = 20$ Hz.

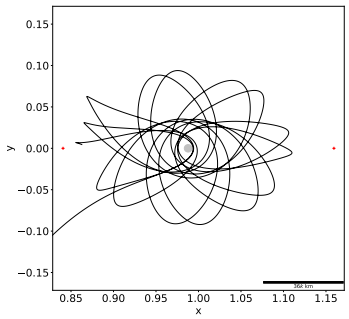

(b) Zoom in centered at the Moon for $f_S = 20$ Hz.

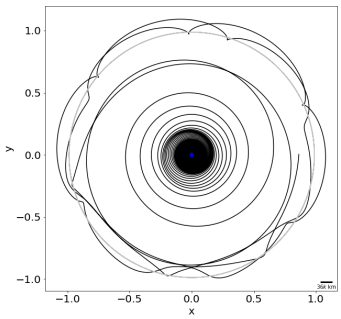

(c) Non rotating frame for $f_S = 20$ Hz.

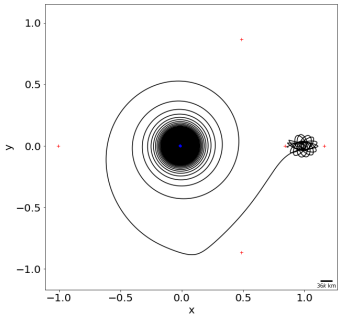

(d) $f_S = 25$ Hz.

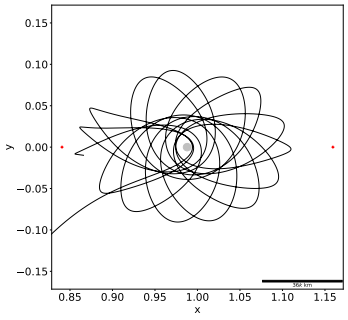

(e) Zoom in centered at the Moon for $f_S = 25$ Hz.

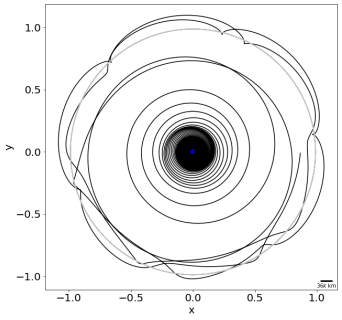

(f) Non rotating frame for $f_S = 25$ Hz.

Figure 4.22: Transfer orbits for $f_1 = 10$ Hz, $t_1 = 8$ T, $f_2 = 7$ Hz, $t_2 = 4$ T, with $f_S = 20$ Hz and $f_S = 25$ Hz.

Figure 4.23 shows transfer orbits for $f_1 = 20$ and $t_1 = 4$ T, sweeping on f_2, from 4 to 15 Hz. This suggest that $f_2 = 6$ Hz and over, until $f \approx 10$ Hz could be appropriate frequencies to try an orbit to the Moon.

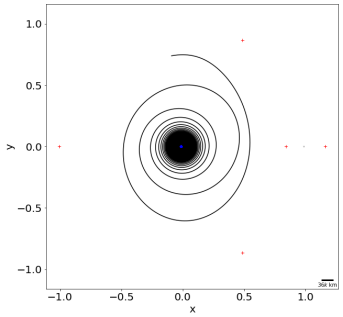

(a) $f_2 = 4$ Hz.

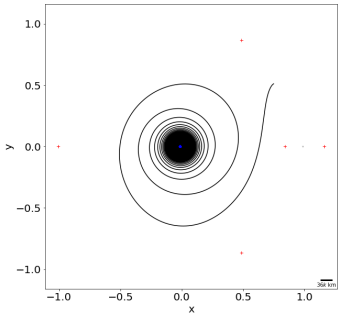

(b) $f_2 = 5$ Hz.

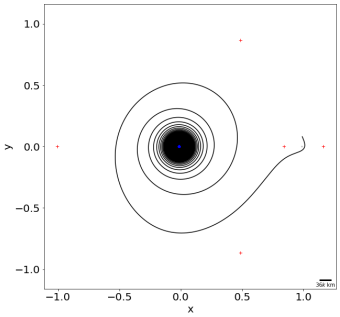

(c) $f_2 = 6$ Hz.

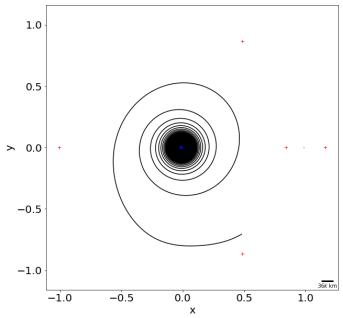

(d) $f_2 = 7$ Hz.

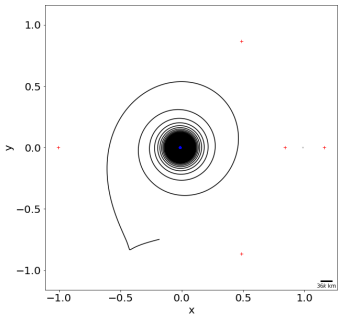

(e) $f_2 = 8$ Hz.

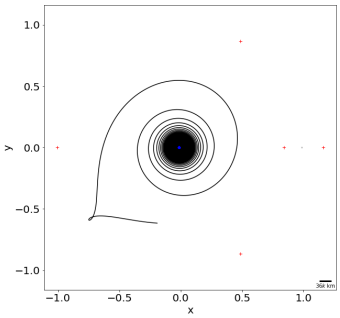

(f) $f_2 = 9$ Hz.

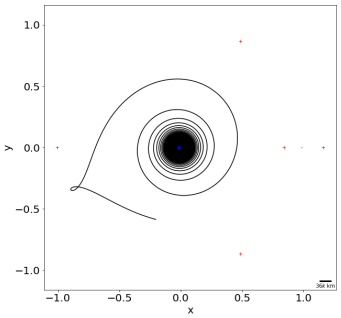

(g) $f_2 = 10$ Hz.

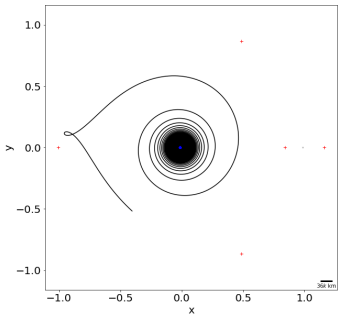

(h) $f_2 = 12$ Hz.

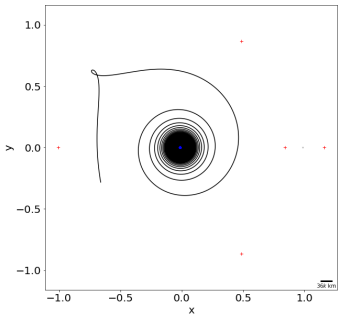

(i) $f_2 = 15$ Hz.

Figure 4.23: Transfer orbits sweeping on f_2 for $f_1 = 20$ Hz and $t_1 = 4$ T. Frequency f_2 is swept from 4 to 15 Hz. Frequency $f_2 = 6$ Hz seems a suitable choice for a transfer orbit to the Moon in this range of values for f_2.

Figure 4.24 shows transfer orbits for $f_1 = 20$ Hz, $t_1 = 4$ T, $f_2 = 6$ Hz, $t_2 = 4$ T and $f_S = 15$ Hz and $f_S = 25$ Hz.

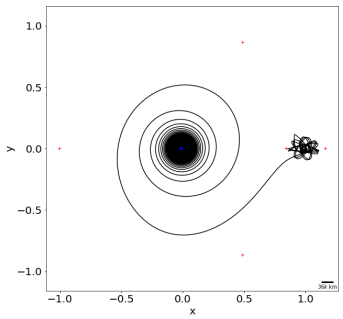

(a) $f_S = 15$ Hz.

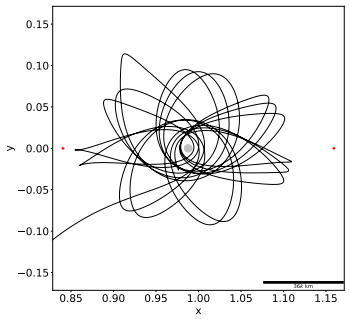

(b) Zoom in centered at the Moon for $f_S = 15$ Hz.

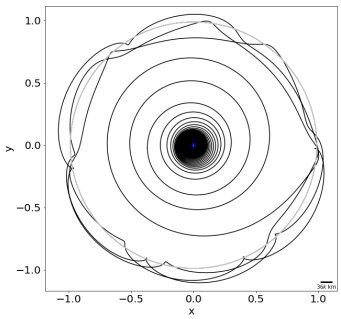

(c) Non rotating frame for $f_S = 15$ Hz.

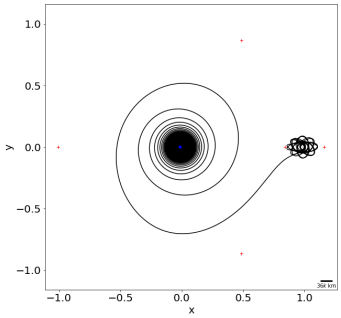

(d) $f_S = 25$ Hz.

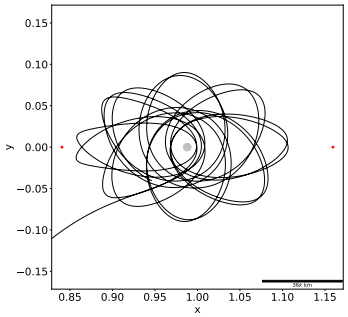

(e) Zoom in centered at the Moon for $f_S = 25$ Hz.

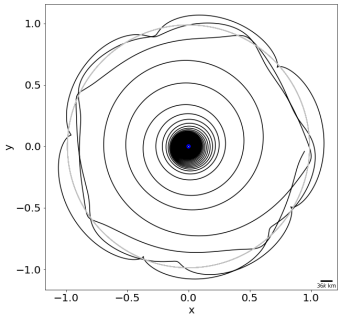

(f) Non rotating frame for $f_S = 25$ Hz.

Figure 4.24: Transfer orbits for $f_1 = 20$ Hz, $t_1 = 4$ T, $f_2 = 6$ Hz, $t_2 = 4$ T and $f_S = 15$ Hz and $f_S = 25$ Hz.

Figure 4.25 shows transfer orbits for $f_1 = 20$ Hz, $t_1 = 4$ T, $f_2 = 7$ Hz, $t_2 = 4$ T and $f_S = 20$ Hz and $f_S = 25$ Hz.

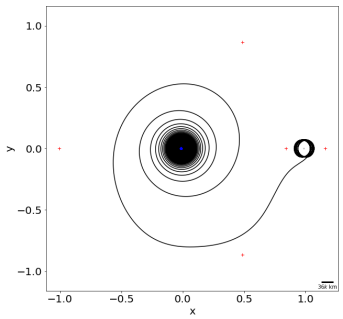

(a) $f_S = 20$ Hz.

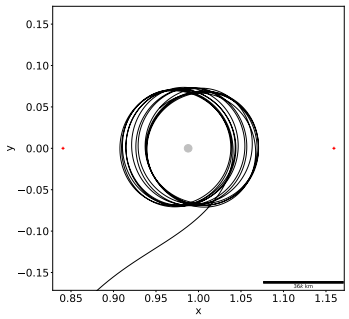

(b) Zoom in centered at the Moon for $f_S = 20$ Hz.

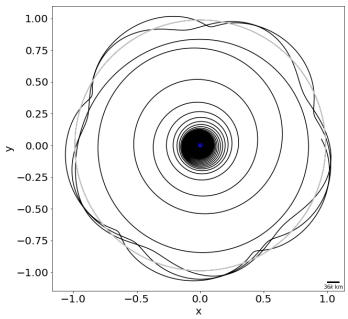

(c) Non rotating frame for $f_S = 20$ Hz.

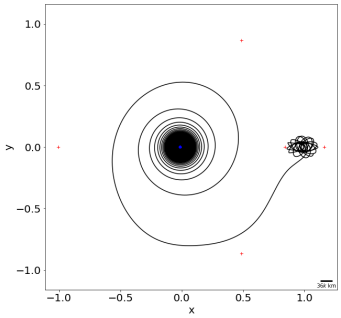

(d) $f_S = 25$ Hz.

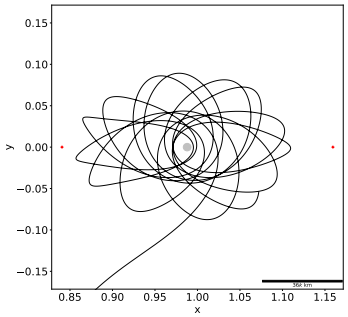

(e) Zoom in centered at the Moon for $f_S = 25$ Hz.

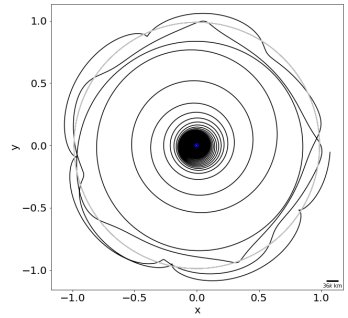

(f) Non rotating frame for $f_S = 25$ Hz.

Figure 4.25: Transfer orbits for $f_1 = 20$ Hz, $t_1 = 4$ T, $f_2 = 7$ Hz, $t_2 = 4$ T and $f_S = 20$ Hz and $f_S = 25$ Hz.

Figure 4.26 shows transfer orbits for $f_1 = 20$ Hz, $t_1 = 4$ T, $f_2 = 8$ Hz, $t_2 = 4$ T and $f_S = 20$ Hz and $f_S = 25$ Hz.

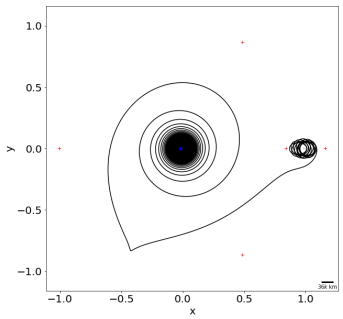

(a) $f_S = 20$ Hz.

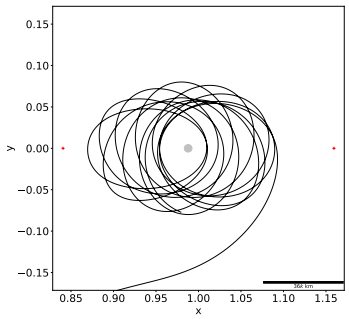

(b) Zoom in centered at the Moon for $f_S = 20$ Hz.

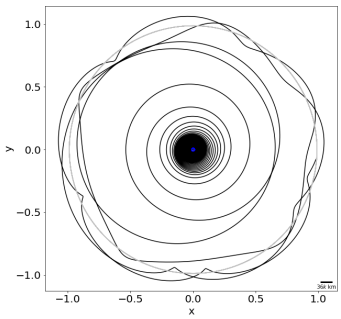

(c) Non rotating frame for $f_S = 20$ Hz.

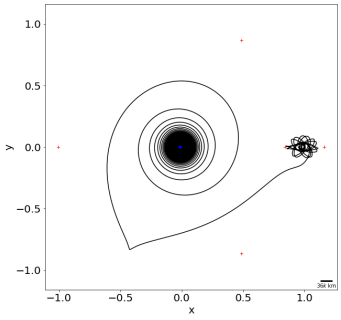

(d) $f_S = 25$ Hz.

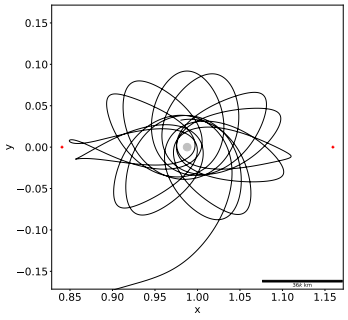

(e) Zoom in centered at the Moon for $f_S = 25$ Hz.

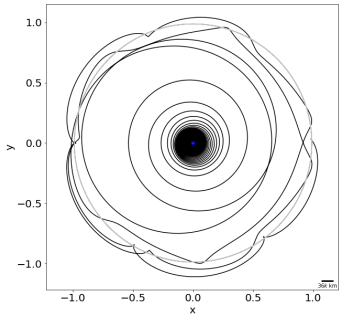

(f) Non rotating frame for $f_S = 25$ Hz.

Figure 4.26: Transfer orbits for $f_1 = 20$ Hz, $t_1 = 4$ T, $f_2 = 8$ Hz, $t_2 = 4$ T and $f_S = 20$ Hz and $f_S = 25$ Hz.

Table 4.1 displays the values for transfer orbits presented in section 4.3. The mean value of the propeller mass is $\overline{m}_p = 0.516$ kg and the mean total energy used for the whole orbit is $\overline{E}_p = 59.155$ kWh $= 212.959$ MJ. Two results are highlighted at table 4.1. These two orbits seems to display a more regular behaviour than the rest of the orbits, this regularity could be useful to find the satellite in the sky from the Moon.

Table 4.1: Values of the propeller, time and energy used for every transfer orbit from LEO to lunar.

f_1[Hz]	t_1[T]	f_2[Hz]	t_2[T]	f_S[Hz]	$H_{l\min}$[km]	m_p[kg]	E_p[kWh]	E_p[MJ]
5	16	6	4	20	359	0.512	58.620	211.030
5	16	6	4	25	1075	0.508	57.750	207.900
10	8	6	4	11	1752	0.523	60.667	218.401
10	8	6	4	12	1897	0.531	60.803	218.891
10	8	6	4	13	1950	0.527	60.419	217.508
20	4	6	4	15	790	0.512	58.672	211.219
20	4	6	4	25	2475	0.506	57.962	208.663
20	**4**	**7**	**4**	**20**	**16915**	**0.513**	**58.774**	**211.586**
20	4	7	4	25	1092	0.512	58.707	211.345
20	**4**	**8**	**4**	**20**	**6667**	**0.518**	**59.337**	**213.613**
20	4	8	4	25	1720	0.515	58.996	212.356

4.4. Stationary Orbits

Some orbits shows a stationary behaviour, i.e. the satellite orbits around the center of mass in a circular orbit with an angular velocity equal to n, then the satellite appears fixed in the rotating frame. This is consequence of the forces on the satellite are equal to zero. The propulsion and the gravity forces cancel out to each other. This stationary orbit will remain as long as the thruster is operating.

Figure 4.27 shows transfer orbits for $f_1 = 5$ Hz, $t_1 = 16$ T, $f_2 = 7$ Hz, $t_2 = 2$ T, with $f_S = 15$ Hz and $f_S = 25$ Hz. When the satellite reaches an altitude of $350k$ km, it stays at that point.

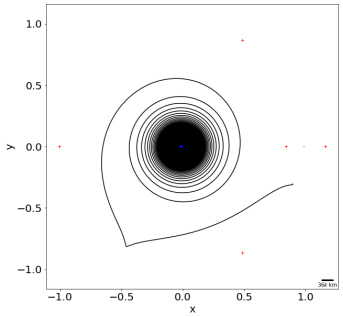

(a) Stationary orbit for $f_S = 15$ Hz.

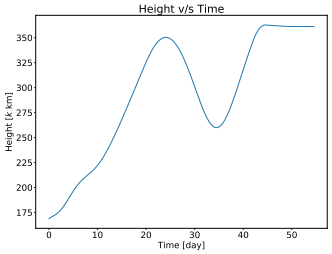

(b) Height reached for $f_S = 15$ Hz.

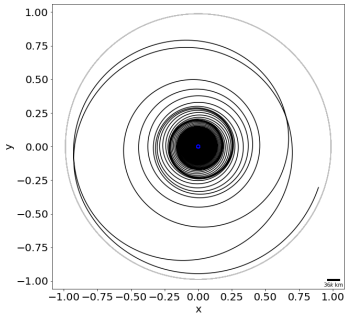

(c) Non rotating frame for $f_S = 15$ Hz.

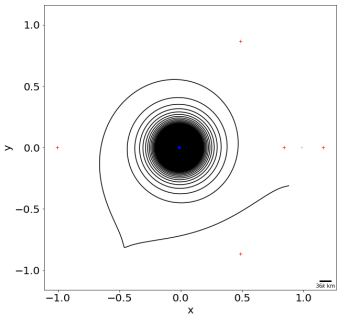

(d) Stationary orbit for $f_S = 25$ Hz.

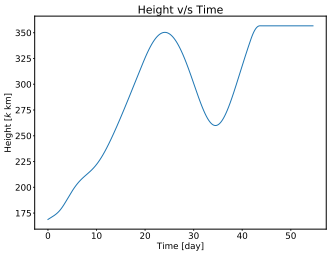

(e) Height reached for $f_S = 25$ Hz.

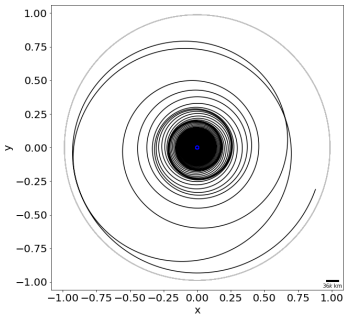

(f) Non rotating frame for $f_S = 25$ Hz.

Figure 4.27: Stationary orbits for $f_1 = 5$ Hz, $t_1 = 16$ T, $f_2 = 7$ Hz, $t_2 = 2$ T, with $f_S = 15$ Hz and $f_S = 25$ Hz.

In the non rotating frame (inertial frame), as can be expected, the orbit is circular at its final part with angular velocity equal to n, so the satellite appears stationary in the rotating frame (non inertial frame) as the Earth and the Moon do. The next results present the same behaviour.

Figure 4.28 shows transfer orbits for $f_1 = 10$ Hz, $t_1 = 8$ T. With $f_2 = 6$ Hz, $t_2 = 2$ T and $f_S = 20$ Hz and $f_S = 25$ Hz. When the satellite reaches an altitude of $350k$ km, it stays at that point.

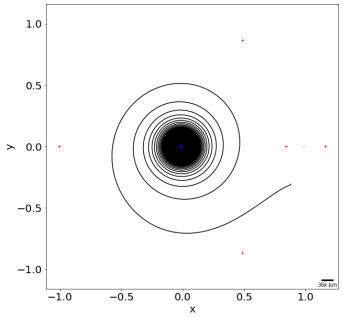

(a) Stationary orbit for $f_S = 20$ Hz.

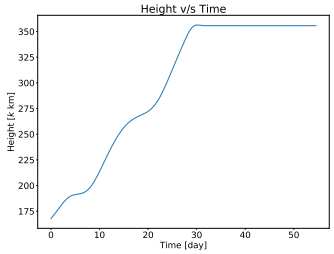

(b) Height reached for $f_S = 20$ Hz.

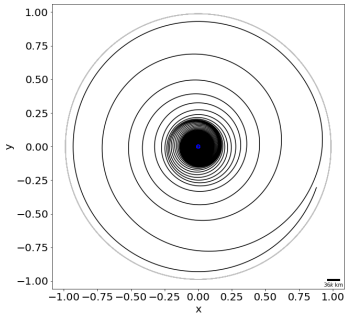

(c) Non rotating frame for $f_S = 20$ Hz.

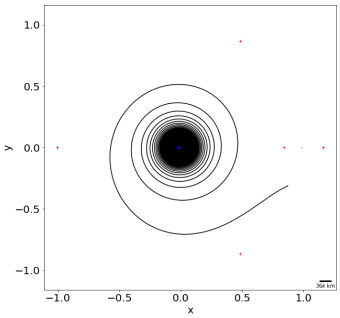

(d) Stationary orbit for $f_S = 25$ Hz.

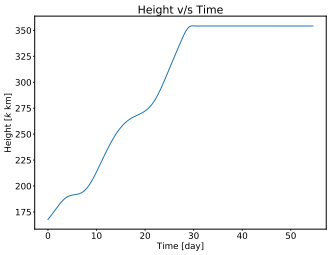

(e) Height reached for $f_S = 25$ Hz.

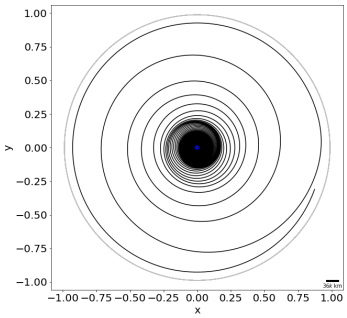

(f) Non rotating frame for $f_S = 25$ Hz.

Figure 4.28: Stationary orbits for $f_1 = 10$ Hz, $t_1 = 8$ T. In the second part $f_2 = 6$ Hz, $t_2 = 2$ T, with $f_S = 20$ Hz and $f_S = 25$ Hz.

Figure 4.29 shows transfer orbits for $f_1 = 20$ Hz and $t_1 = 4$ T. First result $f_2 = 8$ Hz, $t_2 = 2$ T and $f_S = 18$ Hz; in this case the altitude reached is around $450k$ km. Second result $f_2 = 9$ Hz, $t_2 = 2$ T and $f_S = 25$ Hz, reaching an altitude of $350k$ km and staying at that point.

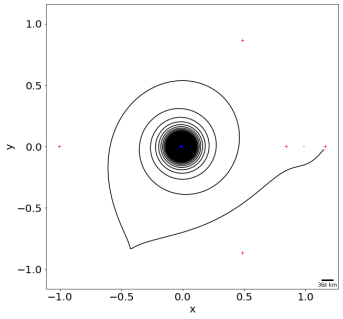

(a) Stationary orbit for $f_S = 18$ Hz.

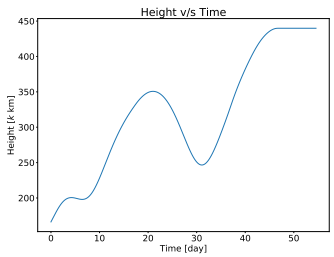

(b) Height reached for $f_S = 18$ Hz.

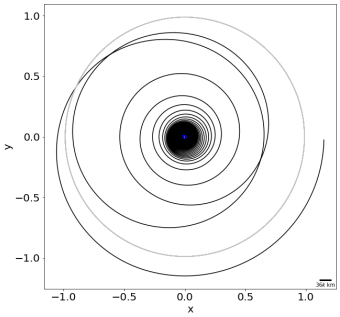

(c) Non rotating frame for $f_S = 18$ Hz.

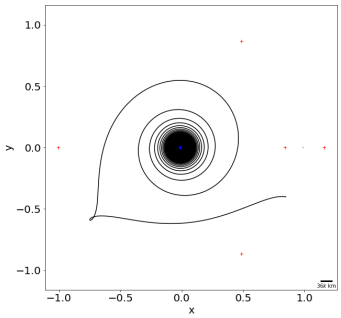

(d) Stationary orbit for $f_S = 25$ Hz.

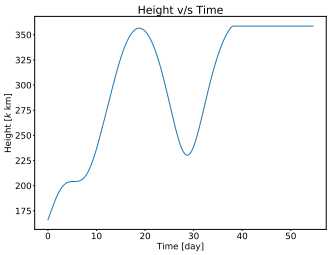

(e) Height reached for $f_S = 25$ Hz.

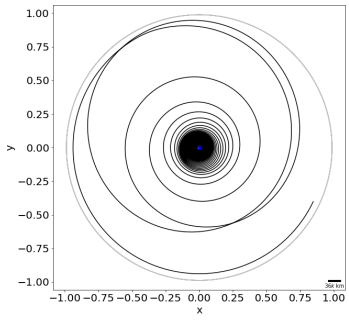

(f) Non rotating frame for $f_S = 25$ Hz.

Figure 4.29: Stationary orbits for $f_1 = 20$ Hz and $t_1 = 4$ T. In the first result $f_2 = 8$ Hz, $t_2 = 2$ T and $f_S = 18$ Hz, reaching an altitude of approximately $450k$ km. In the second result $f_2 = 9$ Hz, $t_2 = 2$ T and $f_S = 25$ Hz, reaching an altitude of approximately $350k$ km. In both cases, the satellite stays at the final point it reaches.

Figure 4.30 shows transfer orbits for $f_1 = 20$ Hz, $t_1 = 4$ T. With $f_2 = 20$ Hz, $t_2 = 4$ T, $f_S = 20$ Hz and $f_S = 25$ Hz. When the satellite reaches an altitude of $350k$ km, it stays at that point.

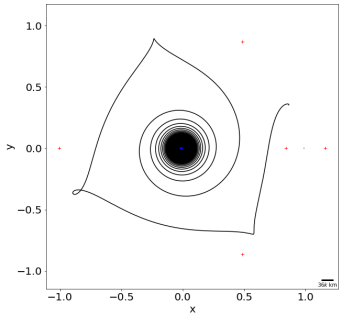

(a) Stationary orbit for $f_S = 20$ Hz.

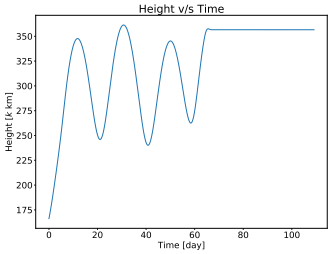

(b) Height reached for $f_S = 20$ Hz.

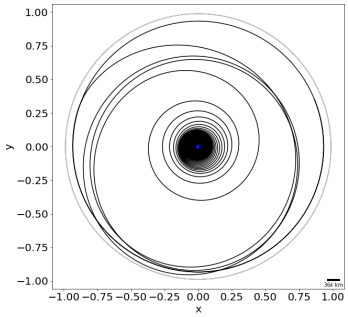

(c) Non rotating frame for $f_S = 20$ Hz.

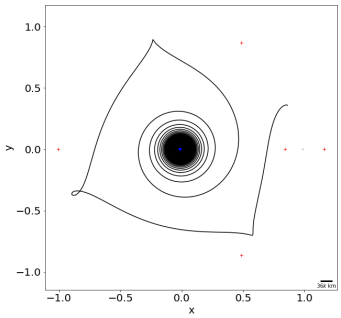

(d) Stationary orbit for $f_S = 25$ Hz.

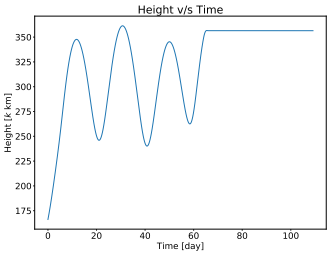

(e) Height reached for $f_S = 25$ Hz.

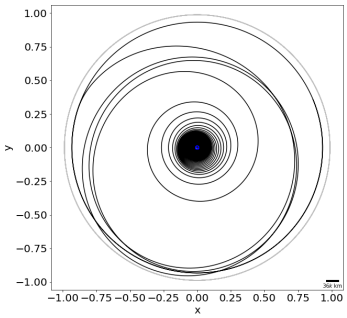

(f) Non rotating frame for $f_S = 25$ Hz.

Figure 4.30: Stationary orbits for $f_1 = 20$ Hz, $t_1 = 4$ T, $f_2 = 20$ Hz, $t_2 = 4$ T, with $f_S = 20$ Hz and $f_S = 25$ Hz. When the satellite reaches an altitude of $350k$ km, it stays at that point.

Table 4.2 displays the values for stationary orbits presented in section 4.4. Two results are highlighted in table 4.2. One has almost $50k$ km of distance to the Moon surface, which is the shortest distance among the stationary orbits here presented; this result could be useful to make surface Moon observation. The other result has a distance of around $160k$ km, which is the highest among the stationary orbits presented here; this orbit could have the potential to make observations to outside the Earth-Moon System.

Table 4.2: Values of the propeller, time and energy used for every stationary orbit.

f_1[Hz]	t_1[T]	f_2[Hz]	t_2[T]	f_S[Hz]	$H_{l\min}$[km]	m_p[kg]	E_p[kWh]	E_p[MJ]
5	16	7	2	15	125055	0.524	60.035	216.126
5	16	7	2	25	125011	0.524	60.035	216.126
10	8	6	4	20	122767	0.538	69.817	251.341
10	8	6	4	25	125533	0.538	69.817	251.341
20	**4**	**8**	**2**	**18**	**49809**	**0.535**	**61.273**	**220.583**
20	**4**	**9**	**2**	**25**	**161679**	**0.535**	**61.346**	**220.846**
20	4	20	4	20	108391	0.696	79.727	287.017
20	4	20	4	25	108391	0.696	79.727	287.017

4.5. Landing Orbits

This method can produce orbits that reach the surface of Moon. These orbits could become useful if they are considered as possible paths to land a satellite on the Moon.

Figure 4.31 shows a landing orbit for $f_1 = 5$ Hz, $t_1 = 16$ T, $f_2 = 5$ Hz, $t_2 = 1.013$ T, with $f_S = 25$ Hz.

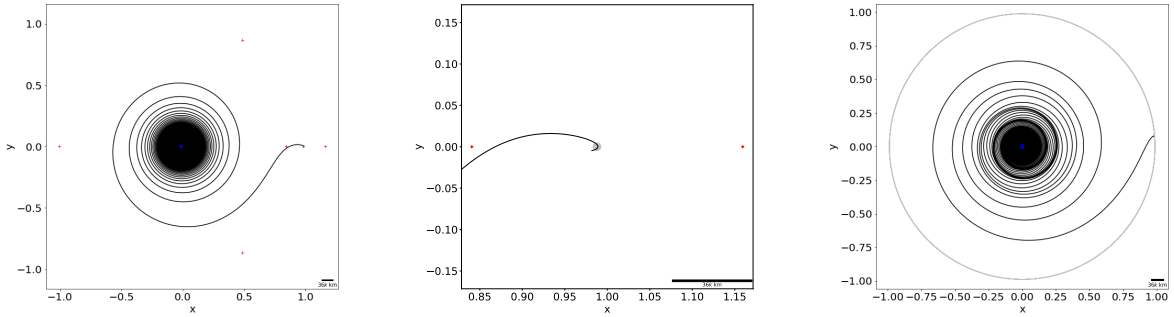

(a) Landing orbit for $f_2 = 5$ Hz and $t_2 = 1.013$ T, $f_S = 25$ Hz.

(b) Zoom in of landing orbit for $f_2 = 5$ Hz and $t_2 = 1.013$ T, $f_S = 25$ Hz.

(c) Non rotating frame of landing orbit for $f_2 = 5$ Hz and $t_2 = 1.013$ T, $f_S = 25$ Hz.

Figure 4.31: Landing orbit for $f_1 = 5$ Hz, $t_1 = 16$ T, $f_2 = 5$ Hz, $t_2 = 1.013$ T, with $f_S = 25$ Hz.

Figure 4.32 shows a landing orbit for $f_1 = 10$ Hz, $t_1 = 8$ T, with $f_2 = 6$ Hz, $t_2 = 1.684$ T, $f_S = 15$ Hz and $f_2 = 8$ Hz, $t_2 = 2.261$ T, $f_S = 12$ Hz.

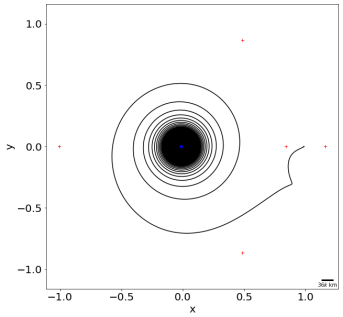

(a) Landing orbit for $f_2 = 6$ Hz and $t_2 = 1.684$ T, $f_S = 15$ Hz.

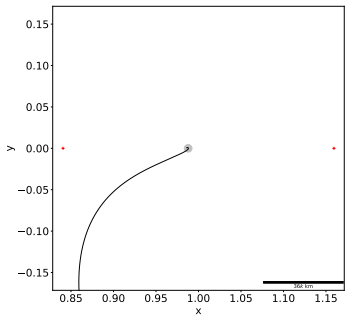

(b) Landing orbit for $f_2 = 6$ Hz and $t_2 = 1.684$ T, $f_S = 15$ Hz.

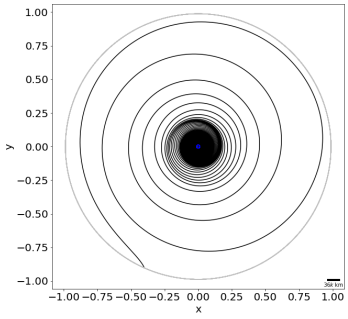

(c) Non rotating frame of landing orbit for $f_2 = 6$ Hz and $t_2 = 1.684$ T, $f_S = 15$ Hz.

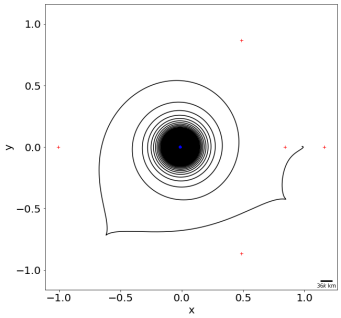

(d) Landing orbit for $f_2 = 6$ Hz and $t_2 = 2.261$ T, $f_S = 12$ Hz.

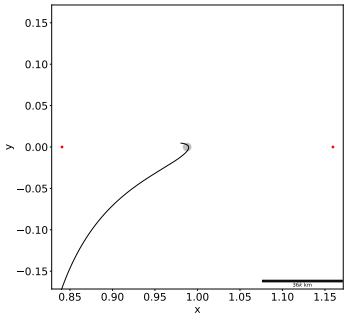

(e) Landing orbit for $f_2 = 6$Hz and $t_2 = 2.261$T, $f_S = 12$ Hz.

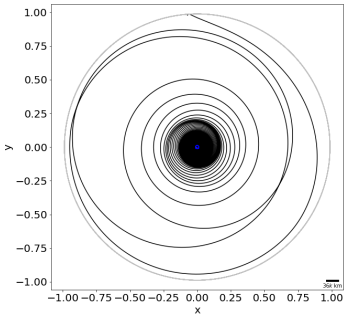

(f) Non rotating frame of landing orbit for $f_2 = 6$ Hz and $t_2 = 2.261$ T, $f_S = 12$ Hz.

Figure 4.32: Landing orbits for $f_1 = 10$ Hz, $t_1 = 8$ T. Then, $f_2 = 6$ Hz, $t_2 = 1.684$ T, with $f_S = 15$ Hz and $f_2 = 8$ Hz, $t_2 = 2.261$ T, with $f_S = 12$ Hz.

Figure 4.33 shows landing orbits for $f_1 = 20$ Hz and $t_1 = 4$ T. In the second part $f_2 = 6$ Hz, with $t_2 = 3.730$ T and $f_S = 10$ Hz, and $t_2 = 1.433$ T and $f_S = 20$ Hz.

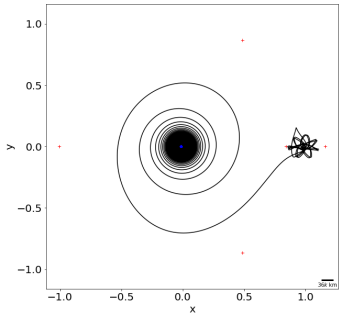

(a) Landing orbit for $f_2 = 6$ Hz and $t_2 = 3.730$ T, $f_S = 10$ Hz.

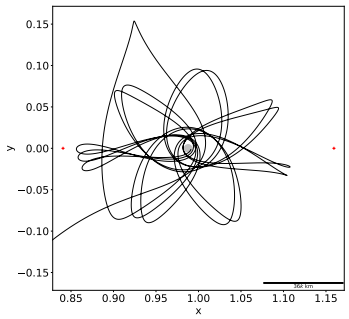

(b) Landing orbit for $f_2 = 6$ Hz and $t_2 = 3.730$ T, $f_S = 10$ Hz.

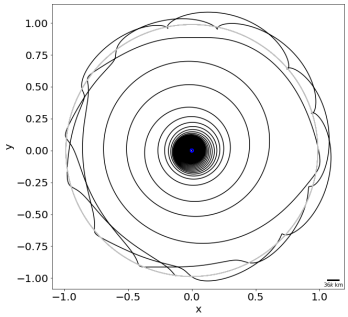

(c) Non rotating frame of landing orbit for $f_2 = 6$ Hz and $t_2 = 3.730$ T, $f_S = 10$ Hz.

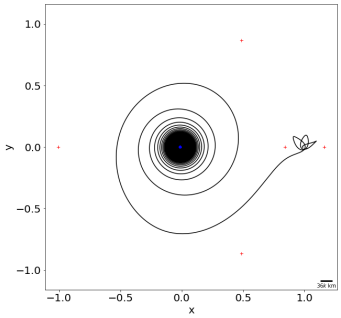

(d) Landing orbit for $f_2 = 6$ Hz and $t_2 = 1.433$ T, $f_S = 20$ Hz.

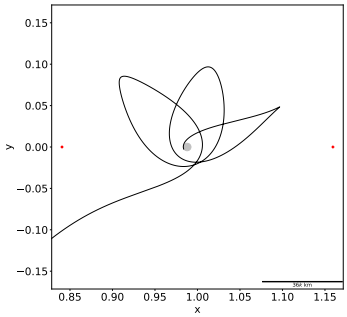

(e) Landing orbit for $f_2 = 6$ Hz and $t_2 = 1.433$ T, $f_S = 20$ Hz.

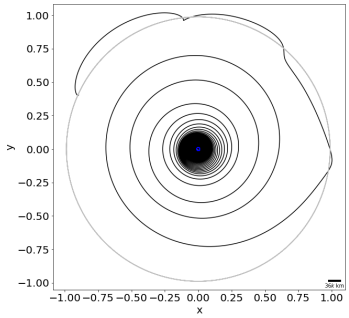

(f) Non rotating frame of landing orbit for $f_2 = 6$ Hz and $t_2 = 1.433$ T, $f_S = 20$ Hz.

Figure 4.33: Landing orbits for $f_1 = 20$ Hz and $t_1 = 4$ T. Then, $f_2 = 6$ Hz, with $t_2 = 1.433$ T and $f_S = 20$ Hz, and $t_2 = 3.730$ T and $f_S = 10$ Hz.

Figure 4.34 shows landing orbits for $f_1 = 20$ Hz and $t_1 = 4$ T. In the second part $f_2 = 7$ Hz, with $t_2 = 1.886$ T and $f_S = 15$ Hz, and $f_2 = 9$ Hz, $t_2 = 1.867$ T and $f_S = 10$ Hz.

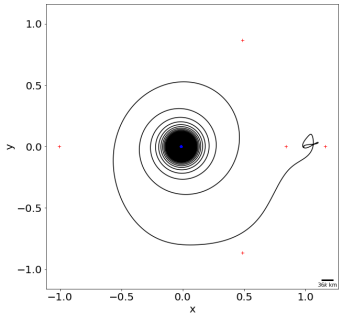

(a) Landing orbit for $f_2 = 7$ Hz and $t_2 = 1.886$ T, $f_S = 15$ Hz.

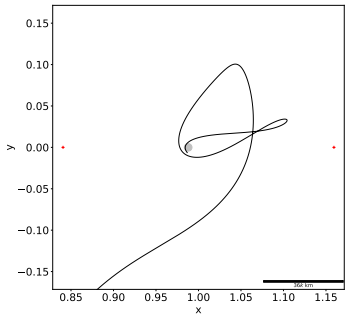

(b) Landing orbit for $f_2 = 7$ Hz and $t_2 = 1.886$ T, $f_S = 10$ Hz.

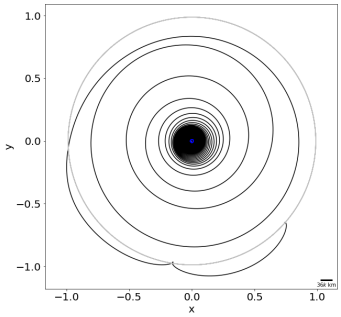

(c) Non rotating frame of landing orbit for $f_2 = 7$ Hz and $t_2 = 1.886$ T, $f_S = 15$ Hz.

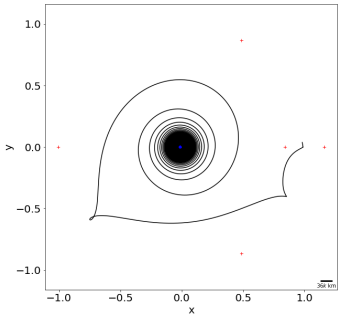

(d) Landing orbit for $f_2 = 6$ Hz and $t_2 = 1.867$ T, $f_S = 10$ Hz.

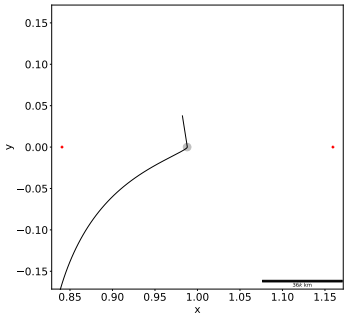

(e) Landing orbit for $f_2 = 6$ Hz and $t_2 = 1.867$ T, $f_S = 10$ Hz.

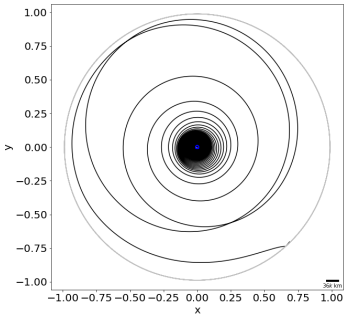

(f) Non rotating frame of landing orbit for $f_2 = 6$ Hz and $t_2 = 1.867$ T, $f_S = 10$ Hz.

Figure 4.34: Landing orbits for $f_1 = 20$ Hz and $t_1 = 4$ T. Then, $f_2 = 7$ Hz, with $t_2 = 1.886$ T and $f_S = 15$ Hz, and $f_2 = 9$ Hz, $t_2 = 1.867$ T and $f_S = 10$ Hz.

Table 4.3 displays the values for landing orbits presented in section 4.5. Two orbits are highlighted at table 4.3. These two orbits has the characteristic that the satellite orbits around the Moon before landing, this could be useful at the time of landing to give more time of maneuvering before landing.

Table 4.3: Values of the propeller, time and energy used for every landing orbit.

f_1[Hz]	t_1[T]	f_2[Hz]	t_2[T]	f_S[Hz]	$H_{l\min}$[km]	m_p[kg]	E_p[kWh]	E_p[MJ]
5	16	5	1.013	25	–	0.504	57.750	207.900
10	8	6	1.684	15	–	0.527	60.383	217.379
10	8	8	2.261	12	–	0.531	60.796	218.866
20	**4**	**6**	**3.730**	**10**	–	**0.519**	**59.525**	**214.290**
20	**4**	**6**	**1.433**	**20**	–	**0.509**	**58.300**	**209.880**
20	4	7	1.886	15	–	0.517	59.288	213.437
20	4	9	1.867	10	–	0.523	59.884	215.582

4.6. Geostationary Initial Orbit

The satellite can be considered initially at a geostationary orbit, this is an initial altitude of $36k$ km approximately.

Figure 4.35 shows transfer orbits with initial altitude of $36k$ km for $f_1 = 5$ Hz and $t_1 = 4$ T. In the second part $f_2 = 5$ Hz, $t_2 = 5$ T and $f_S = 20$ Hz and and $f_S = 25$ Hz.

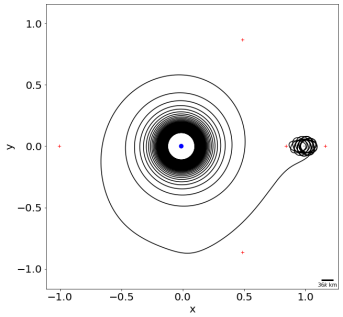

(a) Transfer orbit for $f_2 = 5$ Hz and $t_2 = 5$ T, $f_S = 20$ Hz.

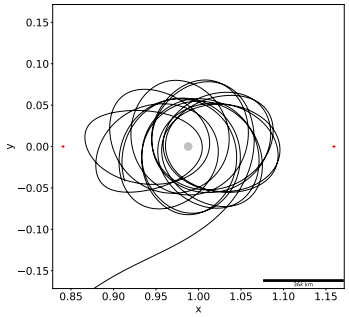

(b) Zoom in at the Moon to transfer orbit for $f_2 = 5$ Hz and $t_2 = 5$ T, $f_S = 20$ Hz.

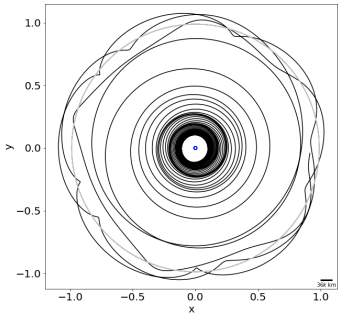

(c) Transfer orbit in non rotating frame for $f_2 = 5$ Hz and $t_2 = 5$ T, $f_S = 20$ Hz.

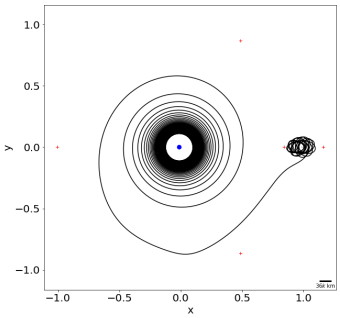

(d) Transfer orbit for $f_2 = 5$ Hz and $t_2 = 5$ T, $f_S = 25$ Hz.

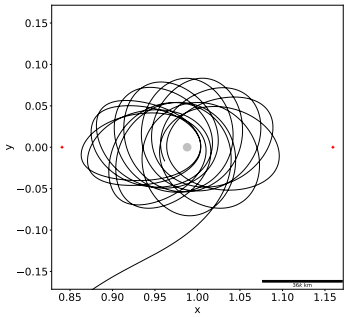

(e) Zoom in at the Moon to Transfer orbit for $f_2 = 5$ Hz and $t_2 = 5$ T, $f_S = 25$ Hz.

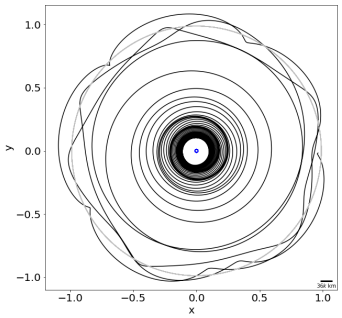

(f) Transfer orbit in non rotating frame for $f_2 = 5$ Hz and $t_2 = 5$ T, $f_S = 25$ Hz.

Figure 4.35: Transfer orbit for $f_1 = 20$ Hz and $t_1 = 4$ T. Then, $f_2 = 5$ Hz, with $t_2 = 5$ T and $f_S = 20$ Hz and $f_S = 25$ Hz.

Figures 4.36 and 4.37 shows transfer orbits with initial altitude of $36k$ km for $f_1 = 10$ Hz and $t_1 = 2$ T.

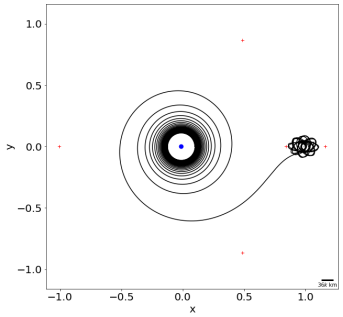

(a) Transfer orbit for $f_2 = 9$ Hz and $t_2 = 4$ T, $f_S = 25$ Hz.

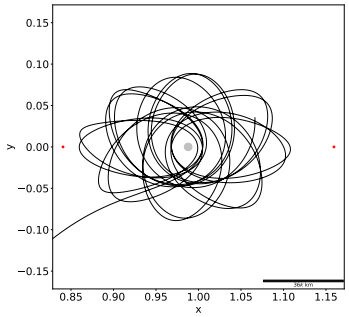

(b) Zoom in at the Moon to transfer orbit for $f_2 = 9$ Hz and $t_2 = 4$ T, $f_S = 25$ Hz.

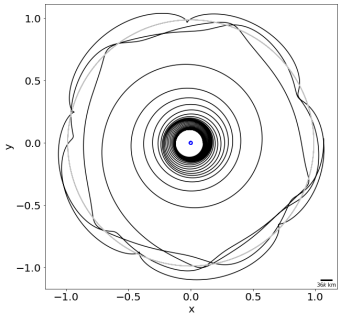

(c) Transfer orbit in non rotating frame for $f_2 = 9$ Hz and $t_2 = 4$ T, $f_S = 25$ Hz.

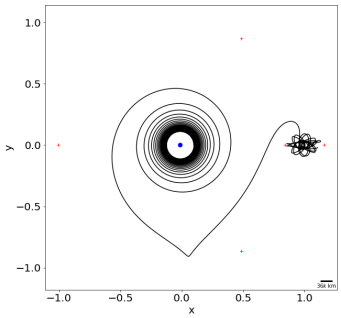

(d) Transfer orbit for $f_2 = 12$ Hz and $t_2 = 4$ T, $f_S = 15$ Hz.

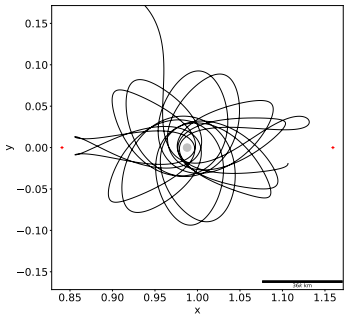

(e) Zoom in at the Moon to transfer orbit for $f_2 = 12$ Hz and $t_2 = 4$ T, $f_S = 15$ Hz.

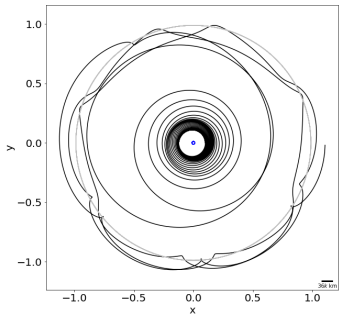

(f) Transfer orbit in non rotating frame for $f_2 = 12$ Hz and $t_2 = 4$ T, $f_S = 15$ Hz.

Figure 4.36: Transfer orbit for $f_1 = 10$ Hz and $t_1 = 2$ T. Then, $f_2 = 9$ Hz, with $t_2 = 4$ T and $f_S = 25$ Hz; $f_2 = 12$ Hz, with $t_2 = 4$ T and $f_S = 15$ Hz

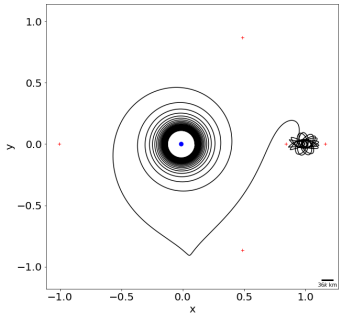

(a) Transfer orbit for $f_2 = 12$ Hz and $t_2 = 4$ T, $f_S = 20$ Hz.

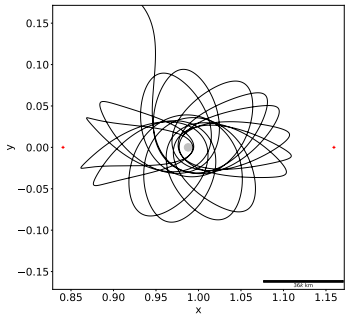

(b) Transfer orbit for $f_2 = 12$ Hz and $t_2 = 4$ T, $f_S = 20$ Hz.

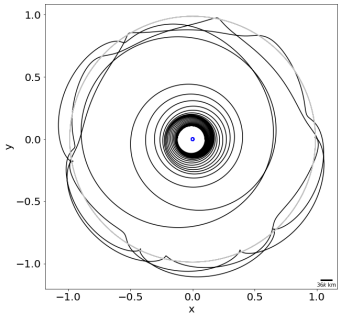

(c) Transfer orbit in non rotating frame for $f_2 = 12$ Hz and $t_2 = 4$ T, $f_S = 20$ Hz.

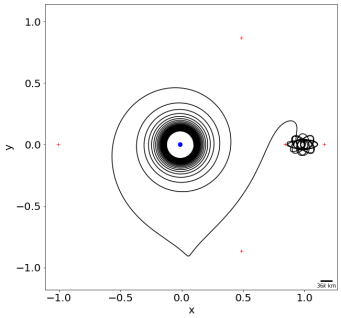

(d) Transfer orbit for $f_2 = 12$ Hz and $t_2 = 4$ T, $f_S = 25$ Hz.

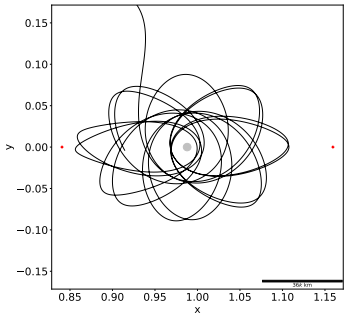

(e) Transfer orbit for $f_2 = 12$ Hz and $t_2 = 4$ T, $f_S = 25$ Hz.

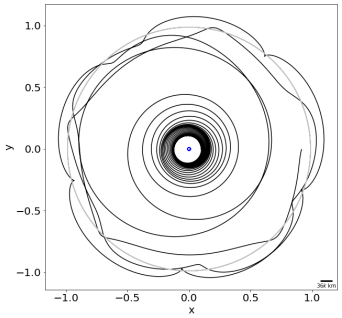

(f) Transfer orbit in non rotating frame for $f_2 = 12$ Hz and $t_2 = 4$ T, $f_S = 25$ Hz.

Figure 4.37: Transfer orbit for $f_1 = 10$ Hz and $t_1 = 2$ T. Then, $f_2 = 12$ Hz, with $t_2 = 4$ T and $f_S = 20$ Hz and $f_S = 25$ Hz.

Figures 4.38 shows transfer orbits with initial altitude of $36k$ km for $f_1 = 10$ Hz and $t_1 = 2$ T.

Table 4.4 displays the results of the orbits with initial altitude of $36k$ km or GEO orbit. Two results are highlighted at table 4.4, these two orbits present the same regularity mentioned at table 4.1 in section 4.3. the mean propeller mass of these orbits is $\overline{m}_p = 0.166$ kg and the mean total energy used of the whole orbit is $\overline{E}_p = 18.992$ kWh $= 68.370$ MJ.

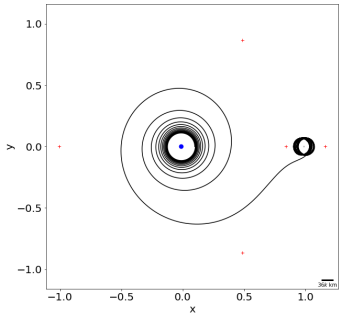

(a) Transfer orbit for $f_2 = 9$ Hz and $t_2 = 4$ T, $f_S = 25$ Hz.

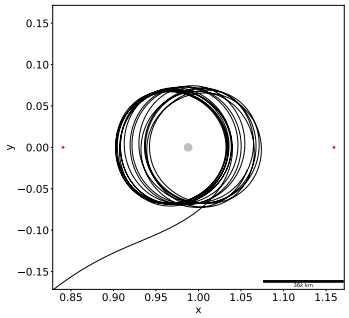

(b) Transfer orbit for $f_2 = 9$ Hz and $t_2 = 4$ T, $f_S = 25$ Hz.

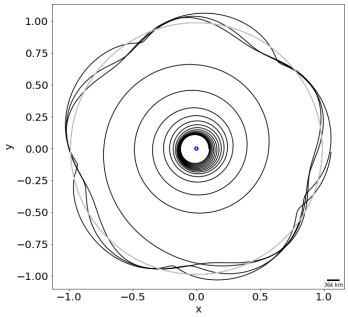

(c) Transfer orbit in non rotating frame for $f_2 = 9$ Hz and $t_2 = 4$ T, $f_S = 25$ Hz.

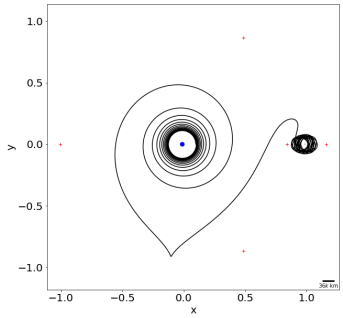

(d) Transfer orbit for $f_2 = 12$ Hz and $t_2 = 4$ T, $f_S = 25$ Hz.

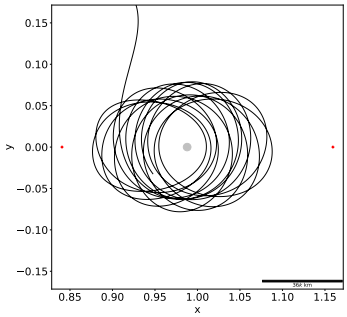

(e) Transfer orbit for $f_2 = 12$ Hz and $t_2 = 4$ T, $f_S = 25$ Hz.

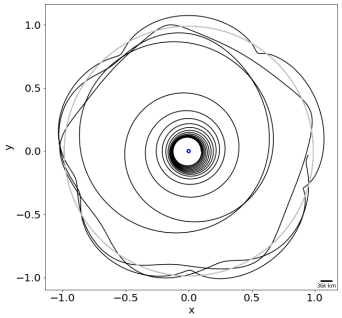

(f) Transfer orbit in non rotating frame for $f_2 = 12$ Hz and $t_2 = 4$ T, $f_S = 25$ Hz.

Figure 4.38: Transfer orbit for $f_1 = 20$ Hz and $t_1 = 1$ T. Then, $f_2 = 9$ Hz, with $t_2 = 4$ T and $f_S = 20$ Hz and $f_S = 25$ Hz.

Table 4.4: Values of the propeller, time and energy used for every transfer orbit from a geostationary orbit.

f_1[Hz]	t_1[T]	f_2[Hz]	t_2[T]	f_S[Hz]	$H_{l\min}$[km]	m_p[kg]	E_p[kWh]	E_p[MJ]
5	4	5	5	20	4620	0.163	18.702	67.327
5	4	5	5	25	4335	0.162	18.580	66.888
10	2	9	4	25	2547	0.158	18.121	65.236
10	2	12	4	15	1587	0.180	20.655	74.358
10	2	12	4	20	371	0.167	19.095	68.742
10	2	12	4	25	2732	0.167	19.102	68.767
20	**1**	**9**	**4**	**25**	**15371**	**0.161**	**18.430**	**66.348**
20	**1**	**12**	**4**	**20**	**6966**	**0.168**	**19.249**	**69.296**

It is interesting to see that the fuel and the total energy needed to make a transfer orbit from a GEO orbit to a lunar orbit is around one third the needed to make a transfer orbit from a LEO orbit to a lunar orbit. This indicates that the fuel and energy requirements from LEO to GEO orbit is two thirds of the total fuel and energy requirements of a transfer orbit

from a LEO to a lunar orbit.

4.7. A 10 % Reduction of Δm and c

In this section results on transfer orbits are presented where the propeller mass Δm and the velocity of the mass ejected from the thruster c are reduced in a 10 %. The objective of this section is to find if it is still possible to find transfer orbits to the Moon from LEO orbit after the reduction in parameters Δm and c. Additional results (orbits) are left at the appendix I.

4.7.1. A 10 % Reduction of Δm

This section presents results on a reduction of a 10 % on the ejected mass from the satellite. The value $\Delta m = 1 \cdot 10^{-10}$ kg is reduced to $\Delta m = 9 \cdot 10^{-11}$ kg.

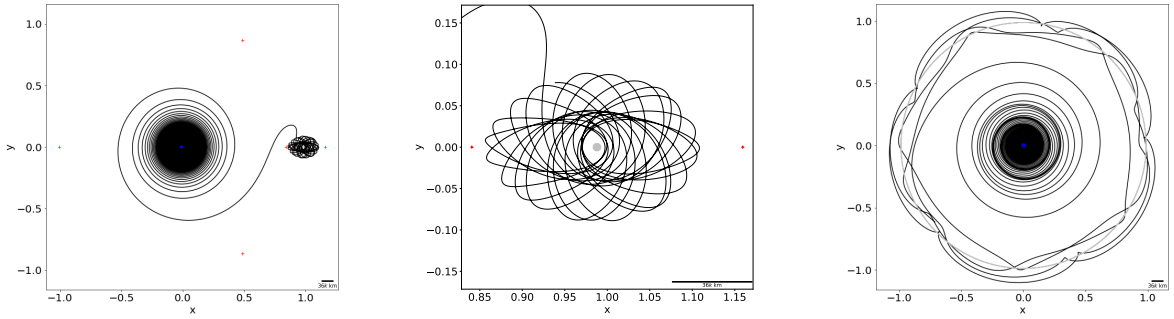

(a) Transfer orbit for $f_2 = 7$ Hz and $t_2 = 5$ T, $f_S = 25$ Hz.

(b) Zoom in at the Moon to transfer orbit for $f_2 = 7$ Hz and $t_2 = 5$ T, $f_S = 25$ Hz.

(c) Transfer orbit in non rotating frame for $f_2 = 7$ Hz, $t_2 = 5$ T and $f_S = 25$ Hz.

Figure 4.39: Transfer orbit for $f_1 = 5$ Hz and $t_1 = 17.6$ T. Then, $f_2 = 7$ Hz, $t_2 = 5$ T and $f_S = 25$ Hz.

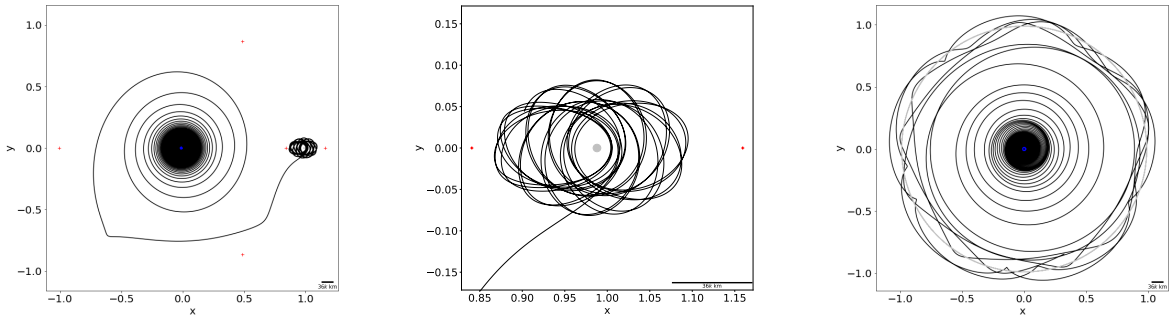

(a) Transfer orbit for $f_2 = 5$ Hz and $t_2 = 7$ T, $f_S = 25$ Hz.

(b) Zoom in at the Moon to transfer orbit for $f_2 = 5$ Hz and $t_2 = 7$ T, $f_S = 25$ Hz.

(c) Transfer orbit in non rotating frame for $f_2 = 5$ Hz and $t_2 = 7$ T, $f_S = 25$ Hz.

Figure 4.40: Transfer orbit for $f_1 = 10$ Hz and $t_1 = 8.8$ T. Then, $f_2 = 5$ Hz, with $t_2 = 7$ T and $f_S = 25$ Hz.

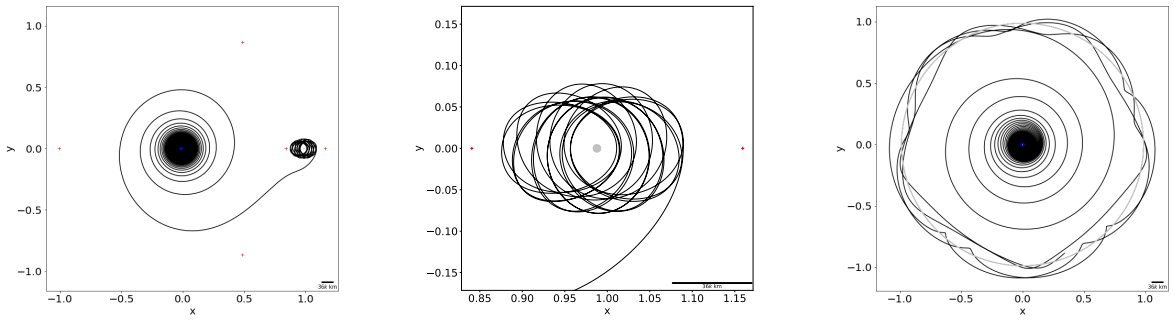

(a) Transfer orbit for $f_2 = 9$ Hz and $t_2 = 4.4$ T, $f_S = 20$ Hz.

(b) Zoom in at the Moon to transfer orbit for $f_2 = 9$ Hz and $t_2 = 4.4$ T, $f_S = 20$ Hz.

(c) Transfer orbit in non rotating frame for $f_2 = 9$ Hz and $t_2 = 4.4$ T, $f_S = 20$ Hz.

Figure 4.41: Transfer orbit for $f_1 = 20$ Hz and $t_1 = 4.4$ T. Then, $f_2 = 9$ Hz, with $t_2 = 4.4$ T and $f_S = 20$ Hz.

Table 4.5: Values of the propeller, time and energy used for every transfer orbit from a LEO orbit to a lunar orbit with a 10 % reduction in Δm.

f_1[Hz]	t_1[T]	f_2[Hz]	t_2[T]	f_S[Hz]	$H_{l\min}$[km]	m_p[kg]	E_p[kWh]	E_p[MJ]
5	17.6	7	5	25	1918	0.508	64.692	232.891
10	8.8	5	7	25	4532	0.510	64.895	233.622
20	4.4	9	4.4	20	7177	0.519	66.055	237.798

If the cases studied in section 4.5 are called initial case, we can see from table 4.5 that the propeller mass is not different from the one from the initial case, but the energy required and the time are higher in around 10 %. The time in this case and in the initial case it is the time required to the satellite achieve an altitude of approximately $160k$ km.

4.7.2. A 10 % Reduction of c

In this section results with a 10 % reduction on the velocity of the mass ejected c are presented. The velocity $c = 1 \cdot 10^5$ m/s is reduced in a 10 %, to the value $c = 9 \cdot 10^4$ m/s.

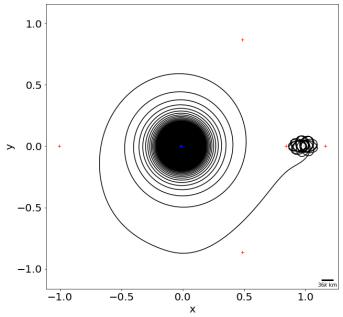

(a) Transfer orbit for $f_2 = 5$ Hz and $t_2 = 5$ T, $f_S = 25$ Hz.

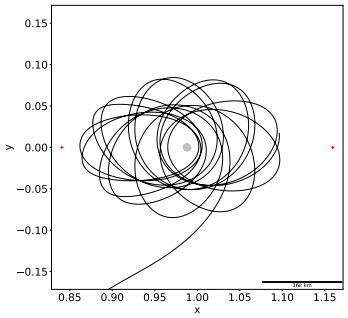

(b) Zoom in at the Moon to transfer orbit for $f_2 = 5$ Hz and $t_2 = 5$ T, $f_S = 25$ Hz.

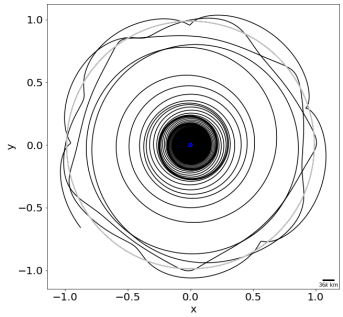

(c) Transfer orbit in non rotating frame for $f_2 = 5$ Hz and $t_2 = 5$ T, $f_S = 25$ Hz.

Figure 4.42: Transfer orbit for $f_1 = 5$ Hz and $t_1 = 17.6$ T. Then, $f_2 = 5$ Hz, with $t_2 = 5$ T and $f_S = 25$ Hz.

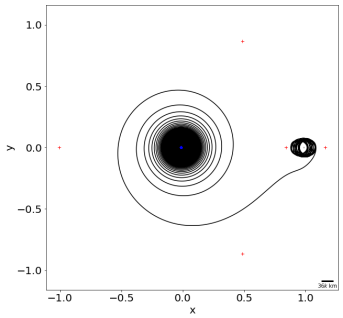

(a) Transfer orbit for $f_2 = 9$ Hz and $t_2 = 4.4$ T, $f_S = 20$ Hz.

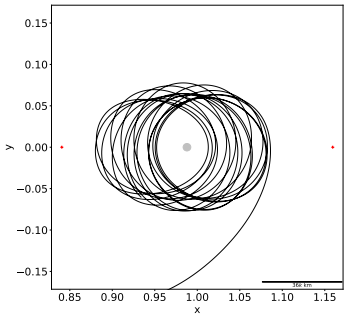

(b) Zoom in at the Moon to transfer orbit for $f_2 = 9$ Hz and $t_2 = 4.4$ T, $f_S = 20$ Hz.

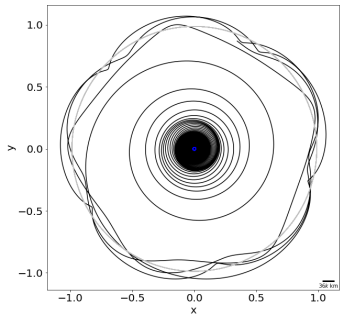

(c) Transfer orbit in non rotating frame for $f_2 = 9$ Hz and $t_2 = 4.4$ T, $f_S = 20$ Hz.

Figure 4.43: Transfer orbit for $f_1 = 10$ Hz and $t_1 = 8.8$ T. Then, $f_2 = 9$ Hz, with $t_2 = 4.4$ T and $f_S = 20$ Hz.

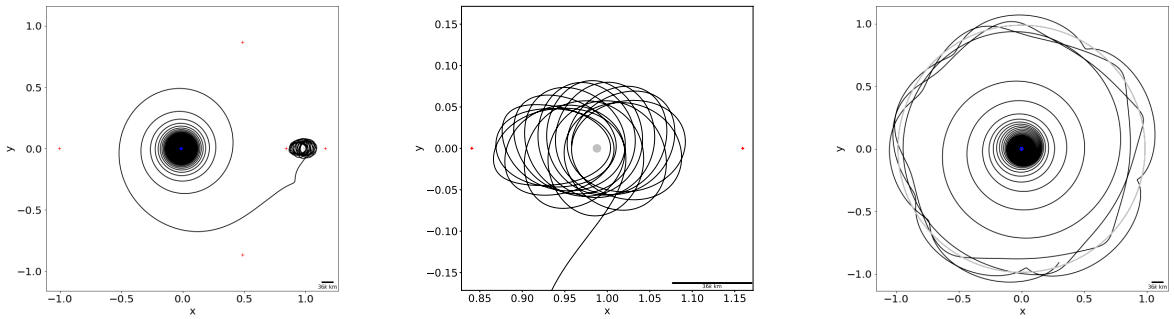

(a) Transfer orbit for $f_2 = 9$ Hz and $t_2 = 4.4$ T, $f_S = 15$ Hz.

(b) Zoom in at the Moon to transfer orbit for $f_2 = 9$ Hz and $t_2 = 4.4$ T, $f_S = 15$ Hz.

(c) Transfer orbit in non rotating frame for $f_2 = 9$ Hz and $t_2 = 4.4$ T, $f_S = 15$ Hz.

Figure 4.44: Transfer orbit for $f_1 = 20$ Hz and $t_1 = 4.4$ T. Then, $f_2 = 9$ Hz, with $t_2 = 4.4$ T and $f_S = 15$ Hz.

Table 4.6: Values of the propeller, time and energy used for three cases of transfer orbit from a LEO orbit to a lunar orbit with a 10 % reduction in c.

f_1[Hz]	t_1[T]	f_2[Hz]	t_2[T]	f_S[Hz]	$H_{l\min}$[km]	m_p[kg]	E_p[kWh]	E_p[MJ]
5	17.6	5	5	25	4545	0.567	65.025	234.090
10	8.8	9	4.4	20	7915	0.574	65.787	236.833
20	4.4	9	4.4	15	4400	0.589	67.546	243.166

It is interesting to see that in this case both, the propeller mass and the energy requirements, are higher in approximately 10 % than the initial case. The time of flight is also around 10 % higher than the initial case.

4.7.3. Simultaneous Reduction of a 10 % in Δm and c

In this section the results are presented with both reductions at the same time, a 10 % reduction in Δm and a 10 % reduction in the velocity c.

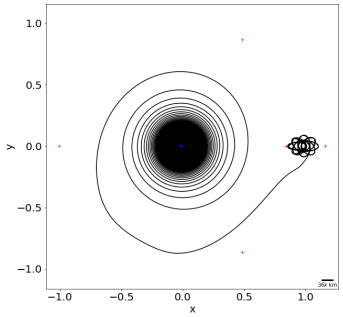

(a) Transfer orbit for $f_2 = 5$ Hz and $t_2 = 6$ T, $f_S = 25$ Hz.

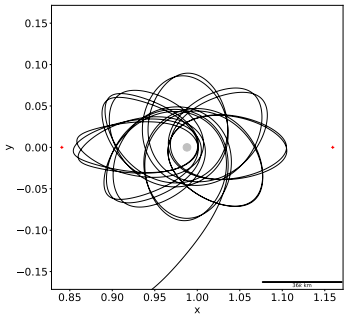

(b) Zoom in at the Moon to transfer orbit for $f_2 = 5$ Hz and $t_2 = 6$ T, $f_S = 25$ Hz.

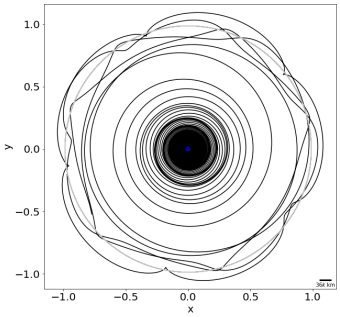

(c) Transfer orbit in non rotating frame for $f_2 = 5$ Hz and $t_2 = 6$ T, $f_S = 25$ Hz.

Figure 4.45: Transfer orbit for $f_1 = 5$ Hz and $t_1 = 19.6$ T. Then, $f_2 = 5$ Hz, with $t_2 = 6$ T and $f_S = 25$ Hz.

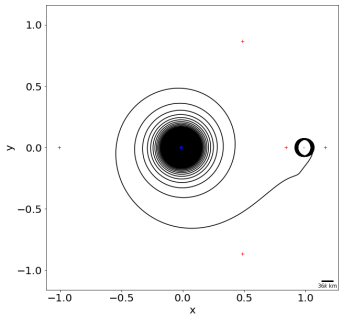

(a) Transfer orbit for $f_2 = 9$ Hz and $t_2 = 4.9$ T, $f_S = 20$ Hz.

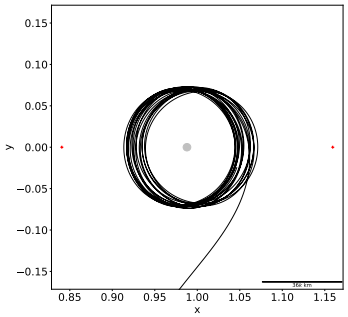

(b) Zoom in at the Moon to transfer orbit for $f_2 = 9$ Hz and $t_2 = 4.9$ T, $f_S = 20$ Hz.

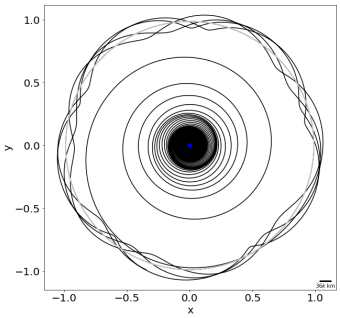

(c) Transfer orbit in non rotating frame for $f_2 = 9$ Hz and $t_2 = 4.9$ T, $f_S = 20$ Hz.

Figure 4.46: Transfer orbit for $f_1 = 10$ Hz and $t_1 = 9.8$ T. Then, $f_2 = 9$ Hz, with $t_2 = 4.9$ T and $f_S = 20$ Hz.

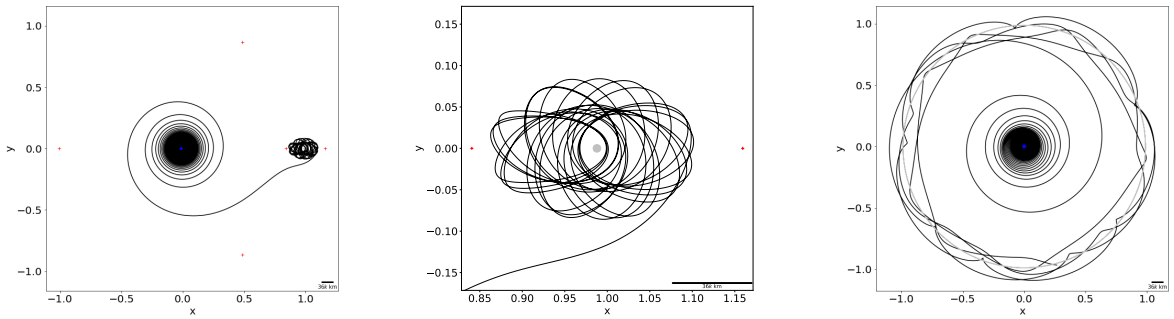

(a) Transfer orbit for $f_2 = 19$ Hz and $t_2 = 4.9$ T, $f_S = 25$ Hz.

(b) Zoom in at the Moon to transfer orbit for $f_2 = 19$ Hz and $t_2 = 4.9$ T, $f_S = 25$ Hz.

(c) Transfer orbit in non rotating frame for $f_2 = 19$ Hz and $t_2 = 4.9$ T, $f_S = 25$ Hz.

Figure 4.47: Transfer orbit for $f_1 = 20$ Hz and $t_1 = 4.9$ T. Then, $f_2 = 19$ Hz, with $t_2 = 4.9$ T and $f_S = 25$ Hz.

Table 4.7: Values of the propeller, time and energy used for three cases of transfer orbit from a LEO orbit to a lunar orbit with a 10 % reduction in Δm and a 10 % reduction in c.

f_1[Hz]	t_1[T]	f_2[Hz]	t_2[T]	f_S[Hz]	$H_{l\min}$[km]	m_p[kg]	E_p[kWh]	E_p[MJ]
5	19.6	5	6	25	3030	0.568	72.316	260.338
10	9.8	9	4.9	20	17015	0.577	73.490	264.564
20	4.9	19	4.9	25	2523	0.578	73.557	264.805

In this case, the time of flight is 22.5 % higher than the initial case so the satellite can reach the altitude of approximately $160k$ km. The propeller mass is approximately 12 % higher than the initial case and the energy requirements around 24 % higher than the initial case.

Chapter 5

Conclusions

In this section the conclusions of this work are presented. Also a future work is proposed. The main conclusions of this work are:

1. It was possible to implement the equations of the Planar and Circular Restricted 3 Body Problem (PCR3BP), on a *jupiter notebook* using codes written in Python 3, and solve them using the fourth order Runge-Kutta method (rk4).

2. The expected results were obtained in the cases of LEO, GEO and LLO orbits, as circular orbits around the Earth and the Moon, respectively.

3. It was possible to compute transfer orbits from a LEO orbit to a lunar orbit, all of this in the context of the PCR3BP, for a satellite of standard Cubesat of six units or eight kilograms of total initial mass.

4. It was found that the satellite needs around one half of a kilogram of propeller to complete the whole transfer orbit, from a LEO orbit to a HEO orbit, transiting from the Earth to the Moon and finally decelerating to orbit the Moon.

5. The total time of flight of the satellite from a LEO orbit to a lunar orbit depends on the applied force. In this case, the thruster fixed its force by choosing an operation frequency. For frequencies of 5, 10 and 20 Hz, the total time was 16, 8 and 4 periods of time of the Earth-Moon system (with one period equal to 27.3 days approximately), respectively, to reach an altitude of $160k$ km approximately. Then the satellite took between 1 and 2 periods to reach a lunar orbit.

6. Some orbits showed a stationary behaviour, i.e. the satellite remained at the same position in the rotating frame of reference, as the Earth and the Moon do. This particular case of orbit occurred at an altitude of $350k$ km in every case, with an exception where it stayed at an altitude of $450k$ km approximately. These cases are because the thruster force is equal and opposite to the net gravity forces at that point, leaving the satellite at rest in the rotating frame.

7. In some cases, the orbit of the satellite reached the surface of the Moon. These kinds of orbits could be useful if they are considered as possible paths to make a satellite land on the Moon. These types of orbits must be avoided if the satellite is meant to orbit the Moon.

8. Transfer orbits from a geostationary orbit (GEO) were obtained (orbit with an initial altitude of $36k$ km). It was found that the propeller mass and energy requirements was one third of the case of transfer orbit from a LEO orbit to a lunar orbit. Also, the time of flight of the transfer orbit from LEO to an altitude of approximately $160k$ km was reduced to a one quarter of every case of study.

9. The ejected mass Δm and the velocity of the ejected mass c were reduced in a 10 %, individually and simultaneously. For the case that Δm was reduced, the time of flight to $160k$ km of altitude and the total energy required increased in a 10 %, the mass propeller was approximately the same as the case without reduction in Δm. For the case that c was reduced in a 10 %, the time of flight to $160k$ km of altitude, the propeller mass and the total energy requirement increased in a 10 %, approximately. For the case Δm and c were reduced in a 10 %, the time of flight to $160k$ km of altitude increased in a 22.5 %, the propeller mass increased in a 10 % approximately and the total energy required increased in a 20 % approximately.

Future Work

A next step of this research would be the extension to the three dimensional case, the circular restricted three body problem (CR3BP). In general, the satellite will be orbiting the Earth out of the Earth-Moon plane. To make a better approximation of the orbit of the satellite will require to consider the z component of the movement of it. Nevertheless, the PCR3BP can still be a good approach to the satellite orbit in the Earth-Moon system if the movement of the satellite is restricted to the Earth-Moon plane.

Attitude dynamics must be considered to make a better approximation of the evolution of the thrust force. In general, the satellite will spin around some axis. To estimate where the thrust force is aiming, the attitude of the satellite needs to be considered.

In this work it is considered a perturbation aspect of the gravity field of the Earth ($J2$ factor), but this is not in the case of the Moon. The Moon presents mass concentrations, or the so called mascons. Mascons make the gravitational field near of the Moon vary such that it is necessary to consider them to make a better approximation to the orbit of the satellite when it is in lunar orbit[70].

The thruster can be modeled in more detailed if the electromagnetic aspects of the pulsed plasma thruster (PPT) are considered. In general, the PPT can be modeled as an RLC circuit and the thrust can be computed using the square of the current, the plasma inductance and the geometry of the thruster[71].

Even this work considers some perturbation aspects on the orbit of the satellite like the atmospheric drag and the Sun gravity, there are other perturbation phenomena that could be integrated gradually in the model as it becomes more complex. Some of these perturbations could be the Sun radiation pressure (see Curtis, chapter 12.9[25]), Earth radiation pressure[72], solar wind, among others.

Bibliography

[1] P. J. Stooke, *The international atlas of lunar exploration*. Cambridge University Press, 2007.

[2] G. Heiken and E. Jones, *On the Moon: The Apollo Journals*. Springer Science & Business Media, 2007.

[3] M. von Ehrenfried *et al.*, *Apollo Mission Control*. Springer International Publishing:, 2018.

[4] P. Conchie, C. Hempsell, and R. Parkinson, "Potential evolution of an international moon base programme," *Acta Astronautica*, vol. 26, no. 12, pp. 889–897, 1992.

[5] B. Sherwood, "Principles for a practical moon base," *Acta Astronautica*, vol. 160, pp. 116–124, 2019.

[6] C. Heinicke and B. Foing, "Human habitats: prospects for infrastructure supporting astronomy from the moon," *Philosophical Transactions of the Royal Society A*, vol. 379, no. 2188, p. 20190568, 2021.

[7] M. Smith, D. Craig, N. Herrmann, E. Mahoney, J. Krezel, N. McIntyre, and K. Goodliff, "The artemis program: An overview of nasa's activities to return humans to the moon," in *2020 IEEE Aerospace Conference*, pp. 1–10, IEEE, 2020.

[8] D. Folta and T. Sweetser, "Artemis mission overview: from concept to operations," tech. rep., NASA/Goddard Space flight Center and Jet Propulsion Laboratory, 2011.

[9] T. H. Sweetser, S. B. Broschart, V. Angelopoulos, G. J. Whiffen, D. C. Folta, M.-K. Chung, S. J. Hatch, and M. A. Woodard, "Artemis mission design," *Space science reviews*, vol. 165, no. 1-4, pp. 27–57, 2011.

[10] V. Angelopoulos, "The artemis mission," *The ARTEMIS mission*, pp. 3–25, 2010.

[11] M. Woodard, D. Folta, and D. Woodfork, "Artemis: the first mission to the lunar libration orbits," in *21st International Symposium on Space Flight Dynamics, Toulouse, France*, 2009.

[12] C. Chantal, S. Battistini, and B. K. Malphrus, *Cubesat Handbook. From Mission Design to Operations-*. Elsevier, 2020.

[13] J. Bouwmeester and J. Guo, "Survey of worldwide pico- and nanosatellite missions, distributions and subsystem technology," *Acta Astronautica*, vol. 67, no. 7, pp. 854–862, 2010.

[14] M. Swartwout, "The first one hundred cubesats: A statistical look," *Journal of small Satellites*, vol. 2, no. 2, pp. 213–233, 2013.

[15] M. Swartwout, "Attack of the cubesats: a statistical look," *Journal of small Satellites*, 2011.

[16] M. Swartwout, "Reliving 24 years in the next 12 minutes: a statistical and personal history of university-class satellites," *Journal of small Satellites*, 2018.

[17] T. Villela, C. A. Costa, A. M. Brandão, F. T. Bueno, and R. Leonardi, "Towards the thousandth cubesat: A statistical overview," *International Journal of Aerospace Engineering*, vol. 2019, 2019.

[18] R. Funase, S. Ikari, K. Miyoshi, Y. Kawabata, S. Nakajima, S. Nomura, N. Funabiki, A. Ishikawa, K. Kakihara, S. Matsushita, *et al.*, "Mission to earth–moon lagrange point by a 6u cubesat: Equuleus," *IEEE Aerospace and Electronic Systems Magazine*, vol. 35, no. 3, pp. 30–44, 2020.

[19] D. C. Folta, N. Bosanac, A. Cox, and K. C. Howell, "The lunar icecube mission design: Construction of feasible transfer trajectories with a constrained departure," in *AAS/AIAA Space Flight Mechanics Meeting, Napa Valley, CA*, 2016.

[20] C. Hardgrove, R. Starr, I. Lazbin, A. Babuscia, B. Roebuck, J. DuBois, N. Struebel, A. Colaprete, D. Drake, E. Johnson, *et al.*, "The lunar polar hydrogen mapper cubesat mission," *IEEE Aerospace and Electronic Systems Magazine*, vol. 35, no. 3, pp. 54–69, 2020.

[21] S. Speretta, A. Cervone, P. Sundaramoorthy, R. Noomen, S. Mestry, A. Cipriano, F. Topputo, J. Biggs, P. Di Lizia, M. Massari, *et al.*, "Lumio: an autonomous cubesat for lunar exploration," in *Space operations: inspiring Humankind's future*, pp. 103–134, Springer, 2019.

[22] M. Tsay, J. Frongillo, K. Hohman, and B. K. Malphrus, "Lunarcube: a deep space 6u cubesat with mission enabling ion propulsion technology," *Small Satellite Conference*, 2015.

[23] M. Diaz, J. Zagal, C. Falcon, M. Stepanova, J. Valdivia, M. Martinez-Ledesma, J. Diaz-Pena, F. Jaramillo, N. Romanova, E. Pacheco, *et al.*, "New opportunities offered by cubesats for space research in latin america: The suchai project case," *Advances in Space Research*, vol. 58, no. 10, pp. 2134–2147, 2016.

[24] C. Gonzalez, C. Rojas, A. Becerra, J. Rojas, T. Opazo, and M. Diaz, "Lessons learned from building the first chilean nano-satellite: The suchai project," *Small Satellite Conference*, 2018.

[25] H. D. Curtis, *Orbital mechanics for engineering students*. Butterworth-Heinemann, 2013.

[26] M. Valtonen and H. Karttunen, *The three-body problem*. Cambridge University Press, 2006.

[27] S. G. Rajeev, *Advanced mechanics: from Euler's determinism to Arnold's chaos*. OUP Oxford, 2013.

[28] R. Broucke, "Periodic orbits in the restricted three-body problem with earth-moon masses. nasa jet propulsion laboratory," tech. rep., Technical Report 32-1168, 1968.

[29] S. Ugai and A. Ichikawa, "Lunar synchronous orbits in the earth-moon circular-restricted three-body problem," *Journal of guidance, control, and dynamics*, vol. 33, no. 3, pp. 995–

1000, 2010.

[30] E. Sheila Widnall, John Deyst, "16.07 dynamics," Fall 2009.

[31] "Atmosphere properties." http://www.braeunig.us/space/atmos.htm. Accessed: 2021-02-16.

[32] C. D. Murray, "Dynamical effects of drag in the circular restricted three-body problem: I. location and stability of the lagrangian equilibrium points," *Icarus*, vol. 112, no. 2, pp. 465–484, 1994.

[33] F. J. Regan and S. M. Anandakrishnan, *Dynamics of atmospheric re-entry*. American Institute of Aeronautics and Astronautics, 1993.

[34] T. KATO, B. RIEVERS, and M. LIST, "Generic computation method of free-molecular flow effects on space objects," *TRANSACTIONS OF THE JAPAN SOCIETY FOR AERONAUTICAL AND SPACE SCIENCES, AEROSPACE TECHNOLOGY JAPAN*, vol. 14, no. ists30, pp. Pd_105–Pd_110, 2016.

[35] D. Oltrogge and K. Leveque, "An evaluation of cubesat orbital decay," *25th Annual Conference on Small Satellites*, 2011.

[36] R. E. Fischell, "Gravity gradient stabilization of earth satellites," 1964.

[37] W. S. Koon, M. W. Lo, J. E. Marsden, and S. D. Ross, "Dynamical systems, the three-body problem and space mission design," in *Equadiff 99: (In 2 Volumes)*, pp. 1167–1181, World Scientific, 2000.

[38] D. M. Goebel and I. Katz, *Fundamentals of electric propulsion: ion and Hall thrusters*, vol. 1. John Wiley & Sons, 2008.

[39] R. G. Jahn, *Physics of electric propulsion*. Courier Corporation, 2006.

[40] K. Lemmer, "Propulsion for cubesats," *Acta Astronautica*, vol. 134, pp. 231–243, 2017.

[41] J. Mueller, R. Hofer, and J. Ziemer, "Survey of propulsion technologies applicable to cubesats," *Jet Propulsion Laboratory*, 2010.

[42] I. Maldonado, "Evaluación de un propulsor electrospray para misiones de cubesats de tres unidades," 2018.

[43] D. Krejci, F. Mier-Hicks, C. Fucetola, P. Lozano, A. H. Schouten, and F. Martel, "Design and characterization of a scalable ion electrospray propulsion system," in *Joint Conference of 30th ISTS, 34th IEPC and 6th NSAT, Hyogo-Kobe, Japan*, 2015.

[44] P. R. L. Burton, "Pulsed plasma thruster," *JOURNAL OF PROPULSION AND POWER*, vol. 14, no. 5, pp. 716–735, 1998.

[45] R. L. Burton, "Pulsed plasma thrusters," *Encyclopedia of Aerospace Engineering*, 2010.

[46] L. Soto, "New trends and future perspectives on plasma focus research," *Plasma Physics and Controlled Fusion*, vol. 47, no. 5A, p. A361, 2005.

[47] C. Leakeas, "Parametric studies of dense plasma focus for fusion space propulsion with d-he3," tech. rep., PHILLIPS LAB EDWARDS AFB CA, 1991.

[48] G. Miley, R. Nachtrieb, J. Nadler, and C. Choi, "Use of a plasma focus device for space propulsion," in *Conference on Advanced SEI Technologies*, p. 3617, 1991.

[49] B. Temple, O. Barnouin, and G. Miley, "Plasma focus device for use in space propulsion," *Fusion Technology*, vol. 19, no. 3P2A, pp. 846–851, 1991.

[50] T. Kammash, *Fusion energy in space propulsion*. American Institute of Aeronautics and Astronautics, 1995.

[51] R. Thomas, Y. Yang, G. Miley, and F. Mead, "Advancements in dense plasma focus (dpf) for space propulsion," in *AIP Conference Proceedings*, vol. 746-1, pp. 536–543, American Institute of Physics, 2005.

[52] S. D. Knecht, R. E. Thomas, F. B. Mead, G. H. Miley, and D. Froning, "Propulsion and power generation capabilities of a dense plasma focus (dpf) fusion system for future military aerospace vehicles," in *AIP Conference Proceedings*, vol. 813-1, pp. 1232–1239, American Institute of Physics, 2006.

[53] L. Soto, C. Pavez, J. Moreno, M. Barbaglia, and A. Clausse, "Nanofocus: an ultra-miniature dense pinch plasma focus device with submillimetric anode operating at 0.1 j," *Plasma Sources Science and Technology*, vol. 18, no. 1, p. 015007, 2008.

[54] W. H. Loh, *Jet, rocket, nuclear, ion and electric propulsion: theory and design*, vol. 7. Springer Science & Business Media, 2012.

[55] a. Manuel Martinez-Sanchez, "16.522 space propulsion," Spring 2015.

[56] S. Mazouffre, "Electric propulsion for satellites and spacecraft: established technologies and novel approaches," *Plasma Sources Science and Technology*, vol. 25, no. 3, p. 033002, 2016.

[57] M. Martinez-Sanchez and J. E. Pollard, "Spacecraft electric propulsion-an overview," *Journal of propulsion and power*, vol. 14, no. 5, pp. 688–699, 1998.

[58] A. R. Tummala and A. Dutta, "An overview of cube-satellite propulsion technologies and trends," *Aerospace*, vol. 4, no. 4, p. 58, 2017.

[59] M. Keidar and I. Beilis, *Plasma engineering: applications from aerospace to bio and nanotechnology*. Academic Press, 2013.

[60] D. Krejci, B. Seifert, and C. Scharlemann, "Endurance testing of a pulsed plasma thruster for nanosatellites," *Acta Astronautica*, vol. 91, pp. 187–193, 2013.

[61] L. Zeng, Z. Wu, G. Sun, T. Huang, K. Xie, and N. Wang, "A new ablation model for ablative pulsed plasma thrusters," *Acta Astronautica*, vol. 160, pp. 317–322, 2019.

[62] H. Wagner and M. Auweter-Kurtz, "Slug model and snowplow model for pulsed plasma thruster description," in *40th AIAA/ASME/SAE/ASEE Joint Propulsion Conference and Exhibit*, p. 3466, 2004.

[63] M. Igarashi, N. Kumagai, K. Sato, K. Tamura, H. Takegahara, H. Okamoto, T. Wakizono, and H. Hashimoto, "Performance improvement of pulsed plasma thruster for micro satellite," *27th IEPC*, 2001.

[64] P. H. Gleichauf, "Electrical breakdown over insulators in high vacuum," *Journal of Applied Physics*, vol. 22, no. 5, pp. 535–541, 1951.

[65] L. Cranberg, "The initiation of electrical breakdown in vacuum," *Journal of Applied Physics*, vol. 23, no. 5, pp. 518–522, 1952.

[66] A. Van Oostrom and L. Augustus, "Electrical breakdown between stainless-steel electrodes in vacuum," *Vacuum*, vol. 32, no. 3, pp. 127–135, 1982.

[67] R. V. Latham, *High voltage vacuum insulation: Basic concepts and technological practice*. Elsevier, 1995.

[68] R. K. Parker, "Explosive electron emission and the characteristics of high-current electron flow," tech. rep., AIR FORCE WEAPONS LAB KIRTLAND AFB NM, 1974.

[69] M. Keidar, T. Zhuang, A. Shashurin, G. Teel, D. Chiu, J. Lukas, S. Haque, and L. Brieda, "Electric propulsion for small satellites," *Plasma Physics and Controlled Fusion*, vol. 57, no. 1, p. 014005, 2014.

[70] J. Arkani-Hamed, "The lunar mascons revisited," *Journal of Geophysical Research: Planets*, vol. 103, no. E2, pp. 3709–3739, 1998.

[71] Y. Ou, J. Wu, Y. Zhang, J. Li, and S. Tan, "Theoretical modeling and parameter analysis of micro-pulsed plasma thruster," *Energies*, vol. 11, no. 5, p. 1146, 2018.

[72] P. Knocke, J. Ries, and B. Tapley, "Earth radiation pressure effects on satellites," in *Astrodynamics Conference*, p. 4292, 1988.

[73] R. Frnka, "The circular restricted three-body problem," 2010.

Anexo A

Miscellaneous Content

This appendix presents some miscellaneous content, mainly audiovisual content from the YouTube platform.

- The Moon.
- Landing on the Moon.
- Space Race.
- The Apollo Mission.
- Moon base.
- Artemis program.
- Artemis Lunar Exploration program overview.
- The Three Body Problem.
- Planar Circular Restricted Three Body Problem (PCR3BP).

Anexo B

Derivation of μ factor

To derive the μ factor present in the equations of motion of the Planar and Circular Restricted 3 Body Problem (PCR3BP), first calculate the center of mass or barycenter of the Earth-Moon system.

The center of mass is defined as:

$$R_{CM} = \frac{M_e r_e + M_l r_l}{M_e + M_l} \tag{B.1}$$

Where M_e is the mass of Earth, M_l is the mass of the Moon, r_e is the distance from the center of mass to the center of the Earth and r_l is the distance from the center of mass to the center of the Moon.

To find a frame of reference centered at the center of mass, it is imposed that $R_{CM} = 0$. With this, the equation (B.1) can be reduced to

$$-M_e r_e = M_l r_l \tag{B.2}$$

Furthermore, the distances can be normalized by the mean distance between the Earth and the Moon, D. Because now the distance between Earth and the Moon is 1, it can be noted that if $\frac{|r_e|}{D} = \mu$, then $\frac{|r_l|}{D} = 1 - \mu$.

The Earth-Moon system can be thought as depicted in figure 2.1, then the quantity r_e is negative, thus $|r_e| = -r_e$. With all of this, equation (B.2) reduces to

$$M_e \mu = M_l (1 - \mu) \tag{B.3}$$

From equation, (B.3) it can be find an expression for the factor μ

$$\mu = \frac{M_l}{M_e + M_l} \tag{B.4}$$

The factor μ defines or determines the PCR3BP. Every system of two massive bodies has its own μ factor. For the case of Earth-Moon system $\mu \approx 0.012$. Table B.1 shows values for different primaries of the factor μ. Note that by definition, the μ factor is the normalized mass of the Moon or the normalized of the lighter of the primaries. In consequence, the normalized mass of the heavier primary, the Earth in the case of interest of this work, is equal to $1 - \mu$,

Table B.1: Values for the factor μ for different primaries. Extracted from Frnka 2010[73].

System	m_1[kg]	m_2[kg]	μ
Earth-Moon	$5.9736 \cdot 10^{24}$	$7.7477 \cdot 10^{22}$	$1.12151 \cdot 10^{-2}$
Titan-Saturn	$5.8460 \cdot 10^{26}$	$1.3452 \cdot 10^{23}$	$2.3660 \cdot 10^{-4}$
Sun-Earth	$1.9891 \cdot 10^{30}$	$5.9736 \cdot 10^{24}$	$3.0039 \cdot 10^{-7}$
Sun-Saturn	$1.9891 \cdot 10^{30}$	$5.8460 \cdot 10^{26}$	$2.8571 \cdot 10^{-4}$
Sun-Jupiter	$1.9891 \cdot 10^{30}$	$1.4313 \cdot 10^{27}$	$7.1904 \cdot 10^{-4}$

as it can be seen below

$$\frac{M_e}{M_e + M_l} = \frac{M_e + M_l - M_l}{M_e + M_l} = \frac{M_e + M_l}{M_e + M_l} - \frac{M_l}{M_e + M_l} = 1 - \mu$$

Thus, the factor μ defines the distance of the center of the Earth to the barycenter and the normalized mass of the Moon. Equivalently, the factor $1 - \mu$ defines the distance of the center of the Moon to the barycenter and the normalized mass of the Earth.

Anexo C

Derivation of the Equations of Motion

For the case of a satellite in PCR3BP, the equation to solve is the next one

$$m\ddot{\mathbf{r}} = \mathbf{F_1} + \mathbf{F_2} \tag{C.1}$$

Where m is the mass of the satellite and $\ddot{\mathbf{r}}$ is the acceleration of the satellite in the rotating frame. The forces $\mathbf{F_1}$ and $\mathbf{F_2}$ are the gravity force between the satellite and the Earth and the satellite and the Moon, respectively.

$$\begin{aligned} \mathbf{F_1} &= \frac{GM_e m}{r_1^3}\mathbf{r_1} \\ \mathbf{F_2} &= \frac{GM_l m}{r_2^3}\mathbf{r_2} \end{aligned} \tag{C.2}$$

Where $\mathbf{r_1}$ and $\mathbf{r_2}$ are the position vectors of the satellite respective to the center of the Earth and the center of the Moon, respectively. The acceleration $\ddot{\mathbf{r}}$ must be written considering the relative motion between the inertial frame of reference, which is fixed and centered at the center of mass or barycenter of the Earth-Moon system, and the non inertial frame of reference, which is rotating such that the Earth and the Moon appears fixed in this frame of reference. From Curtis, chapter 1.7 of relative motion [25] is used the next expression:

$$\ddot{\mathbf{r}} = \mathbf{a_G} + \dot{\mathbf{n}} \times \mathbf{r} + \mathbf{n} \times (\mathbf{n} \times \mathbf{r}) + 2\mathbf{n} \times \mathbf{v}_{\text{rel}} + \mathbf{a}_{\text{rel}} \tag{C.3}$$

The term $\mathbf{a_G}$ is the linear acceleration between frames, which in PCR3BP is zero. The term $\mathbf{n}$ is the angular velocity of the rotating frame and in the case of PCR3BP $\mathbf{n} = n\hat{k}$, with $n = \sqrt{\dfrac{GM_eM_l}{D}}$ is the mean motion of the Earth and/or the Moon around the barycenter (this factor is set to 1 in the PCR3BP). The mean motion is constant, then $\dot{\mathbf{n}} = 0$. The remaining terms: $\mathbf{n} \times (\mathbf{n} \times \mathbf{r}) = -n^2\left(x\hat{\mathbf{i}} + y\hat{\mathbf{j}}\right)$, $2\mathbf{n} \times \mathbf{v}_{\text{rel}} = 2n\left(x\hat{\mathbf{i}} - y\hat{\mathbf{j}}\right)$ and $\mathbf{a}_{\text{rel}} = \ddot{x}\hat{i} + \ddot{y}\hat{j} + \ddot{z}\hat{k}$. Replacing this terms in C.1 and eliminating the mass m results

$$\begin{aligned} \ddot{x} - 2n\dot{y} - n^2x &= -\frac{(1-\mu)}{r_1^3}(x+\mu) - \frac{\mu}{r_2^3}(x+\mu-1) \\ \ddot{y} + 2n\dot{x} - n^2y &= -\frac{\mu}{r_1^3}y - \frac{\mu}{r_2^3}y \end{aligned} \tag{C.4}$$

These last equations can be written as

$$\begin{aligned} \ddot{x} &= 2n\dot{y} + \frac{\partial \Omega}{\partial x} \\ \ddot{y} &= -2n\dot{x} + \frac{\partial \Omega}{\partial y} \end{aligned} \tag{C.5}$$

With $\Omega = \dfrac{n^2\left(x^2+y^2\right)}{2} + \dfrac{1-\mu}{r_1} + \dfrac{\mu}{r_2}$ as an effective potential.

Setting the value of $n = 1$ as it is in PCR3BP in equations (C.5), the equations of motion of the satellite in PCR3BP are obtained and they are the same as presented in equations (2.1). The effective potential Ω is also obtained as it is presented in equation (2.2).

Anexo D

Frames of Reference and Initial Conditions

To derive the initial velocity used in equation (2.5) the force of gravity is considered equal to a centripetal force

$$\begin{aligned} F_g &= F_c \\ \frac{GM_e m}{(R_e + H_0)^2} &= \frac{m v_0^2}{R_e + H_0} \\ v_0 &= \sqrt{\frac{GM_e}{R_e + H_0}} \end{aligned} \tag{D.1}$$

The velocity of a satellite in a LEO orbit can be approximated by this formula, because this orbit is approximately circular. Please note this expression must be normalized by a factor $\frac{1}{nD}$ to be used in the PCR3BP. Here, n is the mean motion of the Earth-Moon system and D is the mean distance between Earth and the Moon. For simplicity the notation v_0 will be kept to refer the velocity in equation (D.1) but normalized by $\frac{1}{nD}$.

This velocity is in a frame of reference centered at Earth, then it is necessary to transform it to a frame of reference centered at the center of mass (so it can be used as an initial velocity for the PCR3BP).

The expressions (D.2) are proposed by Curtis[25] in chapter 1.7 of relative motion to transform velocities between inertial and non inertial frame of reference

$$\begin{aligned} \mathbf{r} &= \mathbf{r_G} + \mathbf{r}_{\text{rel}} \\ \mathbf{v} &= \mathbf{v_G} + \mathbf{n} \times \mathbf{r}_{\text{rel}} + \mathbf{v}_{\text{rel}} \end{aligned} \tag{D.2}$$

Where $\mathbf{r}$ is the position of the satellite in the inertial frame, $\mathbf{r_G}$ is the position of the origin of the non inertial frame of reference respect to the inertial frame and $\mathbf{r}_{\text{rel}}$ is the position of the satellite in the non inertial frame of reference, $\mathbf{v}$ is the velocity of the satellite in the inertial frame, $\mathbf{v_G}$ is the velocity of the origin of the non inertial frame respect to the inertial frame, $\mathbf{n}$ is the angular velocity of the non inertial frame and $\mathbf{v}_{\text{rel}}$ is the velocity of the satellite in the non inertial frame of reference. Because the expression for v_0 is in a non inertial frame of reference respect to the barycenter, the equation (D.2) can be applied to use this value of the initial velocity but in the frame of reference with origin at the center of mass or barycenter.

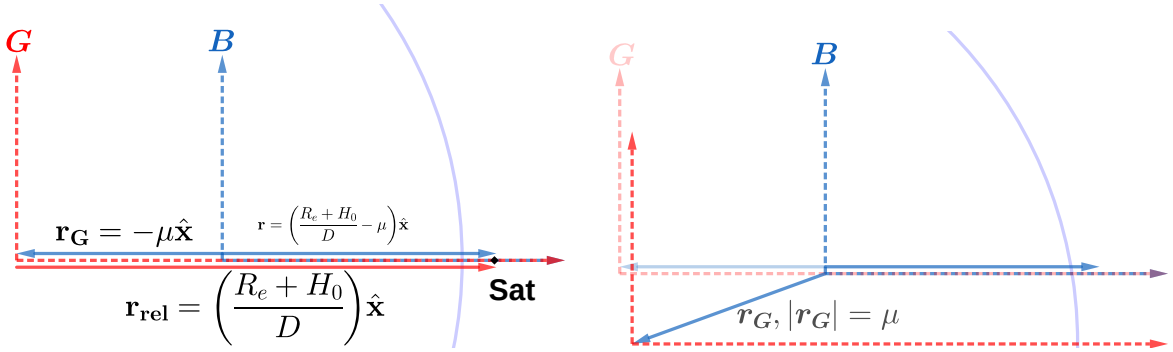

(a) $t = 0$ (b) $t > 0$

Figure D.1: Frames of reference centered at Earth G and at the barycenter B. The arc of circle represents the surface of the Earth. The initial conditions of the satellite are known in G. At $t > 0$ the origin of G rotates around the origin of B with angular velocity equal to n and radius μ. The vectors $\mathbf{r_G}$, $\mathbf{r}_{\text{rel}}$ and $\mathbf{r}$ at $t = 0$ are slightly off axis x so they can be readable. The distances are not at scale.

Figure D.1 shows the reference centered at Earth G and the reference centered at the barycenter B at $t = 0$ and at $t > 0$. The initial position can be defined in G as the initial altitude of the satellite plus the radius of the Earth. Also, the initial velocity can be defined in G by relation (D.1). Figure D.1 shows the necessary factors to transform initial conditions from G to B.

$$\begin{aligned} \mathbf{r_G} &= -\mu\hat{\mathbf{x}} \\ \mathbf{r}_{\text{rel}} &= \left(\frac{R_e + H_0}{D}\right)\hat{\mathbf{x}} \\ \mathbf{v_G} &= -n\mu\hat{\mathbf{y}} \\ \mathbf{n} &= \mathbf{0} \\ \mathbf{v}_{\text{rel}} &= v_0\hat{\mathbf{y}} \end{aligned} \tag{D.3}$$

Using the relations (D.3) with equations (D.2) it is possible to write the transformation from G to B for the initial conditions as shown below.

$$\begin{aligned} \mathbf{r} &= \left(\frac{R_e + H_0}{D} - \mu\right)\hat{\mathbf{x}} \\ \mathbf{v} &= (v_0 - n\mu)\,\hat{\mathbf{y}} \end{aligned} \tag{D.4}$$

Figure D.1 also shows the evolution of the reference G at $t > 0$. Note the Earth rotates represented by an arc of a circle, while the distance between the origin of G and B is constant and equal to μ. To simplify equations consider $x_0 = \dfrac{R_e + H_0}{D} - \mu$.

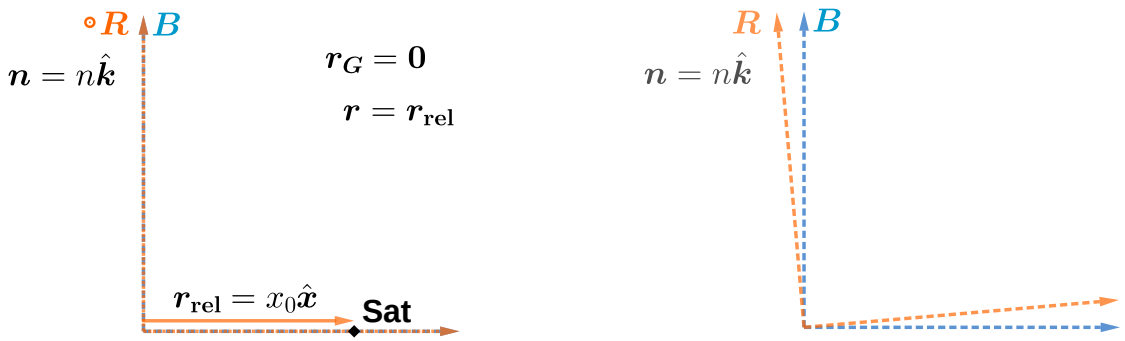

(a) $t = 0$. (b) $t > 0$.

Figure D.2: Frames of reference centered at the barycenter B and the rotating frame R also centered at the barycenter. The initial position of the satellite is known at B. The angular velocity of R is $\mathbf{n} = n\hat{\mathbf{k}}$.

Now, the same process it is repeated to transform the position and velocity from the inertial frame B, fixed at the barycenter, to the non inertial frame R, the rotating frame of reference centered at the barycenter, with the difference that in this case it is found $\mathbf{r}_{\text{rel}}$ and $\mathbf{v}_{\text{rel}}$, known $\mathbf{r}$ and $\mathbf{v}$. From figure D.2 it is found:

$$\begin{aligned} \mathbf{r_G} &= \mathbf{0} \\ \mathbf{r} &= x_0\hat{\mathbf{x}} \\ \mathbf{v_G} &= \mathbf{0} \\ \boldsymbol{\Omega} &= n\hat{\mathbf{k}} \\ \mathbf{v} &= (v_0 - n\mu)\,\hat{\mathbf{y}} \end{aligned} \tag{D.5}$$

In this case $\mathbf{r}_{\text{rel}} = x_0\hat{\mathbf{x}}$, then $\mathbf{n} \times \mathbf{r}_{\text{rel}} = nx_0\hat{\mathbf{y}}$. Using the relations in equation (D.5) with equations (D.2), the initial conditions for the rotating frame in the PCR3BP using LEO initial conditions are

$$\begin{aligned} \mathbf{r}_{\text{rel}} &= x_0\hat{\mathbf{x}} \\ \mathbf{v}_{\text{rel}} &= (v_0 - n\mu - nx_0)\,\hat{\mathbf{y}} \end{aligned} \tag{D.6}$$

Setting $n = 1$, the initial conditions for the PCR3BP are found as presented in equation 2.6. Figure D.2 also shows the evolution of the system R, which rotates with angular velocity $\mathbf{n} = n\hat{\mathbf{k}}$.

Anexo E

Jacobi Constant C Derivation

The *Jacobian integral* constant C can be derived from equations of motion 2.1, multiplying the first one of them by $\dot{x}$ and the second one by $\dot{y}$.

$$\begin{aligned} \dot{x}\ddot{x} &= 2\dot{x}\dot{y} + \dot{x}\frac{\partial \Omega}{\partial x} \\ \dot{y}\ddot{y} &= -2\dot{x}\dot{y} + \dot{y}\frac{\partial \Omega}{\partial y} \end{aligned} \tag{E.1}$$

Adding both equations of E.1 it is obtained

$$\dot{x}\ddot{x} + \dot{y}\ddot{y} = \frac{\partial \Omega}{\partial x}\dot{x} + \frac{\partial \Omega}{\partial y}\dot{y} \tag{E.2}$$

This last expression can be rewritten as

$$\frac{d}{dt}\left(\dot{x}^2 + \dot{y}^2\right) = 2\frac{d\Omega}{dt} \tag{E.3}$$

Integrating over time

$$\left(\dot{x}^2 + \dot{y}^2\right) = 2\Omega - C \tag{E.4}$$

Because $v^2 \geq 0$, it is true that $2\Omega - C \geq 0$, consequently

$$\Omega \geq C/2 \tag{E.5}$$

The relation (E.5) restricted the possible positions of the satellite, restricting the possible orbits that the satellite can transit. Examples of these forbidden zones for the case Earth-Moon system can be seen in figure 4.14.

Anexo F

Gravity-gradient Stabilization for a Cubesat of Six Units

Chapter 10.10 "Gravity-gradient Stabilization" of Curtis[25] develops the theory of gravity gradient and it can be applied to find which will be the orientation of the satellite as it moves along the orbit.

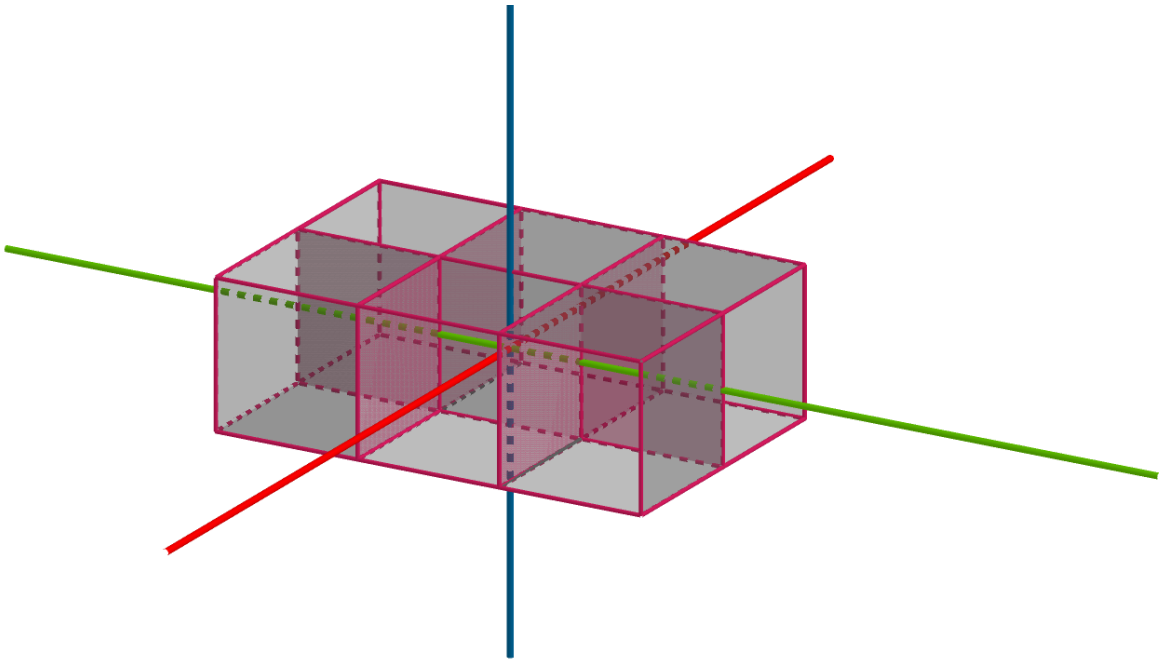

Figure F.1: A six units homogenous Cubesat schematic. The satellite will orbit in the direction of the x axis (the red one). The z axis (the green one) is the radial position of the center of mass of the satellite.

Figure F.1 shows an schematic of the cubesat of six units. For an homogeneus parallelepiped, the principal moments of inertia are $I_{ii} = \frac{m}{12}(j^2 + k^2)$, where i, j, k are a triad, so if $i = x$, then $j = y$ and $k = z$, and so on. The mass of the body is represented by the factor

m. The principal moments of inertia for the parallelepiped will be:

$$\begin{aligned} A &= \frac{8}{12}\left(1^2+3^2\right) = \tfrac{2}{3}10 \\ B &= \frac{8}{12}\left(2^2+3^2\right) = \tfrac{2}{3}13 \\ C &= \frac{8}{12}\left(2^2+1^2\right) = \tfrac{2}{3}5 \end{aligned} \tag{F.1}$$

In this case, the result of equation (F.1) is in arbitrary units, with the mass in kilograms and the distances in cubesat units length (1 unit = 10 cm). To determine if the body is a minor-axis spinner

$$I_{\text{pitch}} = C \qquad I_{\text{yaw}} = A \qquad I_{\text{roll}} = B$$

If $I_{\text{roll}} > I_{\text{yaw}}$, then the satellite will be stable in pitch, as it is in this case

$$k_Y = \frac{I_{\text{pitch}} - I_{\text{roll}}}{I_{\text{yaw}}} = \frac{5-13}{10} = -0.8 \qquad k_R = \frac{I_{\text{pitch}} - I_{\text{yaw}}}{I_{\text{roll}}} = \frac{5-10}{13} \approx -0.4$$

Because $k_Y k_R = 3.2 > 0$ one of the requirements is met. Now it is computed

$$1 + 3k_R + k_Y k_R - 4\sqrt{k_Y k_R} \approx 1 - 1.2 + 3.2 - 7.2 = -4.2 < 0$$

Because this last expression is negative, the satellite will not be a minor-axis spinner.

For the case of major-axis spinner

$$I_{\text{pitch}} = B = \tfrac{2}{3}13 \qquad I_{\text{yaw}} = C = \tfrac{2}{3}5 \qquad I_{\text{roll}} = A = \tfrac{2}{3}10$$

Because $I_{\text{roll}} > I_{\text{yaw}}$ the satellite will be stable in pitch.

$$k_Y = \frac{I_{\text{pitch}} - I_{\text{roll}}}{I_{\text{yaw}}} = \frac{13-10}{5} = 0.6 \qquad k_R = \frac{I_{\text{pitch}} - I_{\text{yaw}}}{I_{\text{roll}}} = \frac{13-5}{10} = 0.8$$

Because $k_Y k_R \approx 0.5 > 0$ the first requirement is met. Now it is computed

$$1 + 3k_R + k_Y k_R - 4\sqrt{k_Y k_R} \approx 1 + 2.4 + 0.5 - 2.8 = 1.1 > 0$$

Because the second requirement is met, the satellite will be oriented with its minor axis along the radial from Earth's center, the major axis aligned with the normal of the orbit and its intermediate axis aligned with the direction of movement. Consequently, the area for the drag will be the area of 3 units of Cubesat, $A = 3 \cdot 10\text{cm} \cdot 10\text{cm}$. Please note this area my be normalized by the factor D^2 to be used in the PCR3BP equations of motion.

Anexo G

Derivation of Factor Associated to $J2$

To consider the effect of the oblateness of the Earth on its potential gravity, the function $\Phi(r_1, \phi)$ is added to the regular expression of the Earth gravity potential.

$$\Phi(r_1, \phi) = \frac{1-\mu}{r_1} \sum_{k=2}^{\infty} J_k \left(\frac{r_e}{r_1}\right)^k P_k(\cos\phi) \tag{G.1}$$

The function P_k are the Legendre's polynomials and can be computed by Rodrigues' formula.

$$P_k(x) = \frac{1}{2!2^k} \frac{d^k}{dx^k} \left(x^2 - 1\right)^k \tag{G.2}$$

For $k = 2$, $P_2(x) = \frac{1}{2}(3x^2 - 1)$. Considering that $x = \cos\phi$ and $\phi = \frac{\pi}{2}$, then $\cos\frac{\pi}{2} = 1 \implies x = 0$. Then $P_2(0) = -\frac{1}{2}$. Then, the correction to the potential until the first term can be written as

$$\Phi(r_1, \phi) = -\frac{1}{2}(1-\mu) r_e^2 J_2 \frac{3\cos^2\phi - 1}{r_1^3} \tag{G.3}$$

Now, the acceleration will be given by -$\nabla\Phi$

$$\begin{aligned} -\hat{\mathbf{r}}_1 \frac{\partial\Phi}{\partial r_1} &= -\frac{3}{2}(1-\mu) r_e^2 J_2 \frac{3\cos^2\phi - 1}{r_1^4} \hat{\mathbf{r}}_1 \\ -\hat{\boldsymbol{\phi}} \frac{1}{r_1} \frac{\partial\Phi}{\partial\phi} &= \frac{1}{2}(1-\mu) r_e^2 J_2 \frac{6\cos\phi(-\sin\phi)}{r_1^4} \hat{\boldsymbol{\phi}} \end{aligned} \tag{G.4}$$

Because in PCR3BP $\phi = \frac{\pi}{2}$, the angular component will not contribute to the perturbation (because $\cos\frac{\pi}{2} = 0$). To determine the x and y components of $\frac{\partial\Phi}{\partial r_1}$,it necessary to compute $\hat{\mathbf{x}} \cdot \hat{\mathbf{r}}_1 \frac{\partial\Phi}{\partial r_1}$ and $\hat{\mathbf{y}} \cdot \hat{\mathbf{r}}_1 \frac{\partial\Phi}{\partial r_1}$, respectively. Note

$$\hat{\mathbf{x}} \cdot \hat{\mathbf{r}}_1 = \frac{x+\mu}{r_1} \qquad \hat{\mathbf{y}} \cdot \hat{\mathbf{r}}_1 = \frac{y}{r_1}$$

Considering this, the expressions for the perturbations due to $J2$ factor by x and y com-

ponents are

$$\begin{aligned} -\hat{\mathbf{x}} \cdot \hat{\mathbf{r}}_1 \frac{\partial \Phi}{\partial r_1}\bigg|_{\phi=\frac{\pi}{2}} &= -\frac{3}{2} J_2 \left(\frac{r_e}{r_1}\right)^2 (1-\mu) \frac{x+\mu}{r_1^3} \\ -\hat{\mathbf{y}} \cdot \hat{\mathbf{r}}_1 \frac{\partial \Phi}{\partial r_1}\bigg|_{\phi=\frac{\pi}{2}} &= -\frac{3}{2} J_2 \left(\frac{r_e}{r_1}\right)^2 (1-\mu) \frac{y}{r_1^3} \end{aligned} \tag{G.5}$$

The result in equations (G.5) is identical to the ideal case (with no perturbations) except for the factor $\frac{3}{2} J_2 \left(\frac{r_e}{r_1}\right)^2$, which appears in both components. With this, it can be concluded that the change in Earth gravity potential due to the oblateness of Earth in function of the J_2 factor is as shown below in equation G.6

$$\begin{aligned} -(1-\mu)\frac{(x+\mu)}{r_1^3} &\rightarrow -(1-\mu)\frac{(x+\mu)}{r_1^3}\left[1+\frac{3}{2} J_2 \left(\frac{r_e}{r_1}\right)^2\right] \\ -(1-\mu)\frac{y}{r_1^3} &\rightarrow -(1-\mu)\frac{y}{r_1^3}\left[1+\frac{3}{2} J_2 \left(\frac{r_e}{r_1}\right)^2\right] \end{aligned} \tag{G.6}$$

As it is presented in equation (2.16).

Anexo H

Zeng's Method to Compute Δm

To compute the factor Δm proposed by Zeng we use the expression below

$$\Delta m = M_{CF2}\frac{\gamma_m E_{gas}\gamma_E}{E_{CC}}$$

Where $M_{CF2} = 50$ gr/mol is the relative molecular weight of CF_2, E_{gas} is the energy that actual ablates the surface of the PTFE, which is usually between 3 % and 4 % of E_0, being E_0 the energy at the capacitor, E_{CC} is the chemical bond energy of the carbon-carbon bonds and is equal to 340 kJ/mol and γ_E is the ratio of energy to successful generates the ejected mass and it is defined as 1/2.

The factor γ_m is the ratio of the ejected mass over the total mass able to be ablated and can be defined as $\gamma_m = \frac{n}{\beta N}$, where n are the ejected molecules of PTFE, N is the total number of molecules of PTFE able to be ablated and β is the fracture density. The parameters associated to γ_m are not specified at Zeng's work, but using the numbers $n = 5200$, $N = 10000$ and $\beta = 1/2$, then $\gamma_m = 1.04$. With this choice of numbers, the theoretical results found at Zeng's work can be obtained with a good approximation.

Given the energy at the capacitor as $E_0 = \frac{1}{2}CV^2$, where C is the capacitance of the capacitor, we can compute the results of Zeng's work considering they used a capacitor with $C = 2\mu$F. Table H.1 shows the results at Zeng's work. The final row of table H.1 is the ejected mass here estimated for Zeng's work, the result is very similar to the values at Zeng's work.

Table H.1: Comparison between Zeng's results and estimation.

Parameter	Case 1	Case 2	Case 3	Case 4
Discharge voltage [kV]	0.75	1.06	1.30	1.50
Discharge energy [mJ]	560	1120	1690	2250
Ejected mass from Zeng's work[61] [μg]	1.29-1.73	2.56-3.44	3.87-5.15	5.19-6.83
Ejected mass, estimation [μg]	1.29-1.72	2.58-3.44	3.88-5.17	5.16-6.88

With these parameters, the graph at figure 3.5 in section 3.4 can be obtained. For more details the reader is refered to Zeng's work[61].

Anexo I

Additional Results of Section 4.7

In this appendix, additional results of section 4 are presented.

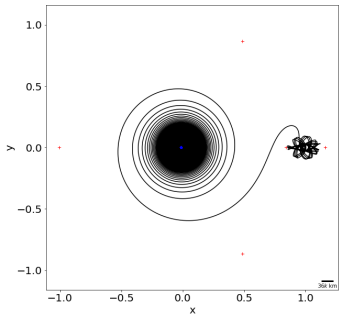

(a) Transfer orbit for $f_2 = 7$ Hz and $t_2 = 5$ T, $f_S = 15$ Hz.

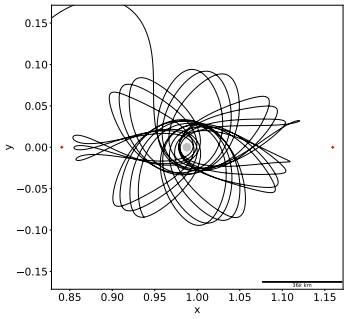

(b) Zoom in at the Moon to transfer orbit for $f_2 = 7$ Hz and $t_2 = 5$ T, $f_S = 15$ Hz.

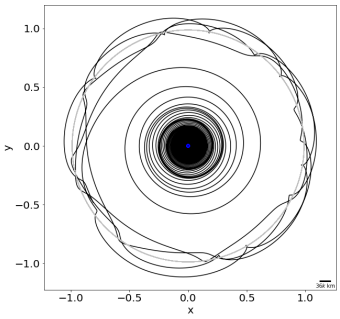

(c) Transfer orbit in non rotating frame for $f_2 = 7$ Hz and $t_2 = 5$ T, $f_S = 15$ Hz.

Figure I.1: Transfer orbit for $f_1 = 5$ Hz and $t_1 = 17.6$ T. Then, $f_2 = 7$ Hz, with $t_2 = 5$ T and $f_S = 15$ Hz. The factor Δm has been reduced in a 10 %.

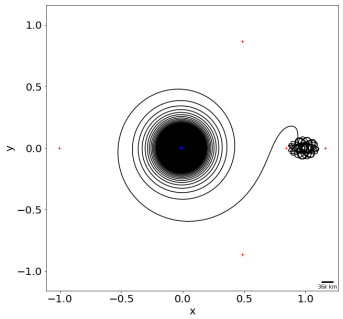

(a) Transfer orbit for $f_2 = 7$ Hz and $t_2 = 5$ T, $f_S = 15$ Hz.

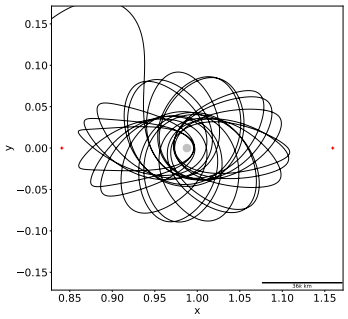

(b) Zoom in at the Moon to transfer orbit for $f_2 = 7$ Hz and $t_2 = 5$ T, $f_S = 15$ Hz.

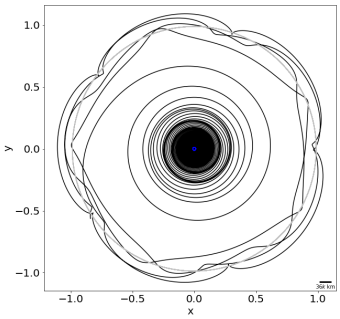

(c) Transfer orbit in non rotating frame for $f_2 = 7$ Hz and $t_2 = 5$ T, $f_S = 15$ Hz.

Figure I.2: Transfer orbit for $f_1 = 5$ Hz and $t_1 = 17.6$ T. Then, $f_2 = 7$ Hz, with $t_2 = 5$ T and $f_S = 20$ Hz. The factor Δm has been reduced in a 10 %.

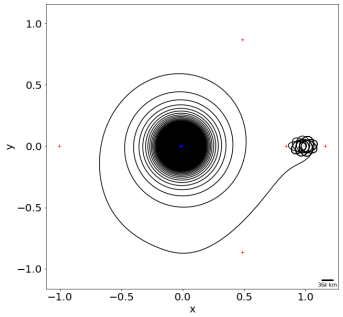

(a) Transfer orbit for $f_2 = 5$ Hz and $t_2 = 5$ T, $f_S = 20$ Hz.

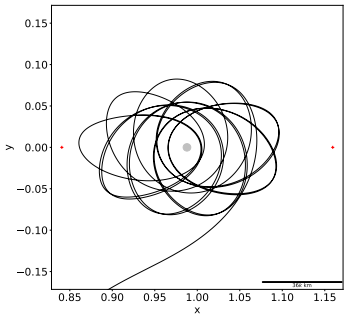

(b) Zoom in at the Moon to transfer orbit for $f_2 = 5$ Hz and $t_2 = 5$ T, $f_S = 20$ Hz.

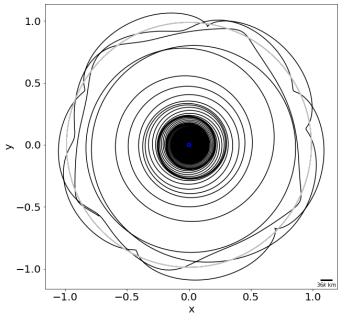

(c) Transfer orbit in non rotating frame for $f_2 = 5$ Hz and $t_2 = 5$ T, $f_S = 20$ Hz.

Figure I.3: Transfer orbit for $f_1 = 5$ Hz and $t_1 = 17.6$ T. Then, $f_2 = 5$ Hz, with $t_2 = 5$ T and $f_S = 20$ Hz. The factor c has been reduced in a 10 %.

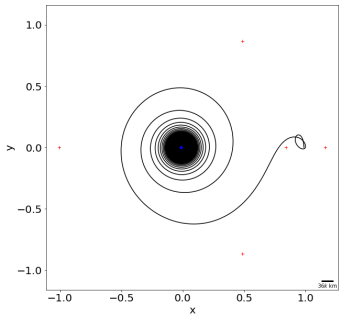

(a) Transfer orbit for $f_2 = 8$ Hz and $t_2 = 0.960$ T, $f_S = 15$ Hz.

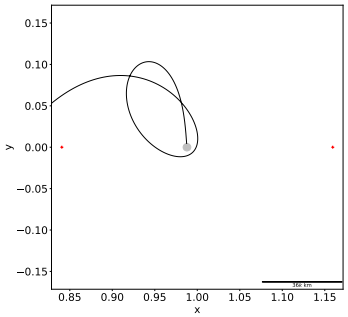

(b) Zoom in at the Moon to transfer orbit for $f_2 = 8$ Hz and $t_2 = 0.960$ T, $f_S = 15$ Hz.

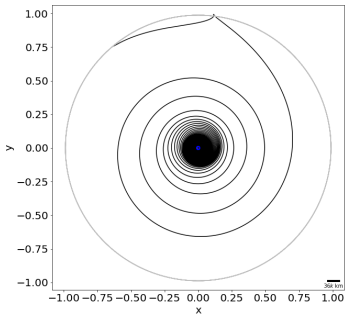

(c) Transfer orbit in non rotating frame for $f_2 = 8$ Hz and $t_2 = 0.960$ T, $f_S = 15$ Hz.

Figure I.4: Landing orbit for $f_1 = 20$ Hz and $t_1 = 4.4$ T. Then, $f_2 = 8$ Hz, with $t_2 = 0.960$ T and $f_S = 15$ Hz. The factor c has been reduced in a 10 %.

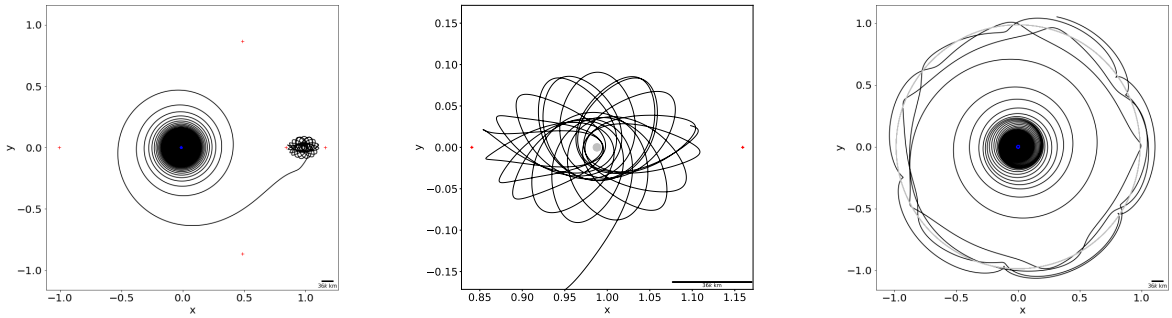

(a) Transfer orbit for $f_2 = 9$ Hz and $t_2 = 4.4$ T, $f_S = 25$ Hz.

(b) Zoom in at the Moon to transfer orbit for $f_2 = 9$ Hz and $t_2 = 4.4$ T, $f_S = 25$ Hz.

(c) Transfer orbit in non rotating frame for $f_2 = 9$ Hz and $t_2 = 4.4$ T, $f_S = 25$ Hz.

Figure I.5: Transfer orbit for $f_1 = 10$ Hz and $t_1 = 8.8$ T. Then, $f_2 = 9$ Hz, with $t_2 = 4.4$ T and $f_S = 25$ Hz. The factor c has been reduced in a 10 %.

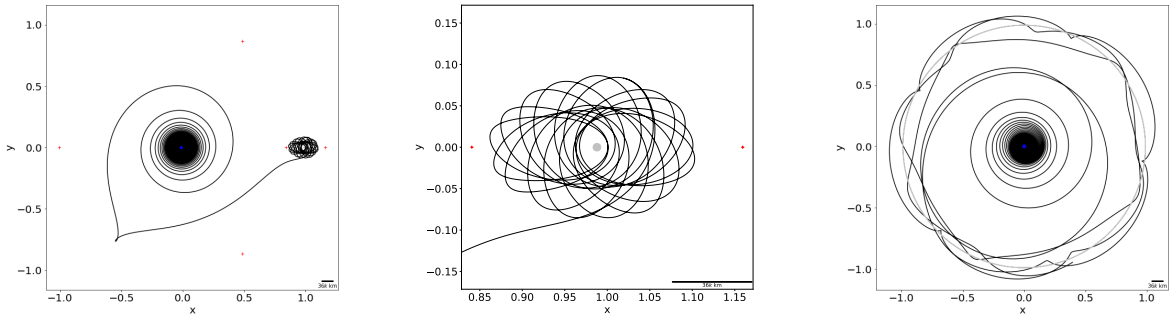

(a) Transfer orbit for $f_2 = 13$ Hz and $t_2 = 4.4$ T, $f_S = 25$ Hz.

(b) Zoom in at the Moon to transfer orbit for $f_2 = 13$ Hz and $t_2 = 4.4$ T, $f_S = 25$ Hz.

(c) Transfer orbit in non rotating frame for $f_2 = 13$ Hz and $t_2 = 4.4$ T, $f_S = 25$ Hz.

Figure I.6: Transfer orbit for $f_1 = 20$ Hz and $t_1 = 4.4$ T. Then, $f_2 = 13$ Hz, with $t_2 = 4.4$ T and $f_S = 25$ Hz. The factor c has been reduced in a 10 %.

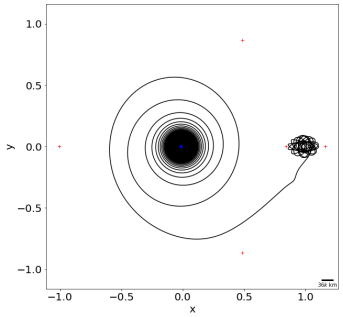

(a) Transfer orbit for $f_2 = 6$ Hz and $t_2 = 4.9$ T, $f_S = 15$ Hz.

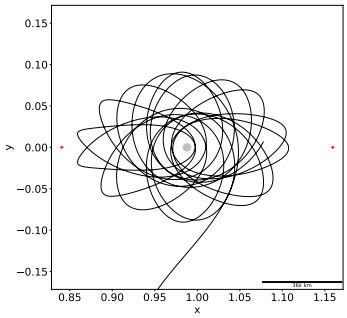

(b) Zoom in at the Moon to transfer orbit for $f_2 = 6$ Hz and $t_2 = 4.9$ T, $f_S = 15$ Hz.

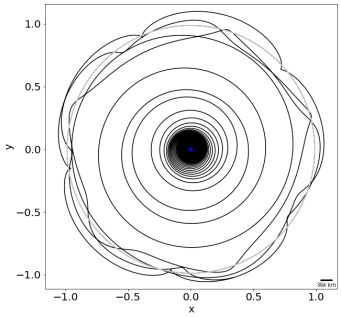

(c) Transfer orbit in non rotating frame for $f_2 = 6$ Hz and $t_2 = 4.9$ T, $f_S = 15$ Hz.

Figure I.7: Transfer orbit for $f_1 = 20$ Hz and $t_1 = 4.9$ T. Then, $f_2 = 6$ Hz, with $t_2 = 4.9$ T and $f_S = 15$ Hz. Both, The factor Δm and the factor c, have been reduced in a 10 %.

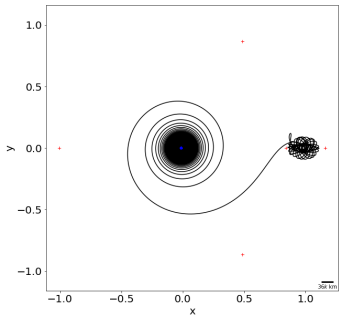

(a) Transfer orbit for $f_2 = 17$ Hz and $t_2 = 4.9$ T, $f_S = 15$ Hz.

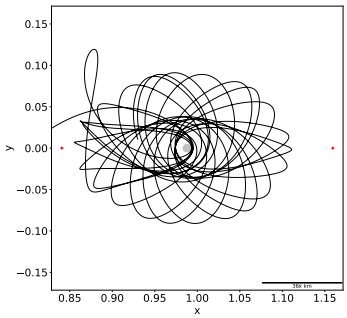

(b) Zoom in at the Moon to transfer orbit for $f_2 = 17$ Hz and $t_2 = 4.9$ T, $f_S = 15$ Hz.

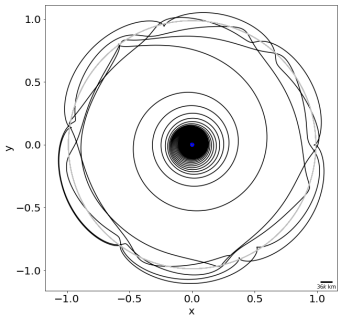

(c) Transfer orbit in non rotating frame for $f_2 = 17$ Hz and $t_2 = 4.9$ T, $f_S = 15$ Hz.

Figure I.8: Transfer orbit for $f_1 = 20$ Hz and $t_1 = 4.9$ T. Then, $f_2 = 17$ Hz, with $t_2 = 4.9$ T and $f_S = 15$ Hz. Both, The factor Δm and the factor c, have been reduced in a 10 %.

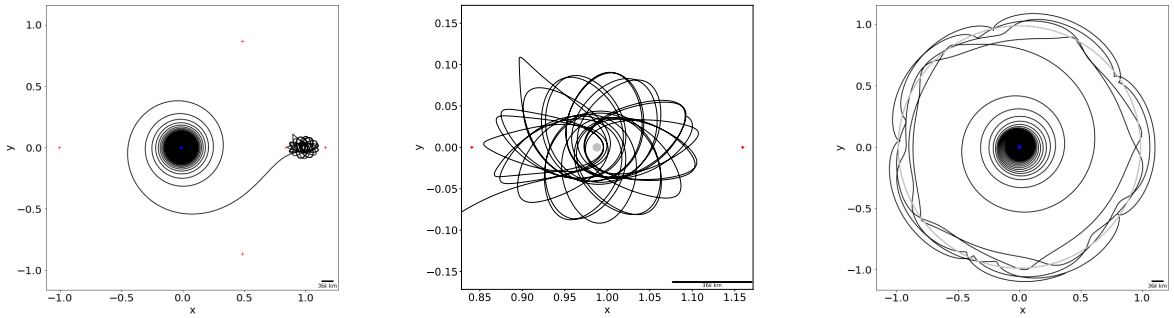

(a) Transfer orbit for $f_2 = 18$ Hz and $t_2 = 4.9$ T, $f_S = 20$ Hz.

(b) Zoom in at the Moon to transfer orbit for $f_2 = 18$ Hz and $t_2 = 4.9$ T, $f_S = 20$ Hz.

(c) Transfer orbit in non rotating frame for $f_2 = 18$ Hz and $t_2 = 4.9$ T, $f_S = 20$ Hz.

Figure I.9: Transfer orbit for $f_1 = 20$ Hz and $t_1 = 4.9$ T. Then, $f_2 = 18$ Hz, with $t_2 = 4.9$ T and $f_S = 20$ Hz. Both, The factor Δm and the factor c, have been reduced in a 10 %.

Anexo J

The Fourth Order Runge-Kutta Method

The fourth order Runge-Kutta method (rk4) is a numerical method to integrate differential equations. It is widely used because its simplicity and its high precision. In equation (J.1) the rk4 solves systems of the form of equation (J.1).

$$\dot{\mathbf{x}} = f(t, \mathbf{x}) \tag{J.1}$$

Given an initial state $\mathbf{x}_0$ and an initial time t_0, rk4 computes as shown below.

$$\begin{aligned} \mathbf{k_1} &= f(t_0, \mathbf{x}_0) \\ \mathbf{k_2} &= f(t_0 + h/2, \mathbf{x}_0 + h\mathbf{k_1}/2) \\ \mathbf{k_3} &= f(t_0 + h/2, \mathbf{x}_0 + h\mathbf{k_2}/2) \\ \mathbf{k_4} &= f(t_0 + h, \mathbf{x}_0 + h\mathbf{k_3}) \end{aligned} \tag{J.2}$$

$$\mathbf{x} = \mathbf{x}_0 + \frac{h}{6}(\mathbf{k_1} + 2(\mathbf{k_2} + \mathbf{k_3}) + \mathbf{k_4}) \tag{J.3}$$

Where $\mathbf{x}$ is the next vector state and h is the time step. In the next iteration $\mathbf{x}$ is used as $\mathbf{x}_0$ and $t_0 + h$ as t_0. This is done as long as required by the number of iterations.

Anexo K

Code

Python modules used

```
import numpy as np
import pandas as pd
import matplotlib.pyplot as plt
from matplotlib.pyplot import figure
import math
import time
import os #to pause with pause()
import winsound
```

The function densityParams(r1) receives the position of the satellite respects to Earth (r_1) and returns the value of the constants ρ_0, h_0 and H. These values are used to define the value of the atmospheric density.

```
def densityParams(r1):
    """Return the constant parameters rho0, h0 and H for density function"""

    global densityCounter
    h = (r1 - r_e)
    flag = True
    while(flag):
        if h > h0_list.iloc[-1]:
            rho0, h0, H = rh0_list.iloc[-1], h, H_list.iloc[-1]        #for the case of no molecular
     ↪  drag
            flag = False
        elif (h <= h0_list.iloc[densityCounter] and h > h0_list.iloc[densityCounter-1]):
            rho0, h0, H = rho0_list.iloc[densityCounter-1], h0_list.iloc[densityCounter-1],
     ↪ H_list.iloc[densityCounter-1]
            flag = False
        elif dh >= 0:
            densityCounter +=1
            #print("densityCounter:", densityCounter, " and h = ", h)
        elif dh < 0:
            densityCounter -=1
            #print("density Counter: ", densityCounter, " and h = ", h)
    return rho0, h0, H
```

The function rk4(x, y, vx, vy, m, t) receives the the position, velocity and mass of the satellite plus the current time. It returns the new or final position, velocity and mass of the satellite after one step.

```
def rk4(x, y, vx, vy, m, t):
    """Return the position (x, y), the velocity (vx,vy) and the mass of the satellite given
     ↪ initial values, step time and mu in
    the context of the Planar Circular Restricted 3 Body Problem (PCR3BP)"""

    xAux = x
    yAux = y
    vxAux = vx
    vyAux = vy
    mAux = m
    tAux = t

    r1Aux = ((xAux+mu)**2 + yAux**2)**0.5
    r2Aux = ((xAux+mu-1)**2 + yAux**2)**0.5
    vAux = (vxAux**2+vyAux**2)**0.5
    hAux = (r1Aux - r_e)
    rhoAux = rho0 * e**(-(hAux-h0)/H)
    vDragAux = ((vxAux - yAux)**2 + (vyAux + xAux)**2)**0.5
    oSAux = -wS*tAux + oS0
    xSAux = aS*np.cos(oSAux)
    ySAux = aS*np.sin(oSAux)
    rSAux = ((xAux-xSAux)**2 + (yAux-ySAux)**2)**0.5

    k11 = vxAux
    k12 = vyAux
    k13 = 2*vyAux + xAux - (1-mu)*(xAux+mu)/r1Aux**3*(1+3*J2/2*(r_e/r1Aux)**2) -
     ↪ mu*(xAux+mu-1)/r2Aux**3 + Th/m*vxAux/vAux - k/m*rhoAux*vDragAux*(
     ↪ vxAux-yAux) - mS*(xAux-xSAux)/rSAux**3 - mS*xSAux/aS**3
    k14 = -2*vxAux + yAux - (1-mu)*yAux/r1Aux**3*(1+3*J2/2*(r_e/r1Aux)**2) - mu*
     ↪ yAux/r2Aux**3 + Th/m*vyAux/vAux - k/m*rhoAux*vDragAux*(vyAux + xAux) -
     ↪ mS*(yAux-ySAux)/rSAux**3 - mS*ySAux/aS**3
    k15 = -NTh * dm * f



    xAux = x + dt/2 * k11
    yAux = y + dt/2 * k12
    vxAux = vx + dt/2 * k13
    vyAux = vy + dt/2 * k14
    mAux = m + dt/2 * k15
    tAux = t + dt/2

    r1Aux = ((xAux+mu)**2 + yAux**2)**0.5
    r2Aux = ((xAux+mu-1)**2 + yAux**2)**0.5
    vAux = (vxAux**2+vyAux**2)**0.5
    hAux = (r1Aux - r_e)
    rhoAux = rho0 * e**(-(hAux-h0)/H)
    vDragAux = ((vxAux - yAux)**2 + (vyAux + xAux)**2)**0.5
```

```
    oSAux = -wS*tAux + oS0
    xSAux = aS*np.cos(oSAux)
    ySAux = aS*np.sin(oSAux)
    rSAux = ((xAux-xSAux)**2 + (yAux-ySAux)**2)**0.5

    k21 = vxAux
    k22 = vyAux
    k23 = 2*vyAux + xAux - (1-mu)*(xAux+mu)/r1Aux**3*(1+3*J2/2*(r_e/r1Aux)**2) -
     ↪ mu*(xAux+mu-1)/r2Aux**3 + Th/m*vxAux/vAux - k/m*rhoAux*vDragAux*(
     ↪ vxAux-yAux) - mS*(xAux-xSAux)/rSAux**3 - mS*xSAux/aS**3
    k24 = -2*vxAux + yAux - (1-mu)*yAux/r1Aux**3*(1+3*J2/2*(r_e/r1Aux)**2) - mu*
     ↪ yAux/r2Aux**3 + Th/m*vyAux/vAux - k/m*rhoAux*vDragAux*(vyAux + xAux) -
     ↪ mS*(yAux-ySAux)/rSAux**3 - mS*ySAux/aS**3
    k25 = -NTh * dm * f



    xAux = x + dt/2 * k21
    yAux = y + dt/2 * k22
    vxAux = vx + dt/2 * k23
    vyAux = vy + dt/2 * k24
    mAux = m + dt/2 * k25
    tAux = t + dt/2

    r1Aux = ((xAux+mu)**2 + yAux**2)**0.5
    r2Aux = ((xAux+mu-1)**2 + yAux**2)**0.5
    vAux = (vxAux**2+vyAux**2)**0.5
    hAux = (r1Aux - r_e)
    rhoAux = rho0 * e**(-(hAux-h0)/H)
    vDragAux = ((vxAux - yAux)**2 + (vyAux + xAux)**2)**0.5
    oSAux = -wS*tAux + oS0
    xSAux = aS*np.cos(oSAux)
    ySAux = aS*np.sin(oSAux)
    rSAux = ((xAux-xSAux)**2 + (yAux-ySAux)**2)**0.5

    k31 = vxAux
    k32 = vyAux
    k33 = 2*vyAux + xAux - (1-mu)*(xAux+mu)/r1Aux**3*(1+3*J2/2*(r_e/r1Aux)**2) -
     ↪ mu*(xAux+mu-1)/r2Aux**3 + Th/m*vxAux/vAux - k/m*rhoAux*vDragAux*(
     ↪ vxAux-yAux) - mS*(xAux-xSAux)/rSAux**3 - mS*xSAux/aS**3
    k34 = -2*vxAux + yAux - (1-mu)*yAux/r1Aux**3*(1+3*J2/2*(r_e/r1Aux)**2) - mu*
     ↪ yAux/r2Aux**3 + Th/m*vyAux/vAux - k/m*rhoAux*vDragAux*(vyAux + xAux) -
     ↪ mS*(yAux-ySAux)/rSAux**3 - mS*ySAux/aS**3
    k35 = -NTh * dm * f



    xAux = x + dt * k31
    yAux = y + dt * k32
    vxAux = vx + dt * k33
    vyAux = vy + dt * k34
    mAux = m + dt * k35
```

```
    tAux = t + dt

    r1Aux = ((xAux+mu)**2 + yAux**2)**0.5
    r2Aux = ((xAux+mu-1)**2 + yAux**2)**0.5
    vAux = (vxAux**2+vyAux**2)**0.5
    hAux = (r1Aux - r_e)
    rhoAux = rho0 * e**(-(hAux-h0)/H)
    vDragAux = ((vxAux - yAux)**2 + (vyAux + xAux)**2)**0.5
    oSAux = -wS*tAux + oS0
    xSAux = aS*np.cos(oSAux)
    ySAux = aS*np.sin(oSAux)
    rSAux = ((xAux-xSAux)**2 + (yAux-ySAux)**2)**0.5

    k41 = vxAux
    k42 = vyAux
    k43 = 2*vyAux + xAux - (1-mu)*(xAux+mu)/r1Aux**3*(1+3*J2/2*(r_e/r1Aux)**2) -
     ↪ mu*(xAux+mu-1)/r2Aux**3 + Th/m*vxAux/vAux - k/m*rhoAux*vDragAux*(
     ↪ vxAux-yAux) - mS*(xAux-xSAux)/rSAux**3 - mS*xSAux/aS**3
    k44 = -2*vxAux + yAux - (1-mu)*yAux/r1Aux**3*(1+3*J2/2*(r_e/r1Aux)**2) - mu*
     ↪ yAux/r2Aux**3 + Th/m*vyAux/vAux - k/m*rhoAux*vDragAux*(vyAux + xAux) -
     ↪ mS*(yAux-ySAux)/rSAux**3 - mS*ySAux/aS**3
    k45 = -NTh * dm * f



    x += dt/6 * (k11+2*(k21+k31)+k41)
    y += dt/6 * (k12+2*(k22+k32)+k42)
    vx += dt/6 * (k13+2*(k23+k33)+k43)
    vy += dt/6 * (k14+2*(k24+k34)+k44)
    m += dt/6 * (k15+2*(k25+k35)+k45)

    return x, y, vx, vy, m
```

The function thruster(f, fStop) receives the operation frequency and the stop frequency of the thruster.

```
def thruster(f, fStop):

    Th = NTh * c * dm * f
    if C[j] <= Cmin and x[j]<=la1:# and r1[j] <= la1:
        Th = 0
    if x[j]>la1:
        Th = (-1) * NTh * c * dm * fStop
    if C[j] >= Cstop and x[j]>la1:# and r1[j] <= la1:
        Th = 0
    return Th
```

This block defines constants associated to the PCR3BP.

```
### GLOBAL CONSTANTS ###
# All constants are measured in MKS units

```

```
G = 6.6743e-11     #Newton's constant
M_e = 5.972e24     # Earth mass
R_e = 6.371e6      # Earth radius
M_l = 7.342e22     # Moon mass
R_l = 1.7371e6     # Moon radius
D = 3.84402e8      # Earth-Moon distance (from their centers)
H_LEO = 5e5        # altitude LEO orbit
H_GEO = 3.6e7                  # Geosyncronus altitute
m0 = 8                        # initial satellite mass
de = 0.5 * 5e-9 * (5e3)**2      # Energy per shoot in Joules for a Capacitor of 5nF and 5kV
pi = np.pi
e = np.exp(1)
#R = 8.31446261815324 #Gas constant
dm = 1e-10         # Ejected mass per shoot of the thruster in kg at 1.5kV
c = 1e5
NTh = 4           # Number of Thrusters used per shoot
Cmin = 3.015
Cstop = 3.189
J2 = 1.0826e-3
mS = 328900.54          # dimensionless Sun mass in E-M units Koon 2011
aS = 388.81114          # dimensionless Sun distance from barycenter in E-M units, Koon
    ↪ 2011
wS = 0.925195985520347    # dimensionless Sun angular velocity in E-M units, Koon 2011
oS0 = 0                 # Sun initial position

### Factors to make variables dimensionless and derived constants

M = M_e + M_l
n = (G*M/D**3)**0.5       # Rajeev, Advanced Mechanics, p.95
mu = M_l/M              # Lunar mass relative to the total mass
T = 2*pi/n              # Period E-M system in seconds
f0 = 1/T                # Frequency E-M system in Hz, it is used to normalize the frequency
    ↪ of the thruster
Tdays = T/3600/24         # Period E-M system in days
dt = 1e-4               # dimensionless step time, equivalent to 235.7 seconds, approximately
r_e = R_e/D
r_l = R_l/D
m0 /= M
dm /= M
c /= (n*D)
```

This block defines the constants associated to the atmospheric drag.

```
### Drag Constants

C_D = 2.2                # Drag coefficient
A = 3 * 0.1 * 0.1 / D**2   # Six units cubesat face area of 3 units, dimless area
k = 0.5 * A * C_D          # Drag constant times mass, IMPORTANT: this numeber must
    ↪ be divided by the mass in the equations.

meanDensityFile = pd.read_csv('density5.csv')
h0_list = meanDensityFile.iloc[:, 0].astype('float') * 1e3/D
```

```
#temp = meanDensityFile.iloc[1:, 1].astype('float')                # temperature
#MolWt = meanDensityFile.iloc[1:, 4].astype('float')               # Molecular Weight in kg/
    ↪ kmol
#g = G*M_e/(R_e+h0_list)**2                                        # gravity at h0

#H_list = (R * temp / (MolWt * g))*1e3/D                           # dimless scale height
#h0_list = h0_list * 1e3/D                                        # dimless h0
rho0_list = meanDensityFile.iloc[:, 3].astype('float') *D**3/M     # dimless density, initial
    ↪ density per altitude segment
H_list = meanDensityFile.iloc[:, 4].astype('float') * 1e3/D
densityCounter0 = 25
```

This block defines the initial conditions of the PCR3BP and initializes all the vectors.

```
### Initial Conditions ###
#Computing initial conditions using Ugai2010
label = 'LEO'
H0 = H_LEO

###Nondimensional Initial conditions around earth
v0 = (G * M_e / (R_e + H0))**0.5 / (n*D)
x0 = (R_e + H0) / D - mu
vy0 = v0 - mu - x0 # this converts v0 from GEO to barycenter vy0

### Null initial conditions
y0, vx0 = 0, 0
m0 = 8/M
oS0 = 0
flag = False
#Initial condition from a final point, this overwrite the Null initial conditions

#x0, y0, vx0, vy0, m0, oS0, t0, flag = xf, yf, vxf, vyf, mf, oSf, tf, True

frac = 0.25 #1-0.175 #/number of Moon periods, use a number/Tdays to count days, eg: for
    ↪ 3 days of orbits use 3/Tdays
N = int(frac*2*pi/dt)

x, y = np.zeros(N), np.zeros(N)
x[0], y[0] = x0, y0

vx, vy = np.zeros(N), np.zeros(N)
vx[0], vy[0] = vx0, vy0

m = np.zeros(N)
m[0] = m0


r01, r02 = ((x0 + mu)**2 + y0**2)**0.5, ((x0 + mu - 1)**2 + y0**2)**0.5
r1, r2 = np.zeros(N), np.zeros(N)
r1[0], r2[0] = r01, r02


```

```
K0 = 0.5 * (vx0**2 + vy0**2)
U0 = - (1-mu)/r01 - mu/r02
K, U = np.zeros(N), np.zeros(N)
K[0], U[0] = K0, U0

t, E = np.zeros(N), np.zeros(N)
t0, E0 = 0, K0 + U0
t[0], E[0] = t0, E0

Omega0 = 0.5 * (x0**2 + y0**2) - U0
Omega = np.zeros(N)
Omega[0] = Omega0

C = np.zeros(N)
C0 = 2 * (Omega0 - K0)
C[0] = C0

Dm, DE = np.zeros(N), np.zeros(N)

densityCounter = densityCounter0
rho0, h0, H = rho0_list[densityCounter], h0_list[densityCounter], H_list[densityCounter]

drag = np.zeros(N)
drag[0]=k/m0*rho0*((vx0-y0)**2+(vy0+x0)**2)*e**(-(r01-r_e-h0)/H)
C0
```

All this code is executed twice. Usually, the first running computes the orbit until a high orbit. The second running computes the transfer orbit and the orbit around the Moon. Considering this, the next block allows to concatenate the position vector obtained in the first and the second running to present an only one total orbit later.

```
### Run this block only in the fisrt loop
if flag:
    x=np.concatenate((X,x[1:]))
    y=np.concatenate((Y,y[1:]))
    tNRF = np.concatenate((tNRF,[ti+tf for ti in t[1:]]))
else:
    X=x
    Y=y
    tNRF = t
```

This block plots the orbit of the satellite close to the Moon. This allows to see the orbit near the Moon. The variable name“ it is used only for printing purposes.

```
Moon = plt.Circle((1-mu, 0), R_1/D, color='silver')
fig, ax = plt.subplots(figsize=(10, 10))
ax.add_artist(Moon)
plt.plot(x, y, color = 'k', linestyle = '-')
#plt.plot(x[260000:300000], y[260000:300000])
plt.plot(la1, 0, color='r', marker='+')
plt.plot(la2, 0, 'r+')
plt.xlim(la1-mu,la2+mu)
```

```
plt.ylim(-(la2-la1)/2-mu,(la2-la1)/2+mu)
plt.xlabel('x',size=20)
plt.ylabel('y', size=20)
plt.xticks(fontsize=20, rotation=0)
plt.yticks(fontsize=20, rotation=0)
print("Minimun distance to moon surface: ", int((min(r2)*D-R_l)*1e-3), "km")

name='f5T16' + 'f' + str(int(f*f0)) + 'T' + str(frac) + 'fS' + str(int(fStop*f0))
name='f' + str(int(f*f0)) + 'T' + str(frac)
name
#plt.savefig('transferOrbits4\' + name + 'Zoom.png')
#plt.savefig('transferOrbits4\' + name + 'Zoom.eps')
```

This block plots the orbit of the PCR3BP. The red crosses represent the 5 Euler-Lagrange points.

```
Earth = plt.Circle((-mu, 0), R_e/D, color='blue')
Moon = plt.Circle((1-mu, 0), R_l/D, color='silver')
fig, ax = plt.subplots(figsize=(10, 10))
ax.add_artist(Earth)
ax.add_artist(Moon)

#plt.plot(-mu, 0, 'bo')
#plt.plot(1-mu, 0, 'k.')
plt.plot(la1, 0, color='r', marker='+')
plt.plot(la2, 0, 'r+')
plt.plot(la3, 0, 'r+')
plt.plot(la4[0], la4[1], 'r+')
plt.plot(la5[0], la5[1], 'r+')
#plt.grid()
#plt.title('H$_0$ = {H_0} km, v$_0$ = {v_0:1.1f} km/s'.format(H_0=int(1e-3*H0), v_0=
    ↪ v0*n*D*1e-3), size=30)
plt.xlabel('x',size=20)
plt.ylabel('y', size=20)
plt.axis('equal')
plt.xticks(fontsize=20, rotation=0)
plt.yticks(fontsize=20, rotation=0)
plt.plot(x, y, color = 'k', linestyle = '-')
#plt.xlim(-mu-0.1,-mu+0.1)
#plt.ylim(-0.12,0.12)
#plt.plot(x[0:500], y[0:500])
#plt.plot(x[0:130000], y[0:130000], color = 'k', linestyle = '-')
#plt.plot(x[0:285446], y[0:285446])
lapse = N*dt/n/3600/24
print("lapse in days = ", lapse)

#plt.savefig('transferOrbits4\Hmax\' + name + '.png')
#plt.savefig('transferOrbits4\Hmax\eps\' + name + '.eps')
```

The next block is used to plot the value of the constant Jacobi C in function of time.

```
#plt.grid()
```

```
fig = plt.figure(figsize=(16,9))
plt.grid()
plt.title('Jacobi Constant $C$', size=25)
plt.xticks(fontsize=20, rotation=0)
plt.yticks(fontsize=20, rotation=0)
plt.xlabel('Time [day]',size=20)
plt.ylabel('Constant $C$ [au]', size=20)
plt.xticks(fontsize=20, rotation=0)
plt.yticks(fontsize=20, rotation=0)
plt.plot(t/n/3600/24, C)
#plt.ylim(C0*.99995,C0*1.00005)
#plt.savefig('transferOrbits\jacobiC\ ' + name + 'JacobiC.png')
#plt.savefig('transferOrbits\jacobiC\ ' + name + 'JacobiC.eps')
print("Minimum value of Cmin = ", min(C), "and final value of Cfinal = ", C[-1])
```

This block plots the high reached by the satellite in function of time.

```
plt.figure(figsize=(12,9))
plt.plot(t/n/3600/24 ,(r1*D-R_e)*1e-6)
plt.title('Height v/s Time', size=25)
plt.xlabel('Time [day]',size=20)
plt.ylabel('Height [$k$ km]', size=20)
plt.xticks(fontsize=20, rotation=0)
plt.yticks(fontsize=20, rotation=0)
print('max height:', max((r1*D-R_e)*1e-3))

#plt.savefig('transferOrbits4\Height_ ' + name + '.png')
#plt.savefig('transferOrbits4\Height_ ' + name + '.eps')
```

This block plots the high reached by the satellite respect to the Moon

```
plt.figure(figsize=(12,9))
plt.plot(t/n/3600/24,(r2-r_l)*D*1e-6)
plt.title('Height Moon v/s Time', size=25)
plt.xlabel('Time [day]',size=20)
plt.ylabel('Height [$k$ km]', size=20)
plt.xticks(fontsize=20, rotation=0)
plt.yticks(fontsize=20, rotation=0)
print("distance from the surface of the Moon to the sat with a minimun: r2_{Min}-r_l = ",
    ↪ int(min(r2*D*1e-3)-R_l*1e-3), 'km')
#plt.savefig('HighMoon'+ Ti + 'T' + Tf + '.png')
#plt.savefig('HighMoon'+ Ti + 'T' + Tf + '.eps')
```

This line of code simply make a sound to let know the computing has finished.

```
# Play Windows exit sound.
winsound.PlaySound("SystemExit", winsound.SND_ALIAS)
```

This line of code defines the new initial condition for the second running, this line of code has to be ran in the first running and only in the first running of the whole code.

```
###Defining new initial condition in function of the last point obtained in the first
    ↪ computing
```

```
xf, yf, vxf, vyf, mf, oSf, tf= x[-1], y[-1], vx[-1], vy[-1], m[-1], -wS*t[-1]+oS0, t[-1]
```

the next lines of code have to be executed one by one, this is because the value obtained in the variables in the first execution are used in the second one.

```
propellerMass = Dm[-1]*M
propellerMass
propellerMass + 0.47399237945192785
DE[-1]/3.6e6
DE[-1]/3.6e6 + 82.29034365442136
```

This block plot the total mass ejected from the thruster in function of time.

```
plt.figure(figsize=(12,9))
plt.plot(t/n/3600/24,Dm*M*1e3)
plt.title("Mass Ejected", size=25)
plt.xlabel('Time [day]',size=20)
plt.ylabel('Mass Propeled [mg]', size=20)
plt.xticks(fontsize=15, rotation=0)
plt.yticks(fontsize=15, rotation=0)
flag1, flag2 = True, True
for i in range(N-1):
    if Dm[i+1] == Dm[i] and flag1 == True:
        print(i-1)
        flag1 = False
    if Dm[i+1] != Dm[i] and flag1 == False and flag2 == True:
        print(i-1)
        flag2 = False

#plt.savefig('Mass'+ Ti + 'T' + Tf + '.png')
#plt.savefig('Mass'+ Ti + 'T' + Tf + '.eps')
```

This block defines labels used in the next plots.

```
### plot parameters ###
Hi='4k'
Hf='120k'
Ti='1'
Tf='4'
```

This block plots the total energy used by the thruster in function of time

```
plt.figure(figsize=(12,9))
plt.plot(t/n/3600/24,DE/3600/1e3)
plt.title("Energy for Propulsion", size=25)
plt.xlabel('Time [day]',size=20)
plt.ylabel('Energy [kWh]', size=20)
plt.xticks(fontsize=15, rotation=0)
plt.yticks(fontsize=15, rotation=0)

#plt.savefig('Energy'+ Ti + 'T' + Tf + '.png')
```

```
#plt.savefig('Energy'+ Ti + 'T' + Tf + '.eps')
```

This block plots the modulus of the acceleration on the satellite due to the thruster in function of time.

```
plt.figure(figsize=(12,9))
plt.plot(t/n/3600/24,Th/m*1e3)
plt.title("Thrust Acceleration", size=25)
plt.xlabel('Time [day]',size=20)
plt.ylabel('Thrust Acceleration [mm/s$^2$]', size=20)
plt.xticks(fontsize=15, rotation=0)
plt.yticks(fontsize=15, rotation=0)

#plt.savefig('forcesComparison\Thrust'+ Ti + 'T' + Tf + '.png')
#plt.savefig('forcesComparison\Thrust'+ Ti + 'T' + Tf + '.eps')
```

This block plots the modulus of the acceleration on the satellite due to the oblateness of Earth ($J2$ factor) in function of time.

```
plt.figure(figsize=(12,9))
plt.figure(figsize=(12,9))
plt.plot((r1-r_e)*D*1e-3,(1-mu)*(3/2*J2*(r_e/r1)**2) * ((((x+mu)/r1**3)**2 + (y/r1**3)
    ↪ **2)**0.5)*n**2*D*1e6)
plt.title('J2 Acceleration',size=25)
plt.xlabel('Height [km]',size=20)
plt.ylabel('J2 Acceleration [$\mu$m/s$^2$]', size=20)
plt.xticks(fontsize=15, rotation=0)
plt.yticks(fontsize=15, rotation=0)

#plt.savefig('forcesComparison3\J2Height_'+ Hi + '_' + Hf + '.png')
#plt.savefig('forcesComparison3\J2Height_'+ Hi + '_' + Hf + '.eps')
```

As the last block, the next one plots the modulus of the acceleration on the satellite due to the oblateness of Earth ($J2$ factor), but this time in function of height of the satellite respect to Earth.

```
plt.figure(figsize=(12,9))
plt.plot(t/n/3600/24,(1-mu)*(3/2*J2*(r_e/r1)**2) * ((((x+mu)/r1**3)**2 + (y/r1**3)**2)
    ↪ **0.5)*n**2*D*1e6)
plt.title('J2 Acceleration',size=25)
plt.xlabel('Time [day]',size=20)
plt.ylabel('Acceleration by J2 [$\mu$m/s$^2$]', size=20)
plt.xticks(fontsize=15, rotation=0)
plt.yticks(fontsize=15, rotation=0)
min((1-mu)*(3/2*J2*(r_e/r1)**2) * ((((x+mu)/r1**3)**2 + (y/r1**3)**2)**0.5)*n**2*D*1
    ↪ e6)
#plt.ylim(0,10)
#plt.xlim(60,85)
#plt.savefig('forcesComparison\J2_Tail'+ Ti + 'T' + Tf + '.png')
#plt.savefig('forcesComparison\J2_Tail'+ Ti + 'T' + Tf + '.eps')
```

This block plots the modulus of the acceleration on the satellite due to the atmospheric

density of Earth in function of time.

```
plt.figure(figsize=(12,9))
plt.plot(t/n/3600/24,drag*D*n**2*1e6)
plt.title('Drag Acceleration',size=25)
plt.xlabel('time [days]',size=20)
plt.ylabel('Drag Acceleration [$\mu$m/s$^2$]', size=20)
plt.xticks(fontsize=15, rotation=0)
plt.yticks(fontsize=15, rotation=0)

#plt.savefig('forcesComparison\Drag'+ Ti + 'T' + Tf + '.png')
#plt.savefig('forcesComparison\Drag'+ Ti + 'T' + Tf + '.eps')
```

As the last block, this one plots the modulus of the acceleration on the satellite due to the atmospheric density of Earth ($J2$ factor), but this time in function of height of the satellite respect to Earth.

```
plt.figure(figsize=(12,9))
plt.plot((r1-r_e)*D*1e-3,drag*D*n**2*1e6)
plt.title('Drag Acceleration',size=25)
plt.xlabel('Height [km]',size=20)
plt.ylabel('Drag Acceleration [$\mu$m/s$^2$]', size=20)
plt.xticks(fontsize=15, rotation=0)
plt.yticks(fontsize=15, rotation=0)

#plt.savefig('forcesComparison\Drag'+ Hi + 'H' + Hf + '.png')
#plt.savefig('forcesComparison\Drag'+ Hi + 'H' + Hf + '.eps')
```

This block computes the position of the Sun as a funtion of time.

```
### SUN ###
oS = -wS*t+ oS0
xS = aS*np.cos(oS)
yS = aS*np.sin(oS)
rS = ((x-xS)**2 + (y-yS)**2)**0.5
```

This block plots the modulus of the acceleration on the satellite due to the Sun's gravity in function of time.

```
plt.figure(figsize=(12,9))
plt.plot(t/n/3600/24,(((- mS*(x-xS)/rS**3 - mS*xS/aS**3)**2+(- mS*(y-yS)/rS**3 - mS*yS
    ↪ /aS**3)**2)**0.5)*n**2*D*1e6)
plt.title('Sun Acceleration', size=25)
plt.xlabel('Time [days]',size=20)
plt.ylabel('Sun Acceleration [$\mu$m/s$^2$]', size=20)
plt.xticks(fontsize=15, rotation=0)
plt.yticks(fontsize=15, rotation=0)

#plt.savefig('forcesComparison\Sun'+ Ti + 'T' + Tf + '.png')
#plt.savefig('forcesComparison\Sun'+ Ti + 'T' + Tf + '.eps')
```

As the last block, this one plots the modulus of the acceleration on the satellite due to the Sun's gravity, but this time in function of height of the satellite respect to Earth.

```
plt.figure(figsize=(12,9))
plt.plot((r1-r_e)*D*1e-3,(((- mS*(x-xS)/rS**3 - mS*xS/aS**3)**2+(- mS*(y-yS)/rS**3 - mS
    ↪ *yS/aS**3)**2)**0.5)*n**2*D*1e6)
plt.title('Sun Acceleration', size=25)
plt.xlabel('Height [km]',size=20)
plt.ylabel('Sun Acceleration [$\mu$m/s$^2$]', size=20)
plt.xticks(fontsize=15, rotation=0)
plt.yticks(fontsize=15, rotation=0)

#plt.savefig('forcesComparison\Sun'+ Hi + 'H' + Hf + '.png')
#plt.savefig('forcesComparison\Sun'+ Hi + 'H' + Hf + '.eps')
```

The next code computes the ablated mass from the Nanofocus using the work of Wagner[62].

```
###    Ablated Mass, Wagner2004slug for Nanofocus    ###
# Wagner gives an empirical expression that can be used directly
# with the number from the nanofocus
# Wagner's formula: m_b = 1.32e-6*A_p^0.65*E_0^0.35

# Constants
pi = np.pi
C = 3.3e-9              #Nanofocus capacitance, [F]
R = 0.85e-3             #exterior radius of the plasma gun
r = 0.25e-3             #interior radius of the plasma gun
A_p = pi * (R**2 - r**2)   #Ablated area

# Equations
N = 10                  #Number of points on the graph
V = np.zeros(N)
E_0 = np.zeros(N)
m_b = np.zeros(N)
for i in range(N):
    V[i] = 5e2 * (i+1);                     #Discharge voltage, [V]
    E_0[i] = 0.5 * C * V[i]**2              #Initial Energy, Energy in the capacitor, (J)
    m_b[i] = 1.32e-6 * A_p**0.65 * E_0[i]**0.35  #mass in kg

plt.figure(figsize=(16,9))
plt.plot(V,m_b, color='b')
xAxis = [i * 1e3 for i in [0.5, 1, 1.5, 2, 2.5, 3, 3.5, 4, 4.5, 5]];
xLabels = ['0.5','1.0','1.5','2.0','2.5','3.0','3.5','4.0','4.5','5.0'];
plt.plot(V,m_b)
yAxis = [i * 1e-10 for i in [ 0.2, 0.3, 0.4, 0.5, 0.6, 0.7, 0.8, 0.9]];
yLabels = ['0.2','0.3','0.4','0.5','0.6','0.7','0.8','0.9'];
plt.title('Ablated Mass Nanofocus', size=30)
plt.xlabel('Voltage [kV]', size=25)
plt.ylabel('Ablated mass [10$^{-10}$kg]', size=25)
plt.xticks(xAxis, xLabels, size=20);
plt.yticks(yAxis, yLabels, size=20);

#plt.savefig('ablatedMass\Wagner2004.png')
#plt.savefig('ablatedMass\Wagner2004.eps')
```

The next code computes the ablated mass from the Nanofocus using the work of Zeng[61] in the other.

```
###   Ablated Mass, zeng2019new  for NANOFOCUS ###
# Description
# This is the implementation of equations from 'zeng2019new'
# It computes the ablated mass from a pulsed plasma thruster
# Constants
n = 5310           #number of simulated CF2 units that break away from the surface,
    ↪ arbitrary yet
beta = 0.5         #fracture density, arbitrary yet
N = 10000           #total number of simulated CF2 units, arbitrary yet
gamma_E = 0.5       #ratio of energy of ablation and total Egas
M_CF2 = 50 * 1e-3    #relative molecular mass of CF2, approx 50 [kg/mol]
E_CC = 348000       #chemical bond energy carbon-carbon [J/mol]
e_gas = 1.5e6       #specific energy breakdowwn PTFE [J/kg], Burton1998
C = 3.3e-9          #capacitance [F] of NANOFOCUS

# Equations
gamma_m = n / (beta * N);      #ratio of mass ablated
points = 10                  #points to be plotted
V = np.zeros(points)
E_0 = np.zeros(points)
m_b1 = np.zeros(points)
m_b2 = np.zeros(points)
m_b3 = np.zeros(points)
m_b4 = np.zeros(points)

for i in range(points):
    V[i] = 5e2 * (i+1);           #Discharge Voltage [V]
    E_0[i] = 0.5 * C * V[i]**2;
    E_gas1 = 0.01 * E_0[i];
    E_gas3 = 0.03 * E_0[i];
    E_gas4 = 0.04 * E_0[i];  #percent, 3 or 4
    m_b1[i] = M_CF2 * gamma_m * (E_gas1 * gamma_E / E_CC);
    m_b3[i] = M_CF2 * gamma_m * (E_gas3 * gamma_E / E_CC);
    m_b4[i] = M_CF2 * gamma_m * (E_gas4 * gamma_E / E_CC);


plt.figure(figsize=(16,9))
plt.plot(V,m_b3)
plt.plot(V,m_b4)
xAxis = [i * 1e3 for i in [0.5, 1, 1.5, 2, 2.5, 3, 3.5, 4, 4.5, 5]];
xLabels = ['0.5','1.0','1.5','2.0','2.5','3.0','3.5','4.0','4.5','5.0'];
yAxis = [i * 1e-10 for i in [0.0, 0.2, 0.4, 0.6, 0.8, 1.0, 1.2]];
yLabels = ['0.0','0.2','0.4','0.6','0.8','1.0','1.2'];
plt.title('Ablated Mass Nanofocus', size=30)
plt.xlabel('Voltage [kV]', size=25)
plt.ylabel('Ablated mass [10$^{-10}$kg]', size=25)
plt.xticks(xAxis, xLabels, size=20);
plt.yticks(yAxis, yLabels, size=20);
plt.legend(['3 % of E$_0$','4 % of E$_0$'], fontsize=20)
```

```
#plt.savefig('ablatedMass\Zeng2019.png')
#plt.savefig('ablatedMass\Zeng2019.eps')
```

The next block computes the Hill's zones given a value for the constant Jacobi C.

```
#Hill's regions

dHill = 1.5
delta = 0.01
Nhill = int(dHill/delta)
xHill = []
yHill = []

C0 = 2.989 #to vary the value of C0
for j in range(0, 2*Nhill + 1):
    for i in range(0, 2*Nhill + 1):
        xH = -dHill + delta * i
        yH = -dHill + delta * j
        r1 = ((xH+mu)**2 + yH**2)**0.5
        r2 = ((xH+mu-1)**2 + yH**2)**0.5
        U = -(1-mu)/r1 - mu/r2
        Omega = (xH**2 + yH**2)/2 - U
        if  Omega <= C0/2:
            xHill.append(xH)
            yHill.append(yH)

plt.figure(figsize=(10, 10))
plt.scatter(xHill,yHill,s=.5,c='k')
plt.plot(-mu,0,'b.')
plt.plot(1-mu,0,'k.')
plt.plot(la1, 0, 'r+')
plt.plot(la2, 0, 'r+')
plt.plot(la3, 0, 'r+')
plt.plot(la4[0], la4[1], 'r+')
plt.plot(la5[0], la5[1], 'r+')
#plt.grid()
plt.title('Hill region for C = %1.3f' % C0, size=30)
plt.xlabel('x',size=20)
plt.ylabel('y', size=20)
print("with C0 = ", C0)
plt.ylim(-1.5,1.5)
plt.xlim(-1.5,1.5)
#plt.ylim(-0.1,0.1)
#plt.xlim(la2*.99,1.01*la2)
#plt.savefig('Hill' + str(int(C0)) + 'C' + str(round(C0-int(C0), 3))[2:] + '.png')
#plt.savefig('Hill' + str(int(C0)) + 'C' + str(round(C0-int(C0), 3))[2:] + '.eps')
```